UNIVERSITA' VITA-SALUTE SAN RAFFAELE

CORSO DI DOTTORATO DI RICERCA INTERNAZIONALE IN MEDICINA MOLECOLARE

Curriculum in Experimental and Clinical Medicine

INTEGRATING PSMA EXPRESSION PATTERNS, MORPHOLOGICAL AND CLINICAL FEATURES TO OPTIMIZE DETECTION OF NODAL METASTASES IN PATIENTS TREATED WITH PSMA RADIO-GUIDED ROBOT-ASSISTED RADICAL PROSTATECTOMY AND EXTENDED PELVIC LYMPH NODE DISSECTION

DoS: Prof. Francesco Montorsi
Second Supervisor: Prof. Freddie Hamdy

Tesi di DOTTORATO di RICERCA di Elio Mazzone

Matricola. 017573
Ciclo di dottorato XXXVI SSD MED/24

Anno Accademico 2022/2023

CONSULTAZIONE TESI DI DOTTORATO DI RICERCA

Il sottoscritto/*I*	Elio Mazzone
Matricola/*registration number*	017573
Nato a/*born at*	*Roma*
Il/*on*	*21/09/1990*

Autore della tesi di Dottorato di ricerca dal titolo / *author of the PhD Thesis titled*
Integrating PSMA expression patterns, morphological and clinical features to optimize detection of nodal metastases in patients treated with PSMA radio-guided robot-assisted radical prostatectomy and extended pelvic lymph node dissection

X AUTORIZZA la Consultazione della tesi / AUTHORIZES *the public release of the thesis*

☐ NON AUTORIZZA la Consultazione della tesi per ..... mesi /DOES NOT AUTHORIZE *the public release of the thesis for ..... months*

a partire dalla data di conseguimento del titolo e precisamente */ from the PhD thesis date, specifically*

Dal / *from* ...../...../..... Al / *to* ...../...../..... Poiché /*because*:

□ l'intera ricerca o parti di essa sono potenzialmente soggette a brevettabilità/ *The whole project or part of it might be subject to patentability;*

□ ci sono parti di tesi che sono già state sottoposte a un editore o sono in attesa di pubblicazione/ *Parts of the thesis have been or are being submitted to a publisher or are in press;*

□ la tesi è finanziata da enti esterni che vantano dei diritti su di esse e sulla loro pubblicazione/ *the thesis project is financed by external bodies that have rights over it and on its publication.*

E' fatto divieto di riprodurre, in tutto o in parte, quanto in essa contenuto /

Copyright the contents of the thesis in whole or in part is forbidden

Data /Date 30/10/2023 Firma /Signature .....

DECLARATION

This thesis has been:
- composed by myself and has not been used in any previous application for a degree. Throughout the text I use both 'I' and 'We' interchangeably.
- written according to the editing guidelines approved by the University.

Permission to use images and other material covered by copyright has been sought and obtained.

Interim analyses and part of the results presented in the current work were previously published by myself and collaborators in the following manuscript: Gandaglia G, Mazzone E, Stabile A, Pellegrino A, Cucchiara V, Barletta F, Scuderi S, Robesti D, Leni R, Samanes Gajate AM, Picchio M, Gianolli L, Brembilla G, De Cobelli F, van Oosterom MN, van Leeuwen FWB, Montorsi F, Briganti A. Prostate-specific membrane antigen Radioguided Surgery to Detect Nodal Metastases in Primary Prostate Cancer Patients Undergoing Robot-assisted Radical Prostatectomy and Extended Pelvic Lymph Node Dissection: Results of a Planned Interim Analysis of a Prospective Phase 2 Study. Eur Urol. 2022 Oct;82(4):411-418. doi: 10.1016/j.eururo.2022.06.002. Epub 2022 Jul 22. PMID: 35879127.

All the results presented here were obtained by myself, except for:

1. Pathological tumor assessment and immunohistochemical analyses – done in collaboration with Dr. Nazario Tenace, Dr. Roberta Luciano' and Prof. Claudio Doglioni and the Pathology Department, IRCCS Ospedale San Raffaele (methods sections 6.6, and data presented in Figures 17,21 and 25)
2. Radiotracers generation – done in collaboration with Dr. Ana Maria Samanes Gajate, Prof. Maria Picchio and the Nuclear Medicine Department, IRCCS Ospedale San Raffaele (methods sections 6.2 and 6.3)

All sources of information are acknowledged by means of reference.

Abstract

Prostate-specific membrane antigen radio-guided surgery (PSMA-RGS) could optimize the identification of lymph node invasion (LNI) during robot-assisted radical prostatectomy (RARP). In this context, despite previous evidence showed that disease with micro-metastatic spread or with low PSMA expression levels are often missed by preoperative PSMA PET, it is unknown whether PSMA-RGS may overcome these limitations. We relied on patients with intermediate- or high-risk cM0 hormone-naïve prostate cancer at conventional imaging with a risk of LNI >5% enrolled in an ongoing Phase II trial. Overall, 30 patients were enrolled and surgically treated between June 2021 and September 2023. 99mTc-PSMA I&S was administered intravenously the day before surgery followed by SPECT/CT. A drop-in gamma probe was used for in-vivo and ex-vivo measurements during PSMA-RGS with extended pelvic lymph node dissection (ePLND). Target to background count rate was used to determine intraoperative positivity at PSMA-RGS. Immune-histochemical (IHC) analyses on the cohort of patients with pN1 disease tested the expression of PSMA, androgen receptor (AR) and SOX-2 on positive and negative nodes and prostate specimens. A semiquantitative evaluation of PSMA expression was performed using H-score index, calculated as follow: ([{% of weak staining} x 1] + [{% of moderate staining} x 2] + [{% of strong staining} x 3]). Thereafter, intra-tumoral heterogeneity was measured using Shannon Diversity Index (SDI) as follow: SDI = -Σ Pi(lnPi), where Pi is the proportion of each PSMA staining level in each pathological sample. Comparisons were determined using the Wilcoxon matched-pair signed rank test. Overall, 9 (30%) patients had LNI at ePLND. Preoperative 99mTc-PSMA SPECT/CT had sensitivity of 55%, specificity of 95%, positive predictive value of 83%, and negative predictive value of 83% (accuracy 83%). At per-patient level combining both in-vivo and ex-vivo measurements and after assessing the optimal target-to-background count rate, the sensitivity, specificity, positive and negative predictive values of PSMA-RGS were 66%, 95%, 86% and 87% (accuracy 87%). At prostate IHC evaluation of pN1 patients, median H-score was 210 with median intratumor PSMA expression heterogeneity of 0.70. Notably, the highest SDI (1.29) were recorded in the only two patients expressing SOX-2 and with reduced AR expression, suggesting their correlation with intra-tumour heterogeneity. At lymph-nodes IHC of pN1 patients, higher H-score and increasing nodal metastatic diameters were both associated with higher

intraoperative count rate. When comparing true-positive and false-negative nodal findings at RGS according to positivity definition, non-significant differences in H-scores were reported (277 vs 212, p=0.08). Conversely, the median maximum diameter of metastatic lesions was significantly smaller in false negative nodes (10 vs 1.2mm, p=0.01), with no metastases smaller than 3mm identified at PSMA RGS. In summary, 99mTc-PSMA-RGS during RARP did not overcome the dimensional limitation of preoperative PSMA PET, since metastases with maximum diameter < 3mm were not detected regardless PSMA expression levels.

1. Table of contents

2. Acronyms and abbreviations

American Urological Association (AUA)

American Joint Committee on Cancer (AJCC)

Androgen deprivation therapy (ADT)

Androgen receptor (AR)

Apparent diffusion coefficient (ADC)

Carbon-11 (11C-)

Clinically significant prostate cancer (csPCa)

Computer tomography (CT)

Deoxyribonucleic acid (DNA)

Diffusion weighted (DWI)

Digital rectal examination (DRE)

Dynamic contrast enhanced (DCE)

European Association of Nuclear Medicine (EANM)

European Association of Urology (EAU)

European Randomized Study of Screening for Prostate Cancer (ERSPC)

European Society for Radiotherapy and Oncology (ESTRO)

European Society of Urogenital Radiology (ESUR)

Extended pelvic lymph node dissection (ePLND)

External beam radiotherapy (EBRT)

Extra-capsular extension (ECE)

Fluorine-18 (18F-)

Folate hydrolase gene (FOLH1)

Food and Drug Administration (FDA)

Formalin-fixed, paraffin-embedded (FFPE)

Gallium-68 (68Ga)

Glutamate carboxypeptidase II (GCP-II)

Hematoxylin & Eosin (H&E)

Immunohistochemistry (IHC)

Image-guided RT (IGRT)

Indium-111 (111In-)

Intensity-modulated RT (IMRT)

International Society of Geriatric Oncology (SIOG)

International Agency for Research on Cancer (IARC)

International Society of Urological Pathology (ISUP)

Lower urinary tract symptoms (LUTS)

Lymph node invasion (LNI)

Magnetic resonance imaging (MRI)

Memorial Sloan Kettering Cancer Center (MSKCC)

Multiparametric MRI (mpMRI)

National Comprehensive Cancer Network (NCCN)

Negative predictive value (NPV)

Pelvic lymph node dissection (PLND)

Positive predictive value (PPV)

Positron emission tomography (PET)

Prostate Cancer (PCa)

Prostate Evaluation for Clinically Important Disease: Sampling Using Image-guidance Or Not? (PRECISION)

Prostate Imaging Reporting and Data System (PI-RADS)

Prostate, Lung, Colorectal and Ovarian (PLCO)

Prostate-specific antigen (PSA)

Prostate-specific membrane antigen (PSMA)

PSMA Imaging & Surgery (PSMA I&S)

PSMA Imaging & Treatment (PSMA I&T)

Radio-guided surgery (RGS)

Robot-assisted radical prostatectomy (RARP)

Seminal vesicle invasion (SVI)

Shannon Diversity Index (SDI)

Single genetic variations (SNPs)

Single positron emission computerized tomography (SPECT)

United States (US)

United States Preventive Services Task Force (USPSTF)

Target-to-Background (TtB)

Technetium-99m (99mTc)

T2-weighted (T2WI)

Tumor, Node, Metastasis (TNM)

Volumetric arc radiation therapy (VMAT)

3. List of figure and tables

List of Figures

List of Tables

4. Introduction

4.1 Epidemiology

The World Cancer Research Association indicates that prostate cancer is the second most frequently identified cancer in men globally, recording 1,414,259 new diagnoses in 2020 (1). In 2020, the all-age rate of prostate cancer incidence stood at 31 per 100,000 males, with a lifetime risk of 3.9%. In that year, prostate cancer was responsible for 375,304 male deaths, positioning it as the fourth leading cancer-causing death in men. Projections for 2040 suggest an increase of 71.6% in incidence and 91.1% in mortality, primarily attributed to the aging and expansion of the global population (1). The prevalence of this ailment reveals distinct regional differences. For instance, the frequency and death rates due to prostate cancer fluctuate significantly across nations (1). Countries like Australia, New Zealand, North America, and North-Western Europe report the highest frequency, while Eastern and South-Central Asia record the lowest - although their numbers are on an upward trend **(FIGURE 1)**. Multiple factors contribute to these geographical disparities. One, there's a clear difference in genetic vulnerability to prostate cancer across ethnic groups . For instance, individuals of African ancestry in developed nations face a higher risk of contracting and succumbing to prostate cancer compared to their Asian counterparts (2). Two, unequal access to healthcare can amplify cancer rates and related deaths. For example, the frequent use of PSA screening and surgeries for benign prostatic growth can lead to the detection of dormant prostate cancer cases where they're commonly advised (3). Also, regional variations in lifespan influence the cancer's prevalence, as it's often detected in older males. Typically, men in underdeveloped regions with shorter life expectancies due to other health challenges are less likely to suffer from prostate cancer-related deaths than those in developed regions with longer life expectancies (4). In essence, the frequency of prostate cancer varies significantly across different regions. Factors such as prolonged life span, increased detection of dormant cases, and genetic tendencies have escalated the frequency of this disease in developed regions in recent times.

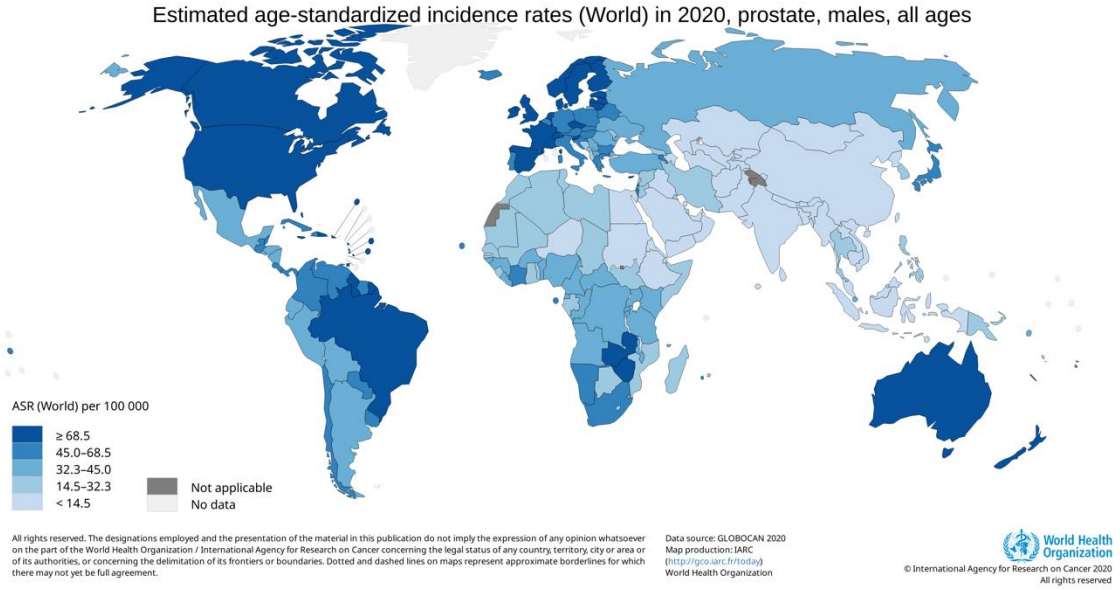

Figure 1. *Estimated age-standardized incidence rates (World) in 2020 for prostate cancer. Reprinted from GLOBOCAN 2020 Graph production: IARC (http://gco.iarc.fr/today) World Health Organization. ©2020, with permission from IARC/WHO.*

4.2 – Biology of prostate cancer

The development of prostate cancer is a result of intricate interactions between various factors in the micro and macro environment, inborn genetic predispositions, and subsequent genetic changes (5). This cancer originates in the prostate gland, positioned in the pelvis and surrounding the initial part of the male urethra. This gland comprises three distinct sections: the central, transition, and peripheral areas (6). The majority of prostate cancer cases begin in the peripheral zone (7). In this zone, both luminal and basal types of prostate epithelial cells can initiate the cancerous transformation **(FIGURE 2)**. Prostate cancer possesses certain distinct biological traits. Primarily, it relies on hormones. Both healthy and cancerous epithelial cells have a high presence of androgen receptors, underscoring the hormone-driven nature of prostate cancer growth, especially in its initial stages (8). Another notable feature is often its multifocal nature. The presence of diverse cancerous foci can have varying genetic modifications and responses to treatments. Hence, detecting prostate cancer through random sampling might not always

provide a complete view of this varied multifocal disease, potentially missing more aggressive tumor sections and leading to unforeseen advancements (9). Chronic inflammation and microbial infections from urine are key factors prompting prostate cancer development. They can promote DNA changes and select mutation-prone cells by inducing oxidative stress and producing reactive oxygen species (10). In such an inflamed setting, proliferating luminal epithelial cells might develop intermediate forms susceptible to genetic and epigenetic changes, eventually resulting in prostatic intraepithelial neoplasia and cancerous evolution.

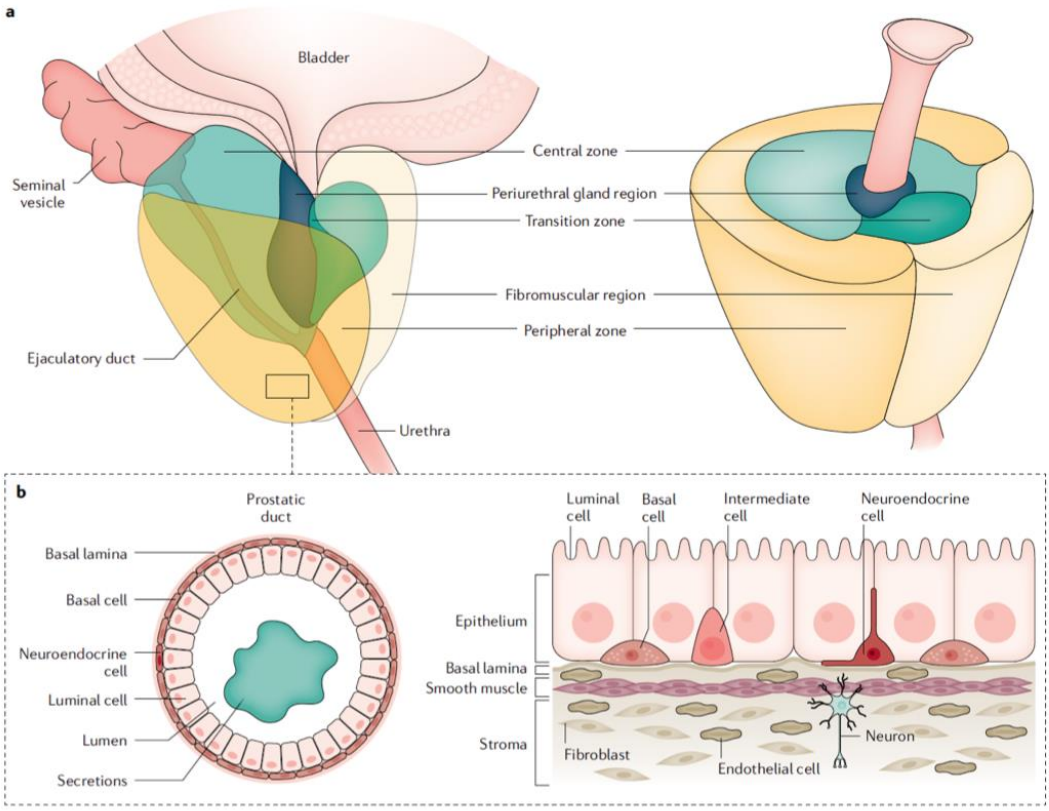

Figure 2. *The adult prostate is composed of three main areas: the central, transition, and peripheral zones; prostate cancer more frequently arises from the peripheral zone. b) Each region comprises ducts and acini embedded in the stroma, which also contains other cell types: smooth muscle cells, fibroblasts, endothelial cells, and neurons. The ducts and acini comprise a single layer of columnar epithelium, surrounded by a layer of basal epithelial cells. Neuroendocrine cells are also present within the duct. Reprinted by permission from Springer Nature ("Springer Nature"), Nature Reviews Disease*

4.3 – Histopathology of prostate cancer

The histopathological appearance of prostate cancer can vary. At one end of the spectrum, it closely resembles benign gland structures, while on the other end, it manifests as high-grade cancerous glandular lesions characterized by small, rounded acini missing a basal epithelial layer and dispersed among non-cancerous glands (11). The Gleason score, a scale from 6 to 10, is utilized to determine prostate cancer's severity upon histopathological examination. Pathologists assign Gleason patterns based on the microscopic look of the cancer, with higher numbers indicating more aggressive forms. This score is derived by adding the two most dominant Gleason patterns together (12) (**FIGURE 3**). In contemporary practices, the Gleason score is translated into the International Society of Urological Pathology (ISUP) grade groups, which are numbered 1 through 5. Specifically, group 1 aligns with Gleason score 3+3, group 2 with 3+4, group 3 with 4+3, group 4 with scores such as 4+4, 3+5, and 5+3, and group 5 with scores like 4+5, 5+4, and 5+5. This ISUP grade system was developed to offer a more precise prognosis for prostate cancer than what the Gleason score alone could provide (13).

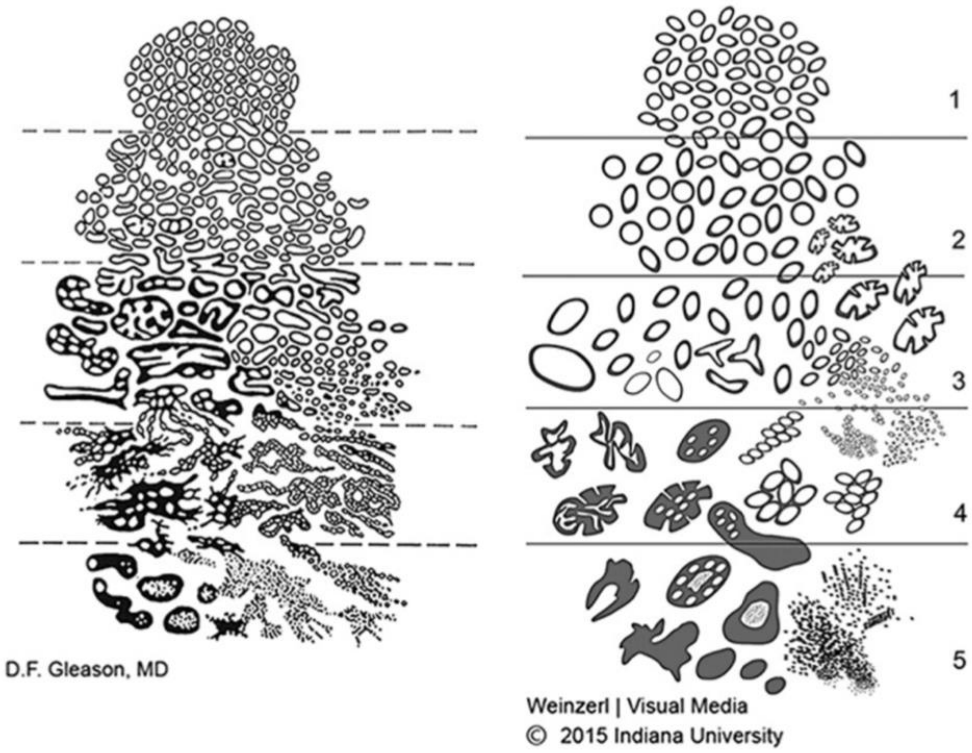

Figure 3. *Histologic patterns of PCa: original Gleason score (left) and modified ISUP 2014 criteria for Grade Group assessment (right). Epstein, Jonathan I et al., The American Journal of Surgical Pathology (2016)*

4.4 – PSA screening

4.4.1 – Understanding PSA

The Prostate-specific antigen (PSA) is a type of glycoprotein found in humans that is secreted by both healthy and cancerous prostate gland cells. A straightforward blood test can assess PSA concentrations. This concentration is typically described as nanograms of PSA in every milliliter (ng/mL) (14). Elevated PSA blood levels can indicate the presence of conditions like prostatic hyperplasia or even prostate cancer (15). In 1986, the FDA gave the nod to the PSA test (16). Initially, it was solely employed to track prostate cancer's evolution in men diagnosed with the ailment. Yet, in 1994, based on a comprehensive study's findings (17), the FDA greenlit the usage of the PSA test alongside a digital rectal exam to aid in identifying prostate cancer in men aged 50 and above (18).

4.4.2 – The Debate Surrounding PSA Screening

Ever since PSA screening became a part of the clinical landscape, it has been a subject of contention. Advocates for PSA-screening posit that it can help decrease mortality rates from prostate cancer by identifying early-stage, symptom-free tumors. However, extensive PSA-screening also leads to the identification of more benign tumors. This spike in benign tumor detection has, in turn, triggered an uptick in aggressive treatments, leading to treatment-induced complications (19). Such issues often overshadowed the advantages of PSA-screening (20). Recognizing these challenges, the US Preventive Services Task Force (USPSTF), a group of specialists in preventive healthcare and evidence-based medicine, advised against using PSA-screening for men 75 years or older in 2008 and all men in 2012 (21,22). They based this on the Prostate, Lung, Colorectal, and Ovarian (PLCO) screening trial findings that didn't highlight any discernable survival advantage for the screened group after 13 years (23). However, this conflicted with European studies, especially the European Randomized Study of Screening for Prostate Cancer (ERSPC), which recorded lower prostate cancer-specific mortality in screened individuals (24). These contradictory findings influenced global health bodies, with some supporting and others opposing PSA-screening. In America, the rejection of PSA-screening led to a surge in metastatic prostate cancer diagnoses (25). Therefore, the USPSTF updated its guidelines in 2018, suggesting that men aged 55-69 years undergo PSA-screening after thorough counseling (26). In contrast, many European nations, including Italy, heed the European Association of Urology (EAU) guidelines, which advocate prostate cancer screening primarily for well-advised individuals over 50 with a projected lifespan of at least a decade or more (27). High-risk demographics, like those with a familial history of the disease, individuals of African origin, or those with BRCA2 mutations, can opt for earlier screening (28). In other regions, the guidelines might fluctuate based on age or inherent risk elements, but the common thread is the emphasis on screening for those over 50, given certain risk factors are in play (**FIGURE 4**).

Country/region	Recommendation			
	Without additional risk factors	Family history of any cancer	*BRCA2* germline mutation carrier	African American ancestry
USA (USPSTF, AUA)	From age 55 to 69 years and if >10 years LE; stop at age 70 years	Individual decision-making before age 55 years	N/A	Individual decision-making before age 55 years
Canada (CUA)	From age 50 to 70 years and if >10 years LE	From age 45 years if >10 years LE	N/A	N/A
Europe (EAU, ESTRO, SIOG)	From age 50 years and only if >10 years LE	From age 45 years if >10 years LE	From age 40 years	From age 45 years if >10 years LE
Japan (JUA)	From age 50 years	From age 40 years	N/A	N/A

Figure 4*. USA, Canada, European, and Japanese recommendations for PSA screening in the adult male population. Reprinted by permission from Springer Nature ("Springer Nature"), Nature Reviews Disease Primers, "Prostate cancer", Richard J. Rebello et al., ©2018*

4.5 – Prostate cancer risk factors

Prominent factors linked to prostate cancer include advancing age, racial background, and familial history from both mother's and father's sides (29). Men with African roots appear to be more susceptible to prostate cancer due to specific genetic tendencies (30,31). Notably, those of African or Caribbean origin residing in the US tend to contract prostate cancer at a younger age and with more severe attributes compared to their Caucasian counterparts, showcasing a relative risk that's twice as high (32). In contrast, Asian men in Asia have a lower incidence of prostate cancer compared to Caucasian men in the US. Interestingly, this protective geographic influence seems to fade when comparing Asian-Americans to Caucasians in the US (33), hinting at environmental factors playing a significant role in these regional differences. Around 20% of men diagnosed with prostate cancer report a family history of the disease (34). It's termed 'familial' when a minimum of three family members are affected, and at least two of them were diagnosed before reaching 55. Thus, having a close relative with the disease increases one's risk by 1.8 times (35). Merely 9% of men with prostate cancer have a genuinely inherited form, generally presenting itself earlier (by 6-7 years) than non-inherited cases (36). The genetic foundations of family predispositions and related hereditary cancer syndromes are intricate. Comprehensive genetic studies have pointed

out more than 100 prevalent genetic markers that heighten prostate cancer risk in high-risk families. Notable among these are BRCA1, BRCA2 (37), HOXB13 (38), MSH2 (39), and specific inherited variations in DNA repair genes that heighten disease risk. Moreover, research has spotlighted over 170 single genetic variations (SNPs) associated with an elevated prostate cancer risk (40). These SNPs assist in creating genetic risk evaluations for early prostate cancer detection in vulnerable individuals. While these metrics don't precisely differentiate between aggressive and milder forms, they're valuable in identifying candidates for proactive screening (41). As for lifestyle determinants, factors like obesity, metabolic conditions (42), alcohol consumption (43), smoking (44), and high protein diets (45) have been explored as possible prostate cancer catalysts. While some show a correlation with increased risk, existing data doesn't conclusively advocate for lifestyle or dietary adjustments as effective preventive measures.

4.6 – Disease classification

4.6.1 – The TNM classification system

Prostate cancer can be categorized using various classification structures. The Tumor, Node, Metastasis (TNM) staging system (46), provided by the American Joint Committee on Cancer (AJCC), applies to the majority of human tumors and delineates prostate cancer into three primary categories: localized, locally advanced, and metastatic. Recent data reveals that 80% of men are diagnosed with disease confined to the organ, 15% with locoregional metastases, and 5% with distant metastases (29) (**FIGURE 6**). Given these findings, a large portion of patients have localized forms of prostate cancer. Men with early-diagnosed localized prostate cancer may have a life expectancy as elevated as 99% over a decade (47). Considering the peak incidence of this tumor in men aged 65 or older, many will pass away before displaying any clinical disease indicators. Therefore, an alternative classification of prostate cancer, considering its clinical impact on patient health and longevity, is crucial for determining treatment recommendations.

T - Primary Tumour (stage based on digital rectal examination [DRE] only)	
TX	Primary tumour cannot be assessed
T0	No evidence of primary tumour
T1	Clinically inapparent tumour that is not palpable
T1a	Tumour incidental histological finding in 5% or less of tissue resected
T1b	Tumour incidental histological finding in more than 5% of tissue resected
T1c	Tumour identified by needle biopsy (e.g. because of elevated prostate-specific antigen [PSA])
T2	Tumour that is palpable and confined within the prostate
T2a	Tumour involves one half of one lobe or less
T2b	Tumour involves more than half of one lobe, but not both lobes
T2c	Tumour involves both lobes
T3	Tumour extends through the prostatic capsule
T3a	Extracapsular extension (unilateral or bilateral)
T3b	Tumour invades seminal vesicle(s)
T4	Tumour is fixed or invades adjacent structures other than seminal vesicles: external sphincter, rectum, levator muscles, and/or pelvic wall
N - Regional (pelvic) Lymph Nodes[1]	
NX	Regional lymph nodes cannot be assessed
N0	No regional lymph node metastasis
N1	Regional lymph node metastasis
M - Distant Metastasis[2]	
M0	No distant metastasis
M1	Distant metastasis
M1a	Non-regional lymph node(s)
M1b	Bone(s)
M1c	Other site(s)

Figure 5*. Clinical Tumor Node Metastasis (TNM) classification of PCa, adapted from EAU Guidelines 2023.*

4.6.2 – Classification according to clinical significance

The terminology "clinically significant" and "clinically insignificant" is commonly utilized to categorize the clinical course of newly identified prostate cancer. A clinically insignificant prostate cancer is described as a localized ailment with a minimal threat to the patient, and its sole risk comes from overtreatment, wherein the treatment's adverse effects overshadow its advantages. Although the utility of a clinical definition for these terms is recognized, the pathological delineation is somewhat ambiguous. Per the Gleason grading system and the 2014 ISUP classification adaptation (12), prostate cancer's ferocity can be segmented into five categories. ISUP Gleason grade groups 2-5 manifest substantial aggressiveness, while group 1 typically demonstrates a lethargic progression. Studies on prostatectomy specimens with ISUP group 1 tumors reveal infrequent

extraprostatic extension and no seminal vesicle invasion or lymph node metastasis (48). Nonetheless, clinically insignificant prostate cancer (ISUP Gleason grade group 1) is commonly identified by biopsy, which can influence management decisions due to possible inaccuracies. The advent of MRI-targeted biopsy has mitigated diagnostic errors, yet inaccuracies, especially when initial MRI indicates a suspicious lesion that is later identified as a Gleason grade group 1 tumor at biopsy, may persist. Additionally, the potential progression of Gleason grade group 1 to more advanced stages over time casts doubt on the definition of insignificant prostate cancer, allowing for potential alterations to its classification. Conversely, clinically significant prostate cancers, characterized by a potent potential for local and systemic advancement, warrant curative treatments that, despite related harm, are justified by enhanced survival prospects. The SPCG-4 (49), PIVOT (50), and Protec-T (51) trials have validated these notions, carving a distinction between clinically significant and insignificant prostate cancers and shaping recommendations for curative treatments. These trials affirm that the clinical relevance of prostate cancer should be ascertained not only based on pathological tumor characteristics (e.g., ISUP Gleason grade groups, T stage, and PSA) but also by considering age expectancy to optimally select curative treatment candidates. A minimum follow-up duration of 10 years is essential to discern benefits from active treatments, while also accommodating treatment complications and disease trajectory. Essentially, prostate cancer is deemed clinically significant when pathological attributes indicate a sufficient disease progression to warrant treatment, taking into account related side effects, and when patient life expectancy exceeds 10 years. This 10-year benchmark is pivotal to accommodate the disease's gradual natural history and to realize the merits of treatment.

4.6.3 – Preoperative risk classification

Alongside the categorization into clinically significant and insignificant prostate cancer, numerous other risk stratifications have emerged to finely delineate patients exhibiting indolent or vehement disease. Amongst these, the D'Amico classification has gained prominence as a frequently applied system (52). Initially conceived to forecast the likelihood of recurrence post-curative treatment (encompassing radiotherapy and radical

prostatectomy) for localized prostate cancer variations, this model segregates patients into three clusters (low, intermediate, and high risk) based on the intrinsic recurrence probability. The risk assessment is formulated using blood PSA concentrations, the Gleason score, and the tumor's T stage. Thus, the recurrence risk is defined as follows:

- Low risk: PSA ≤ 10, ISUP grade group = 1, and clinical stage T1-2a;
- Intermediate risk: PSA between 10 and 20ng/ml, ISUP grade group 2-3, or clinical stage T2b;
- High-risk: PSA > 20ng/ml, ISUP grade group ≥ 4, or clinical stage T2c-3a.

The D'Amico model, albeit with various amendments, has received approval by entities like the National Comprehensive Cancer Network (NCCN) and EAU guidelines to adapt treatment decision-making in localized prostate cancer cases (**FIGURE 6**). Recently, an innovative risk stratification for prostate cancer patients was devised to determine recurrence probability following radical interventions (53). This fresh classification merges clinical and preoperative MRI characteristics, specifically PSA, biopsy ISUP grade groups, MRI T stage, and the lesion's maximum MRI diameter. Analogous to the D'Amico model, the EAU classifier's end-point remains biochemical recurrence post-radical treatment. However, the novel classification by Mazzone et al. (53) exclusively incorporated patients undergoing radical prostatectomy, while D'Amico's model (52) was created in a patient cohort predominantly treated with radiotherapy. The new classification demarcated four patient cohorts: low, intermediate, high, and very-high recurrence risk (**FIGURE 7**). In external validation, the Mazzone classification displayed elevated accuracy in comparison to the D'Amico model (53).

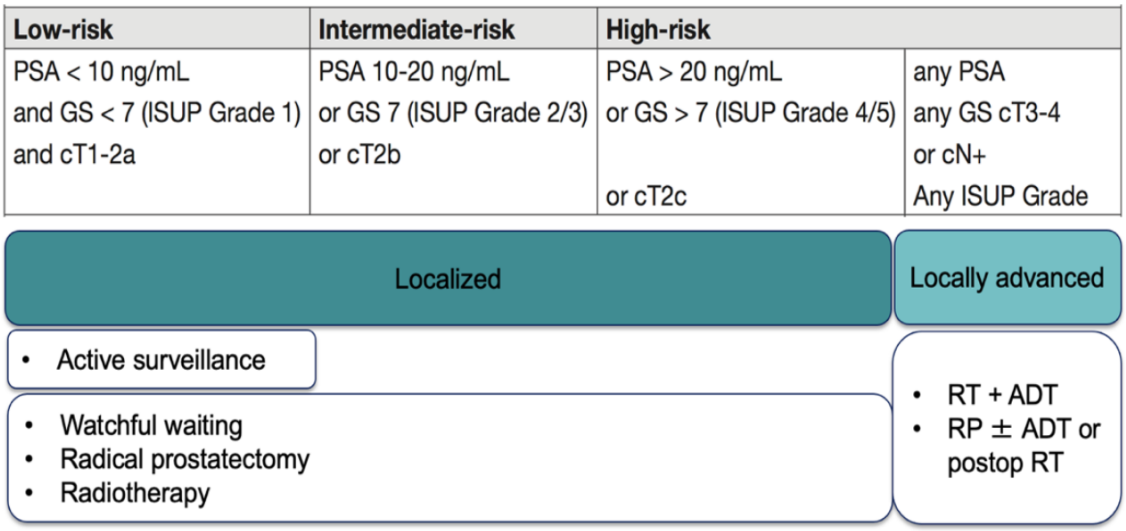

Figure 6*. Risk groups for biochemical recurrence of localized and locally advanced prostate cancer and treatment options, adapted from EAU Guidelines 2023*

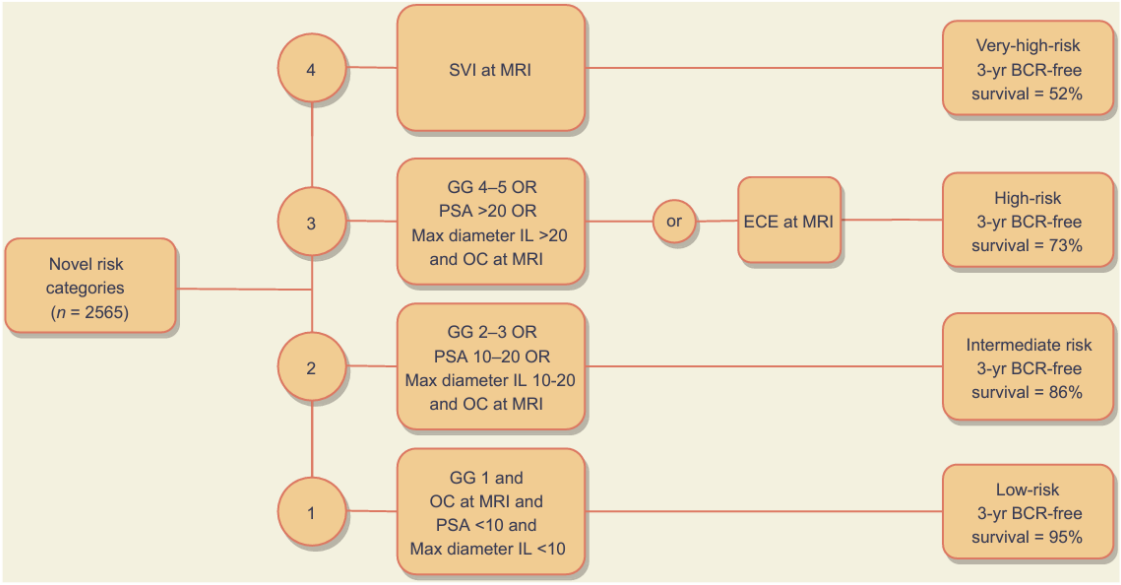

Figure 7*. Novel risk classification stratifying patients into four categories according to grade group, T stage at MRI, maximum diameter of the index lesion at MRI, and preoperative PSA. BCR = biochemical recurrence; ECE = extracapsular extension; GG = grade group; IL = index lesion; MRI = magnetic resonance imaging; OC = organ confined; PSA = prostate-specific antigen; SVI = seminal vesicle invasion. (Reprinted from European Urology, Elio Mazzone et al., "Risk Stratification of Patients Candidate*

to Radical Prostatectomy Based on Clinical and Multiparametric Magnetic Resonance Imaging Parameters: Development and External Validation of Novel Risk Groups", ©2022, with permission from Elsevier).

4.7 – Diagnosis

Prostate cancer frequently presents without symptoms, with diagnoses often emerging serendipitously in men undergoing preventive PSA testing without presenting symptoms. Individuals with PCa may exhibit varied symptoms, including lower urinary tract symptoms (LUTS) — such as nocturia and weak urinary stream —, erectile dysfunction, and noticeable hematuria. Nevertheless, such symptoms scarcely correlate directly with the disease. In contrast, LUTS typically signify the initial clinical manifestation of a widely occurring condition like benign prostatic enlargement, which commonly impacts men within the same age bracket (54). When PCa is suspected, PSA and digital rectal examination (DRE) are generally the initial examinations undertaken, potentially aiding the decision-making procedure to evaluate further explorations (55).

4.7.1 – Digital rectal examination

International clinical guidelines advocate for the use of digital rectal examination in tandem with PSA to identify irregular prostate characteristics warranting additional exploration. In fewer than 10% of instances, PCa is identified solely through anomalous DRE, irrespective of PSA levels (56). A doubtful DRE in patients boasting a PSA level ≤ 2 ng/mL holds a positive predictive value (PPV) ranging from 5–30% (57). An unusual DRE is linked with a heightened risk of a superior ISUP grade and forecasts clinically significant PCa (csPCa) in men undergoing active surveillance (58), serving as a rationale for MRI and biopsy. Clinical staging leans on DRE and robustly predicts advanced PCa (59,60).

4.7.2 – Multiparametric magnetic resonance imaging

In recent history, males with elevated PSA and abnormal DRE suggestive of PCa were straightforwardly referred to random systematic trans-rectal biopsy (61). Nevertheless, this method has associations with sampling inaccuracies, causing up to a 30% failure rate in detecting csPCa. Additionally, contemplating prostate biopsies for all individuals with raised PSA levels could uncover numerous dormant cancers that wouldn't jeopardize the patient, thereby presenting potential overdiagnosis and overtreatment risks in a substantial population (as much as 45% of men diagnosed) (24,62). Magnetic resonance imaging (MRI) initially made its appearance for PCa in the 1980s, initially limited to T1-weighted and T2-weighted sequences. Over the years, additional sequences were developed, and currently, the procedure often utilized for PCa study is termed Multi-Parametric MRI (mpMRI). Over the past few decades, mpMRI has garnered increased attention in urological circles due to its capability to offer data not only linked to tissue anatomy but also attributes like prostate volume, cellularity, and vascularity. Presently, this imaging technique amalgamates T2-weighted imaging with diffusion-weighted imaging (DWI) and dynamic contrast-enhanced imaging (DCE), collectively enhancing diagnostic accuracy for PCa (63). T2-weighted sequence plays a crucial role in prostate gland examination. This sequence showcases cellularity through tissue water content. In a non-cancerous prostate, the peripheral zone (most frequently impacted by PCa) is uniformly hyperintense in T2-weighted imaging due to its ample glandular ductal tissue content. However, with the presence of PCa, cellularity rises, resulting in hypointensity on imaging (64). The dimmer the intensity, the more aggressive the disease manifestation (65). A primary challenge with T2 sequencing is detecting PCa in the transition zone since this region demonstrates high cellular density, translating into a hypointense signal (66,67). To address this challenge, the DWI sequence has been incorporated into prostate studies. This sequence gauges the random motion of water in the relevant tissue (68). In PCa, water molecule motion is notably decreased due to elevated cellularity, leading to restriction areas, which emerge as bright spots encircled by low signal areas (67). From DWI, the apparent diffusion coefficient (ADC) map can be procured, which, in contrast to DWI, depicts PCa as a low-signal lesion, and the further the signal diminishes, the higher the probability of an aggressive disease (69). Diffusion-weighted imaging sequence has also risen in importance due to its capacity to differentiate between benign

prostatic hyperplasia nodules located in the transition zone and malignant transition zone lesions (67). Dynamic contrast-enhanced MRI sequence is acquired before, during, and post-injection of intravenous gadolinium-based contrast media, followed by swift, three-dimensional, T1-Weighted sequences sensitive in detecting the contrast agent's arrival in the tumor. This sequence achieves its peak utility when T2W and DWI are equivocal. Potent early enhancement or rapid contrast media washout from the targeted lesion heightens malignancy suspicions (70). For image acquisition, the application of an endorectal coil is non-mandatory; nonetheless, it is advantageous for local staging by facilitating higher resolution imaging and thus superior delineation of the prostate and seminal vesicles contours. It indeed proves its utility in determining extraprostatic extension (EPE) and seminal vesicle invasion, tumor volume, and tumor laterality (71). After obtaining the prostate gland MRI sequences, imaging interpretation becomes necessary. The Likert scale was the inaugural reporting system developed, constituting a 5-point scale grounded in a radiologist’s subjective evaluation to assess a lesion's PCa likelihood. However, this was associated with a reliability and standardization deficit since it was primarily based on radiologists' familiarity with prostate mpMRI and their technical expertise (63). To circumvent these limitations and to facilitate simpler communication between radiologists and urologists, and to standardize how mpMRI findings are reported, the PI-RADS (Prostate Imaging Reporting And Data System) v1 was devised in 2012 (72). This employed a set of stringent criteria to allocate specific suspicion scores.

PI-RADS scoring relies on the study of mpMRI of the prostate, allocating a score from 1 to 5 to each lesion based on malignancy probability, where 1 denotes a most probable benign lesion while 5 is linked to a high malignancy risk:

- PI-RADS 1: very low (clinically significant cancer is highly improbable to be present);

- PI-RADS 2: low (clinically significant cancer is improbable to be present);

- PI-RADS 3: intermediate (the presence of clinically significant cancer is equivocal);

- PI-RADS 4: high (clinically significant cancer is likely to be present);

- PI-RADS 5: very high (clinically significant cancer is highly probable to be present).

In 2015, PI-RADS version 2 emerged to address some first version limitations. The most notable changes involved introducing a dominant sequence in different anatomical zones: DWI for the peripheral zone and T2-weighted for the transitional zone. In this version, DCE imaging's influence diminishes due to its less crucial role in the PCa diagnosis context (63,67). Dynamic contrast-enhanced is employed when the lesion remains indeterminate (63). In 2019, PI-RADS version 2.1 was developed to diminish the inter-reader variability of the preceding version, without altering the overall scope and principle of PI-RADS v2 (73) (**FIGURE 8**). Clinical indications for prostate mpMRI include detection and localization of primary PCa for MRI-targeted biopsy guidance, local staging, suspected PCa recurrence evaluation, active surveillance, and local treatment (e.g., surgery, radiation therapy, and focal therapy) (48,74,75). Multiparametric MRI stands as a pivotal diagnostic instrument, which should be applied as a triage test before biopsy as standard of care (76). However, several challenges exist to enable a globally high-quality system (77).

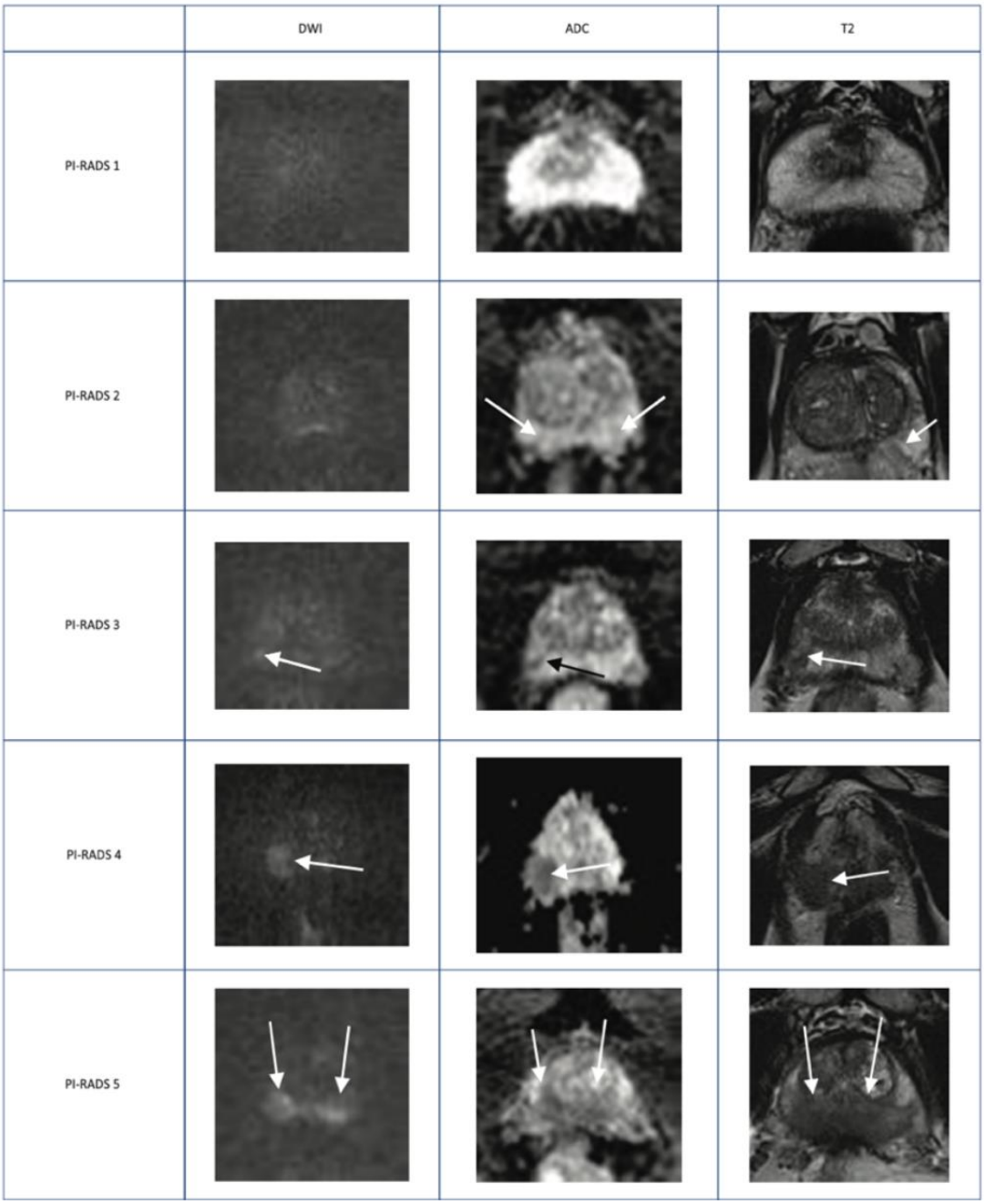

***Figure 8**. PI-RADS classification and mpMRI in prostate cancer; Scott R et al. SA J Radiol. 2021;25(1):2062.*

4.7.3 – Prostate biopsy: approach and techniques

Prostate cancer (PCa) diagnosis mandates a prostate biopsy since imaging alone doesn't suffice. Nonetheless, opting to proceed with a biopsy involves considering preceding test

results, such as PSA levels, DRE, TRUS, and potentially, MRI. Evaluating factors like age, possible co-morbidities, and the subsequent therapeutic interventions are crucial and should be deliberated in advance (78). Utilizing risk stratification can be an effective strategy to minimize unwarranted biopsies (79). An elevated PSA level shouldn't automatically prompt a prostate biopsy. In scenarios where a solitary PSA increase is observed, further PSA testing should be conducted in the ensuing weeks under consistent conditions in the same laboratory utilizing the same assay (e.g., avoiding ejaculation, manipulations, and urinary-tract infections) (80). Currently, the paradigm of care involves MRI-targeted biopsy along with concurrent random systematic biopsy. Although prostate biopsy can be carried out via the transrectal or transperineal method, the latter is favored due to its lower infection risks and enhanced sensitivity in detecting tumors, especially those positioned anteriorly (74,81–83). Over recent years, the significance of pre-biopsy mpMRI in the realm of PCa diagnosis has escalated. The PROMIS study explored whether employing mpMRI before prostate biopsies could prevent unnecessary biopsies for men with a clinical suspicion of PCa, while also enhancing the identification of clinically notable diseases. Within this multicenter trial, participants underwent 1.5 Tesla MRI, and men exhibiting signs of T4 disease or a prostate volume exceeding 100 mL were omitted. Prostates were categorized utilizing the Likert radiology reporting scale, a 5-point scale gauging the likelihood of harboring PCa. Both physicians and patients were blind to the mpMRI reports, and all men were subjected to a prostate biopsy. Simultaneous transperineal-template prostate mapping biopsy and subsequent TRUS biopsy were executed on the same day. The findings indicated that utilizing upfront mp-MRI in patients with unusual PSA and DRE could potentially preclude a primary biopsy for up to 27% of participants, diminish the diagnosis of non-clinically significant cancers by 5%, and if biopsies are directed by mpMRI findings, up to 18% more instances of clinically significant PCa might be identified compared to employing the standard TRUS-biopsy pathway alone (76). However, it's worth noting that while mpMRI exhibited higher sensitivity than TRUS-guided biopsy (87% vs 60%) and a superior NPV (72% vs 65%) for detecting grade group ≥ 2 (i.e., Gleason score PCa ≥3+4) or cancer core length ≥4 mm (76), its specificity and PPV were lower, indicating that mpMRI cannot singularly diagnose PCa. Thus, biopsy based on MRI findings remains imperative for identifying clinically significant PCa (csPCa).

Since PCa is recognized as a multifocal disease (84), a study by Stabile et al. suggested that discovering csPCa foci outside the lesion identified using mpMRI is linked to the PI-RADS score, posing a 70% risk in a lesion with a PI-RADS score of 5 (85). Consequently, amalgamating systematic and target biopsy is advised. For systematic cores, sampling should be bilateral from apex to base, as far posterior and lateral as feasible in the peripheral gland, independent of the technique used. A minimum of 8 systematic biopsies is recommended for prostates of approximately 30 cc (86), whereas 10 to 12 core biopsies are suggested for larger prostates (87). Pertaining to target biopsy, 3 to 5 cores should be extracted from each MRI-visible lesion, achievable through cognitive guidance, US/MRI fusion software, or direct in-bore guidance.

In instances where men have undergone a prior negative systematic biopsy, a prostate MRI should be offered, and if a lesion with a PIRADS exceeds 3, a repeat (targeted) biopsy is warranted. Additional scenarios prompting a repeat biopsy include:

- Elevating and/or persistently high PSA;

- DRE revealing suspicions, translating to a 5 to 30% PCa risk (88);

- Intraductal carcinoma as an isolated discovery, associated with a > 90% risk of concurrent high-grade PCa (89).

4.8 – Staging

The data procured from staging play a pivotal role in ascertaining the disease's scope, which, in turn, influences both prognosis and subsequent treatment strategies. The TNM (tumor, node, metastasis) system, crafted by the International Union Against Cancer alongside the American Joint Committee on Cancer (AJCC), is a prevalently utilized staging methodology. This anatomically oriented system scrutinizes the tumor, evaluating it based on the proliferation and invasion of the principal tumor lesion (T1-4, where an elevated number signifies a more substantial tumor size), nodal involvement acknowledgment (N0 and N1, signifying the absence and presence of involved nodes, respectively), and acknowledgment of metastatic disease (M0 and M1, signifying the

absence and presence of metastases, respectively). Subsequent to evaluating each T, N, and M score (inclusive of the tumor histologic grade G), a concluding stage is derived, typically expressed through Roman numerals ranging from I to IV.

4.8.1 – T staging

Pathologically, extraprostatic extension is identified as the intertwining of carcinoma cells with periprostatic fatty tissue, or tissue that expands beyond the prostate gland (e.g., the neurovascular bundle, anterior prostate, or bladder neck), aligning with stage T3a. This is distinct from seminal vesicle invasion (SVI), which aligns with stage T3b. Various methodologies like imaging, physical examination, and biopsy data can provide insights into T-staging:

- Assessment via DRE: The initial assessment level pertains to the local tumor stage, as the differentiation between organ-confined (T1/T2) and extraprostatic (T3/T4) disease has a significant impact on shaping the treatment plan. Despite its correlation with tumor stage in less than 50% of instances (90), DRE frequently undervalues tumor extension.

- PSA levels: Although PSA levels in serum augment according to tumor stage, their efficacy is curtailed in forecasting the final pathological stage (91).

- Biopsy insight: The percentage of malignant tissue robustly predicts positive surgical margins, SVI, and non-organ-confined disease (92). An escalation in tumor-positive biopsies independently predicts extracapsular extension (ECE), margin involvement, and LNI (93), with serum PSA, GS, and T-stage jointly offering more predictive power for the final pathological stage than when utilized independently (92,94).

- TRUS limitations: The transrectal ultrasound is no longer recommended due to its suboptimal accuracy in predicting organ-confined disease (95).

- mpMRI utility: While T2-weighted imaging retains the highest accuracy for local staging on mpMRI, at 1.5 Tesla, mpMRI displays commendable specificity yet limited sensitivity in identifying T3 stages (96). MpMRI, unable to detect microscopic ECE and its sensitivity escalating with the tumor's radial extension within periprostatic fat, may

enhance the prediction of the pathological stage when amalgamated with clinical data (97,98).

4.8.2 – N staging

Pelvic lymph nodes frequently serve as the initial metastatic destinations for PCa in patients recently diagnosed. Evaluation of LNI encompasses various imaging modalities:

- Utilization of CT and MRI: Abdominal CT scans and T1-T2 weighted MRIs inferentially evaluate nodal invasion through assessing LN diameter and form. However, the dimensions of non-metastatic lymph nodes can significantly fluctuate, potentially matching the size of nodal metastases. Commonly, lymph nodes exhibiting a short axis exceeding 8 mm within the pelvis and over 10 mm externally are deemed malignant. Diminishing these thresholds heightens sensitivity but curtails specificity, leaving an optimal size threshold indeterminate (99,100). CT and MRI exhibit under 40% sensitivity. CT detection rate for microscopic LNI dips below 1% in cases with ISUP grade below 4 cancer, PSA underneath 20 ng/mL, or confined disease (101,102). Despite its potential in identifying metastases within nodes of standard size, a negative DW-MRI does not unequivocally negate lymph nodal metastases existence, and DW-MRI marginally enhances nodal staging compared to traditional imaging (103).

- Choline PET/CT: The introduction of molecular imaging using prostate-specific tracers like Choline aims to augment sensitivity in preoperative detection of LNI. A meta-analysis encompassing 609 patients revealed choline PET/CT's pooled sensitivity and specificity for pelvic lymph-nodal metastases to be 62% (95% CI: 51–66%) and 92% (95% CI: 89–94%), respectively (104). The sensitivity of choline PET/CT escalates to 71% amongst high- and very high-risk disease patients, outstripping contrast-enhanced CT in both instances (105). Nevertheless, due to its limited sensitivity, choline PET/CT hasn't achieved a clinically satisfactory diagnostic precision for lymph-nodal metastases detection, nor to confidently omit a nodal dissection based on risk factors or nomograms.

- PSMA-based PET/CT: Prostate-specific membrane antigen (PSMA) emerges as a pivotal target for molecular imaging amongst PCa patients. Various PSMA inhibitors

have been suggested for PET imaging, with most studies employing 68Ga or 18F labeling. PSMA-PET imaging has demonstrated superior diagnostic precision relative to conventional imaging for pre-treatment staging. While PSMA PET offers enhanced N-staging compared to MRI, abdominal contrast-enhanced CT, or choline PET/CT, diminutive nodal metastases might evade detection due to the spatial resolution constraints of PET (approx. 5 mm). Consequently, this imaging technique is not systematically endorsed to preclude pelvic lymph node dissection in the event of a negative PSMA-PET owing to its subpar sensitivity in lymph node metastasis detection upon diagnosis (106–109).

4.8.3 – M staging

Bone metastases predominantly appear in patients with PCa and evaluating the extent of these metastases is accomplished through various imaging methodologies:

- Bone Scans: Bone scans employing 99mTc are traditional yet highly sensitive imaging tools that assess the skeletal system for active bone formulation associated with both malignant and benign conditions. These scans are typically suggested for certain intermediate and high-risk patients at the initial diagnosis and should also be performed on patients exhibiting symptoms, without regard to PSA levels, ISUP grade, or clinical stage (110).

- Fluoride PET and PET/CT, Choline PET/CT, and MRI: Techniques using 18F-sodium fluoride (18F-NaF) PET or PET/CT, in a similar manner to bone scintigraphy, explore the existence of bone metastases. These tools exhibit comparable specificity but enhanced sensitivity relative to bone scintigraphy when identifying bone metastases in newly diagnosed high-risk PCa patients (111). Choline PET/CT also has the benefit of identifying visceral and nodal metastases. In high-risk PCa cases, Diffusion-weighted whole-body and axial skeleton MRI demonstrate greater sensitivity than bone scans and targeted conventional radiography in pinpointing bone metastases and also prove capable of detecting visceral and nodal metastases. Moreover, compared to a combined approach of bone scans, targeted radiography, and abdominopelvic CT, whole-body MRI demonstrates superior sensitivity and specificity (112). Meta-analysis indicates that on a

per-patient basis, whole-body MRI surpasses choline PET/CT and bone scans in sensitivity, while choline PET/CT maintains the highest specificity.

- PSMA-based PET/CT: A systematic review including 12 studies (n=322) indicated a significant variability in 68Ga-PSMA PET/CT sensitivity during initial staging (varying from 33–99%; median sensitivity during per-lesion analysis was 33–92%, and per-patient analysis was 66–91%), yet showcased robust specificity (per-lesion 82–100%, and per-patient 67–99%) (113). Most studies depicted elevated detection rates relative to traditional imaging models (bone scan and CT) (114). Owing to constrained evidence regarding the prognostic ramifications of implementing PSMA PET imaging in newly identified PCa, its habitual utilization is not yet recommended by clinical guidelines.

4.9 – Conservative Treatment

4.9.1 – Life expectancy in prostate cancer

When considering any proactive treatment for men with prostate cancer, a life expectancy exceeding 10 years is pivotal. Data reflecting survival for prostate cancer patients who forwent active treatment illustrate those rates of survival, specific to cancer, stand at 82-87%, 58-80%, and 32-57% at the 10, 15, and 20-year marks respectively, according to specific sources (115–118). The varied nature of these findings chiefly pertains to the divergent criteria for inclusion among studies, with some originating in the period prior to PSA testing. In the present day, the vast majority of prostate cancer diagnoses are identified in their localized stages, predominantly within ISUP grade groups 1-2. This effect of screening has plummeted the mortality rate from such latent forms of the disease to a mere 7% at 15 years (119). Consequently, conservative management emerges as the optimal strategy to sidestep the morbidity and mortality related to invasive treatments in patients whose life expectancy falls beneath 10 years, or those with a lengthier life expectancy desiring to postpone treatment-related side effects without hindering prolonged survival. Conservative management bifurcates into two separate strategies: i) watchful waiting; ii) active surveillance.

4.9.2 – Watchful waiting

Men who are evaluated as not fit for curative interventions often resort to an alternative approach. The diminished life expectancy nullifies any potential advantages from active treatments, subjecting patients solely to the potential adverse effects of suggested therapeutic strategies. Such patients are generally monitored until symptomatic of the disease, at which point palliative treatment, aimed at preserving a satisfactory quality of life, is administered correlating with their symptoms. Three substantial prospective phase three studies have juxtaposed watchful waiting with active treatments for prostate cancer patients. The SPCG-4 study in Sweden (49), undertaken before the PSA era, randomized 695 men to watchful waiting or radical prostatectomy, revealing a benefit in radical prostatectomy, which only became evident following a decade of monitoring. It supports advocating watchful waiting for those with a more limited life expectancy. In a parallel manner, the PIVOT trial (120) – contrasting radical prostatectomy and watchful waiting in 731 men and executed in the early PSA era – identified minimal to no benefit for radical prostatectomy following over 15 years post-randomization (median follow-up 18.6 years). The VACURG study (121), the smallest of the trio, found no survival advantage for radical prostatectomy after a 15-year observational period, having randomized 111 men to either radical prostatectomy or watchful waiting in the pre-PSA era. A meta-analysis by Cochrane (122), which amalgamated the results of these three pivotal trials, demonstrated that compared to watchful waiting, radical prostatectomy was linked with decreased overall mortality (Hazard ratio: 0.79; 95% confidence interval: 0.70–0.90) and cancer-specific mortality (0.57; 0.44-0.73) over a 29-year follow-up period. It also exhibited a reduced risk of progression (0.43; 0.35-0.54) and metastatic disease (0.56; 0.46-0.70), yet it was allied with heightened instances of urinary incontinence (relative risk: 3.97; 95% confidence interval 2.34-6.74) and erectile dysfunction (2.67; 1.63-4.38) relative to no active intervention. In wrapping up, the advantages stemming from invasive treatment necessitate over a decade post-procedure to manifest. Thus, patients with life expectancies beneath this duration ought to be guided towards watchful waiting.

4.9.3 – Active Surveillance

Opting for this approach is viable for patients whose life expectancy exceeds 10 years and whose tumor characteristics permit a secure postponement of any invasive

procedures. In essence, patients are meticulously tracked to determine the precise moment for active intervention, should it become necessary. Active surveillance in patients involves rigorous monitoring through continual prostatic biopsies, PSA testing, clinical evaluations, and MRI scans to observe the disease's natural progression. Curative interventions are initiated once the tumor exhibits particular characteristics signaling a potential threat to life yet remains within the curable range, while also taking into account the individual's life expectancy. There exists no established randomized controlled trial that compares active surveillance with immediate curative treatments. Multiple cohort-based studies have explored active surveillance in patients with localized prostate cancer. A recent meta-analysis (123) disclosed that approximately one-third of men undergoing active surveillance experienced reclassification during monitoring, with the majority subsequently undergoing active treatment. The most extensive study within this meta-analysis, involving 1298 men with very-low-risk prostate cancer from the Johns Hopkins hospital (124), defined very low-risk disease by clinical stage T1c, PSA density below 0.15 ng/mL, biopsy ISUP grade group 1, two or fewer positive biopsy cores, and no more than 50% cancer involvement in any biopsy core. The surveillance protocol comprised PSA tests and digital rectal examinations semi-annually, coupled with an annual prostate biopsy. Curative intervention was advised if disease reclassification occurred, defined as biopsy results that no longer aligned with the inclusion criteria. The cohort's median follow-up was 5 years, with the cumulative incidence of grade reclassification standing at 26% at 10 years and 31% at 15 years. The cumulative incidence of curative intervention was 50% at 10 years and 57% at 15 years. In sum, this data endorses the implementation of active surveillance for patients with localized prostate cancer, intending to delay active treatments until disease progression is observed, should it transpire.

4.9.4 – The Protec-T trial

The Protec-T trial (51,125) stands out as the sole randomized phase three study contrasting active monitoring with active treatments in the aftermath of the PSA era. It investigated three strategies: radical prostatectomy, external beam radiotherapy, and active monitoring, the last of which is a median approach between active surveillance and watchful waiting. Active monitoring entailed a systematic subsequent biopsy for those

experiencing a PSA surge over 50% within a year. A majority of the patients, 56%, were identified with D'Amico low-risk disease, with breakdowns as follows: 90% had PSA levels below 10 ng/mL, 77% were ISUP grade 1 (with 20% being ISUP grade 2-3), and 76% were classified as T1c. Remaining patients demonstrated tumors categorized as D'Amico intermediate-risk disease. A decade-long follow-up revealed nearly identical cancer-specific survival (98.8% compared to 99%) and overall survival among patients undergoing active monitoring and those receiving invasive treatments. Nonetheless, active monitoring was correlated with an elevated metastatic progression at 6% versus 2.6%. The trial also assessed functional outcomes such as urinary continence, bowel, and erectile function (126). The radical prostatectomy group exhibited decreased sexual and urinary continence in the initial six months, in comparison to the other strategies. Despite some recovery, this group continued to show inferior functional results. Patients undergoing radiotherapy reported the poorest bowel function results in the initial six months. A gradual decline in sexual and urinary function was noted in the active-monitoring group. In aspects of anxiety, depression, and general or cancer-related quality of life markers, no notable disparities were observed among the three trial cohorts. Findings from this pivotal trial further accentuate the necessity of individualized treatment for patients with localized prostate cancer, asserting that active treatments ought to be designated for patients with clinically significant disease, recognizing that survival advantages might take over a decade to counterbalance detriments, while treatment-induced side effects commence instantly.

4.10 – Active Treatment

4.10.1 – Treatment for low-risk tumors

In conditions of low-risk, the primary challenge when determining the most optimal therapeutic strategy lies in avoiding overtreatment. Active surveillance emerges as the advised treatment choice within this category, as it adeptly equates oncological security with the side effects of treatment. Potential alternatives to active surveillance might encompass low-dose-rate brachytherapy or proactive treatments like radical prostatectomy and external beam radiotherapy, particularly for patients willing to

negotiate a balance between toxicity and halting disease progression. On the flip side, due to an absence of survival advantage over mere observation (127), hormonal therapy doesn't constitute a viable substitute for these patients. While active surveillance stands as the normative care in low-risk patients, randomized data affirming this treatment method is still pending publication. Various cohort studies on active surveillance have employed divergent definitions of low-risk disease and numerous surveillance tactics, making result comparisons across studies using existing literature a complex endeavor. Relying on the findings from a systematic review and meta-analysis (128), the EAU-EANM-ESTRO-ESUR-SIOG Prostate Cancer Guideline's multi-society panel crafted a consensus statement delineating the foremost active surveillance strategy for low-risk disease. With insights from the DETECTIVE Study (129), the panel pinpointed ISUP grade group 1, clinical stage cT1c or cT2a, PSA < 10 ng/mL, and PSA-Density < 0.15 ng/mL/cc as the most frequently utilized criteria for active surveillance (130). The panel also scrutinized the role of mp-MRI imaging for patients undergoing active surveillance. In this context, outcomes from The Active Surveillance Magnetic Resonance Imaging Study (ASIST) (131) indicated that employing MRI might curtail the risk of surveillance failure (19% vs. 35%, $p = 0.017$) relative to its non-use, and it also reduced the patient count progressing to ISUP grade group >2 (9.9% vs. 23%, $p = 0.048$) throughout observation. The DETECTIVE panel (129) unanimously agreed that to mitigate the risk of progression and failure during observation, MRI should be proposed to patients suitable for active surveillance. The panel also contemplated whole gland treatments (e.g., cryotherapy, high-intensity focused ultrasound) and focal treatments as alternative therapeutic options for low-risk tumors. They recommended that, due to the absence of compelling supporting evidence, these could be suggested but strictly within a clinical trial environment or a methodically structured prospective cohort study.

4.10.2 – Treatment for intermediate-risk tumors

Engaging in active treatments, such as radical prostatectomy or external beam radiation therapy paired with a brief phase of androgen deprivation therapy (ADT) (4-6 months), have been suggested as viable strategies for patients diagnosed with prostate cancer of intermediate risk, as established by randomized studies (51). An approach of vigilant observation has been explored for individuals with intermediate risk, especially those

keen to bypass immediate surgical or radiative procedures. The consensus panel from the DETECTIVE Study (128) endorsed a watchful waiting strategy for those in the intermediate-risk category who exhibit distinct attributes, such as minimally expansive ISUP grade group 2 tumors or an additional lone feature from the EAU intermediate-risk classification, excluding the occurrence of ISUP 3 disease. The SPCG-4 (49), PIVOT (50), and Protec-T (51) trials collectively substantiate the surgical method as a feasible alternative for intermediate-risk patients. However, the discernible survival advantages of opting for surgery were only apparent a decade post-enrollment in the studies, negating this alternative for individuals with a limited projected lifespan. Due to a not insignificant possibility of lymph node involvement in intermediate-risk individuals (3.7–20.1%) (132), an extended evaluation of the pelvic lymph nodes is advised, in alignment with clinical evaluation mechanisms (133). External beam radiation therapy (EBRT) also stands as an applicable choice for managing intermediate-risk prostate cancer (134–138). Two prevalent techniques of EBRT include intensity-modulated radiation therapy (IMRT) (139) and volumetric arc therapy (VMAT) with image-guided radiation therapy (IGRT) (140). Those eligible for hormone treatment may receive IMRT/VMAT (delivering 76–78 Gy, or moderate hypofractionation over 4 weeks with 20 doses of 60 Gy each, or over 6 weeks with 28 doses of 70 Gy each), supplemented with a concise phase of ADT (4–6 months) (141–143). While subsequent ADT has demonstrated superior results compared to pre-surgical or concurrent ADT (144), the variability among patient factors, scheduling, and hormone therapies in trials involving EBRT and various ADT methods means that ADT maintains its recommendation as a pre-treatment, concurrent, or subsequent intervention. For those who are disqualified for ADT (due to factors like heart issues or other health conditions) or those who refuse it (for reasons like maintaining sexual functionality), IMRT/VMAT (76–78 Gy) or a mix of IMRT/VMAT and internal radiation are the suggested therapies. For intermediate-risk patients, low-dose (145) or high-dose (146) brachytherapy boosts, coupled with IMRT/VMAT and IGRT, may be proposed. In this instance, a short course of ADT (4-6 months) is also recommended per EAU guidelines (147). The urinary function should be evaluated for all patients qualifying for low and high-dose brachytherapy boosts due to the heightened risk of extended (up to 5 years) genitourinary toxicity in comparison to solely using EBRT (148). Full-gland and localized therapies have been trialed with positive findings in

intermediate-risk prostate cancer patients (149). Nonetheless, the supporting evidence originates from non-standardized observational studies, so utilizing these alternate modalities should be restricted to experimental clinical settings (150). Lastly, hormone therapy, as a standalone treatment, was scrutinized in intermediate-risk prostate cancer patients. Insights, derived from the EORTC 30891 trial contrasting immediate and delayed ADT for patients with T0-4N0-2M0 disease, unveiled no associated survival advantages, concluding that hormone therapy isn't advisable in intermediate-risk patients, even if they are unfit for aggressive interventions (132).

4.10.3 – Treatment for high-risk tumors

In patients contending with high-risk prostate cancer, the advocated therapeutic avenues include radical prostatectomy accompanied by ePLND or EBRT paired with an extended regimen of ADT, spanning at least 2-3 years. Preoperatively, it should be communicated to these patients that radical prostatectomy might be one facet of a multi-faceted therapeutic approach, potentially encompassing EBRT and/or hormonal or systemic treatments. In this specific scenario, surgical intervention has been linked with prolonged survival in retrospective study series, showcasing a cancer-specific survival surpassing 60% at a 15-year marker (151). In instances of verified or a high propensity for cancer progression post-radical prostatectomy, consideration should be given to the implementation of hormonal therapy and/or EBRT (152,153). When managing high-risk patients, EBRT in isolation does not suffice to secure extended cancer management. A plethora of trials have revealed that a prolonged supplementary phase of ADT is imperative to amplify the impact of localized radiation (134). Extended supplementary ADT also proves to be more efficacious than a brief initial phase of ADT (135,154). In light of the pronounced risk of lymph node proliferation inherent to high-risk disease, the preventative radiation of the pelvic region has been a topic of substantial discourse. In this regard, a meticulously structured, albeit diminutive, randomized trial juxtaposed the impacts of radiation targeting solely the prostate versus entire pelvic radiotherapy in patients with cN0, high-risk prostate cancer. Outcomes related to metastasis-free survival (95.9% vs. 89.2%, hazard ratio: 0.35, $p = 0.01$) and disease-free survival (89.5% vs.77.2%, $p = 0.02$) tilted in favor of comprehensive pelvic radiotherapy. Nonetheless, such an approach was also correlated with a heightened incidence of late-stage

genitourinary toxicity (grade > 2, 17.7% vs. 7.5%, p = 0.02) (155). Brachytherapy boost can be integrated with EBRT plus ADT in the treatment strategy.

4.11 – Surgical Treatment

4.11.1 – Evolution of radical prostatectomy approaches

The primary objective of radical prostatectomy is to eliminate cancer while maintaining the functionality of the pelvic organs, specifically urinary and sexual functions. This surgical procedure aims to extract the prostate gland, its surrounding capsule, and the seminal vesicles. Depending on the case, this may or may not include conserving the neurovascular bundle, which is then followed by a vesico-urethral linkage. Historically, the method of radical prostatectomy has seen various developments since its first open approach by Hugh Hampton Young in 1904. Young's approach was through the perineum but had the drawback of limited access to pelvic lymph nodes. It wasn't until 1982 that Patrick Wash introduced a technique through the retropubic or suprapubic space (123). This method made accessing the pelvic lymph nodes easier during prostate removal. Additionally, it included an anatomical representation of the neurovascular bundles, focusing on the preservation of the cavernosal nerves, which would potentially lead to quicker post-operative recovery of sexual functions. The retropubic approach soon became the preferred method for prostate cancer surgery. Over subsequent decades, the procedure was refined to decrease potential complications and enhance functional results, including urinary control and sexual performance. In 1997, the medical community saw the introduction of the minimally invasive laparoscopic radical prostatectomy by Schuessler (156) and later by Guillonneau (157), with both methodologies adhering to Walsh's retropubic fundamentals. Fast forward to 2002, and the world witnessed Binder's pioneering work (158) with the da Vinci Surgical System® for robot-assisted radical prostatectomy (RARP). This innovative technology combined the benefits of laparoscopic surgery with enhanced comfort for surgeons, particularly during vesico-urethral stitching. Presently, RARP surpasses the traditional open approach in popularity when treating prostate cancer, assuming both techniques are accessible (159). Its widespread acceptance is partly due to extensive training programs that hasten

proficiency (160,161). Furthermore, studies have shown RARP to be on par with the open method concerning surgical and cancer-related results. A pivotal study that solidified this equivalence involved 326 participants who underwent either the open or robotic method. Updated findings from this study after two years indicated that while both methods yielded similar cancer and functional outcomes (162), the robotic approach had advantages like shorter hospitalization durations and lesser blood loss.

4.11.2 – Techniques for robot-assisted radical prostatectomy

There are two primary variations of the RARP surgical procedure: the extraperitoneal and transperitoneal approaches (163). The extraperitoneal technique initiates by establishing a space between the rectus abdominis and its rear fascia. The posterior fascia is then cut open to access the extraperitoneal space, wherein a balloon is inflated to create the Retzius space (164). Conversely, in the transperitoneal method, insertion points are situated within the peritoneal cavity. This approach has two sub-variations: the anterior and posterior paths. In the posterior path (165), an incision is made at the lower peritoneal fold, leading to the identification and cutting of the vasa deferens, freeing of the seminal vesicles, and marking the base of the prostate. This dissection proceeds with the cutting of the Denonvilliers fascia, tracing the prostate's posterior side from its base to the tip. The next phase starts with the incision of the side peritoneum, freeing the bladder. The Retzius space is then fashioned by removing the surrounding fatty tissue. The prostate is separated from the bladder with efforts to conserve the bladder neck. With the prostate now separated from the incised Denonvilliers fascia, its lateral areas are dissected down to the tip. Finally, the prostatic supports and the primary venous complex are tied, and the urethra is severed. In the anterior approach (166), the dissection begins with a lateral incision to the lateral umbilical ligaments. After freeing the bladder and forming the Retzius space, the decision is made to either conserve or remove the bladder neck. Then, dissection proceeds posteriorly. The retrotrigonal space is crafted to pinpoint the seminal vesicles and vasa deferens. The remaining steps mirror those of the posterior approach. In either method, the neurovascular bundles can be wholly preserved (intrafascial), partially (interfascial), or fully dissected (extra-fascial) (167). After prostate extraction, the lower urinary tract's continuity is restored by linking the bladder neck with the

membranous urethra. This connection aims for a seamless, watertight, accurately aligned, and obstruction-free linkage while maintaining the inherent sphincter mechanism. For this bladder-urethral linkage, both open and robot-aided techniques vary. The open method employs a straightforward technique, using six separate stitches placed in a circular pattern for a primary end-to-end bond between the bladder neck and membranous urethra. In contrast, the robotic technique favors a one-way barbed stitch method using continuous stitching (168). Nevertheless, various other methods for this anastomosis exist, and current research does not particularly favor one technique over another.

4.12 – Pelvic lymph node dissection

Regional lymph nodes are the typical sites for initial spread in prostate cancer (169). In fact, over 30% of men with high-risk prostate cancer undergoing radical prostatectomy and PLND might have lymph node metastases (170). The number of these metastases and their overall impact are influenced by tumor traits and the extent of the PLND (171–176). A broader PLND template increases the likelihood of detecting these metastases, as the spread of the disease doesn't adhere to a fixed route (177). Interestingly, some patients might have micrometastases in distant lymph nodes like the common iliac or sacral, even when closer nodes, such as the obturator or external iliac, remain unaffected (178). This pattern brings up the challenge of determining the most effective PLND template for patients with intermediate or high-risk prostate cancer. Authors have different viewpoints on defining limited and extended PLND. For instance, Touijer and colleagues (179) define limited PLND as removal of just external iliac nodes, while Lestingi's team (180) defines it as the removal of only obturator nodes. The definitions of extended PLND vary even more. Some researchers include obturator, external iliac, and hypogastric nodes (173,179). Others also consider pre-sacral nodes, and yet others extend it up to the common iliac nodes at the ureteric crossing (172,174,180,181). With an even broader scope, some have proposed "super extended PLND", which involves removal up to the aortic and caval bifurcation (182). While lymph node removal can offer valuable staging information, its clear survival advantage remains ambiguous. Two distinct studies didn't show a significant advantage of extended PLND over limited PLND in early cancer outcomes (170,183). Furthermore, while PLND provides the most accurate staging for

localized prostate cancer, it isn't free from potential complications. These complications can significantly escalate the risks associated with radical prostatectomy. A comprehensive review analyzed the repercussions of PLND on perioperative complications in patients undergoing radical prostatectomy (184). This research included 84 studies encompassing over 28,000 patients. Complications were divided into two groups (intraoperative and postoperative) and further classified based on their likelihood of being linked to PLND. For intraoperative complications, issues like external iliac artery injury, internal iliac vein injury, and obturator nerve injury were considered strongly related to PLND. On the other hand, postoperative issues like lymphatic fistula, chronic lymphedema, and lymphocele were also strongly linked to PLND. The study found that intraoperative complications related to PLND occurred in 1.8% of patients, while postoperative complications were found in 14.1%, with lymphocele being the most reported. In defining PLND templates, limited PLND was described as only including obturator nodes, standard as involving obturator and external iliac nodes, extended as including obturator, external, and internal iliac nodes, and super-extended as even more extensive. This meta-analysis indicated that more limited PLND procedures posed lower risks for various complications compared to broader templates. The meta-analysis, however, didn't account for the only two randomized trials on PLND (175). In one of these trials, complications were comparable between limited and extended PLND templates.

4.13 – Selecting candidates for PLND

4.13.1 – Incidence of Lymph Node Involvement according to the D'Amico Risk Group Classification

The occurrence of lymph node involvement (LNI) in alignment with the D'Amico risk group categorization is as follows: In real-world data, the prevalence of lymph node metastases among patients with D'Amico low-risk prostate cancer ranges from 0.5% to 0.7% (170,184). As for D'Amico intermediate-risk patients, the risk of harboring positive nodes varies significantly, spanning from 3.7% to 20.1% (132). Conversely, D'Amico high-risk patients exhibit the highest likelihood of lymph node invasion (LNI), with

reported percentages ranging from 10% to 57% (185) or even reaching 100% in specific sub-categories of this group (186). In light of these statistics, the guidelines provided by the European Association of Urology (EAU) recommend against performing pelvic lymph node dissection (PLND) in cases of low-risk patients when radical prostatectomy is undertaken. Conversely, the guidelines recommend extended pelvic lymph node dissection (ePLND) in instances involving D'Amico high-risk patients to ensure an accurate assessment of tumor staging. The intermediate-risk category poses a more nuanced challenge, where the risk of LNI does not invariably justify the aggressiveness of ePLND. Therefore, for this group of patients, research has explored non-invasive diagnostic modalities to aid in the decision-making process concerning whether to perform or forego ePLND.

4.13.2 – Predicting accuracy of available diagnostic imaging tools

Standard imaging methods like abdominal CT scans and T1-T2 weighted MRI scans have shown limited diagnostic accuracy. These diagnostic techniques evaluate the condition of regional lymph nodes based on their size and shape. However, the size of non-metastatic lymph nodes can vary significantly, sometimes overlapping with the size of metastatic nodes. Combining data from various sources revealed that CT and MRI had a sensitivity for detecting lymph node metastases as low as 40% (187,188). Specifically, CT scans had a less than 1% capacity to detect microscopic LNI in patients with ISUP grade group less than 4, PSA less than 20 ng/mL, or localized disease (189,190). Consequently, the EAU guidelines do not recommend using CT or MRI scans for preoperative assessment of lymph node metastases in patients with intermediate-risk prostate cancer. Whole-body PET/CT with 11C- and 18F-labeled choline has been suggested as an alternative to conventional imaging methods for prostate cancer staging. In a meta-analysis of 609 patients, 11C- and 18F-choline PET/CT exhibited a combined sensitivity of 62% and specificity of 92% for pelvic lymph node metastases (191). However, the accuracy of choline PET/CT is significantly influenced by the characteristics of the primary tumor, being more reliable for locally advanced disease but less sensitive in localized tumors. In a prospective study involving 75 patients with intermediate-risk disease, 11C-choline PET/CT had a sensitivity of only 8.2% in region-

based analysis and 18.9% in patient-based analysis, making it unsuitable for clinical use in intermediate-risk disease (192). More recently, PSMA PET/CT has emerged as a potential game-changer in managing prostate cancer. Its applicability has been examined in primary prostate cancer staging. In a prospective, multi-center study, the use of 68Ga-PSMA PET/CT in newly diagnosed prostate cancer patients demonstrated a per-patient-based sensitivity of 41.5% and specificity of 90.9% (193). Likewise, another multi-center prospective trial reported a sensitivity of 41.2% for assessing lymph node metastases with 18fluorine-labeled PSMA PET/CT scans in newly diagnosed prostate cancer (194). A comprehensive review and meta-analysis, encompassing 37 articles, evaluated the sensitivity and specificity of preoperative PSMA PET/CT in patients with prostate cancer who subsequently underwent radical prostatectomy with ePLND (114). In this analysis, the per-patient-based sensitivity and specificity were found to be 77% and 97%, respectively. The per-lesion-based sensitivity and specificity were 75% and 99%. These preliminary findings suggest that PSMA-based PET/CT imaging is not yet ready to replace diagnostic extended PLND but holds significant promise for this purpose. Until the reliability of PSMA-based PET/CT or other potential alternatives is confirmed, the decision to perform or avoid ePLND in prostate cancer is based on the calculated risk of lymph node metastasis derived from clinical features, also known as the risk of LNI. This risk is assessed using preoperative tumor characteristics obtained from physical examinations, blood tests, and prostate biopsies.

4.13.3 – Preoperative risk tools predicting lymph nodal invasion

Among the various risk assessment tools, the EAU guidelines suggest the utilization of the Roach formula, the Briganti nomogram, the Partin tables, and the MSKCC nomogram. In contrast to alternative risk assessment tools, these four have been validated in numerous patient cohorts (195–198), affirming their ability to predict and distinguish between patients for whom ePLND is recommended and those for whom it might be avoided. The Roach formula computes the risk of LNI by employing the following equation: LNI = 2/3(PSA) + (Gleason score-6) x 10, where PSA is the pre-treatment PSA value, and the Gleason score is determined from the diagnostic systematic biopsy. The Partin tables employ a multivariable logistic regression, using known preoperative

predictors such as PSA, Gleason score, and clinical T stage to determine the risk of LNI. Briganti and the MSKCC are two nomograms that rely on patient and tumor characteristics to evaluate the risk of LNI. Initially, these nomograms were founded on preoperative PSA, systematic biopsy Gleason score, and clinical T stage to determine the risk of LNI (199,200). Over the past fifteen years, several updates to these nomograms have integrated new predictors, enhancing the accuracy of the models. The MSKCC nomogram, utilizing dynamic statistical formulas, draws upon data from over 10,000 prostate cancer patients treated at the Memorial Sloan Kettering Cancer Center. The updated predictors include age, PSA, biopsy Gleason grade group, and clinical T stage. The MSKCC nomogram is consistently updated and freely accessible on the MSKCC website (201). The initial version of the Briganti nomogram was introduced in 2007. It was generated from a cohort of 602 consecutive patients treated at a single Italian institution and included only three predictors: PSA, clinical T stage, and biopsy Gleason score. In 2012, this version was updated to include an additional predictor: the percentage of positive cores in systematic biopsy (202). In 2017, the third updated version of the Briganti nomogram was released (203). In this version, the number of predictors was expanded to five, encompassing PSA, clinical T stage, biopsy Gleason grade group, percentage of cores with the highest-grade prostate cancer, and percentage of cores with lower-grade disease. All these nomograms and predictive models were devised before the MRI era and relied on systematic random biopsy. A risk of LNI exceeding 5% was used as a criterion to select candidates for ePLND during radical prostatectomy. According to this threshold, the 2011 Briganti nomogram permits the avoidance of ePLND in more than 60% of men while missing LNI in only 1% of the population. Unfortunately, it remains suboptimal for two primary reasons: i) Sensitivity is high but not perfect, leading to the potential oversight of some nodal lesions with a 5% cutoff. ii) Specificity is low, resulting in roughly 80% of men with LNI risk above the 5% cutoff undergoing ePLND without nodal metastases. This latter concern is significant, as it exposes many men to unnecessary ePLND procedures, which are time-consuming and associated with possible complications. In recent times, mp-MRI has gained prominence in clinical practice. MRI can provide valuable information about intraprostatic tumor extension and significantly improve the accuracy of prostate biopsy guidance. In light of these developments, a new generation of predictive models has been formulated, incorporating mp-MRI into the

preoperative evaluation of patients with localized disease. The 2019 version of the Briganti nomogram (**FIGURE 9**) resulted from the integration of mp-MRI in determining LNI risk in patients eligible for radical prostatectomy (203). This updated model was developed using a multi-institutional cohort of 497 patients with prostate cancer diagnosed through MRI-targeted biopsies and treated with radical prostatectomy along with ePLND. The model included preoperative PSA, MRI-derived clinical T stage, the maximum diameter of the index lesion on the mpMRI, Gleason grade group determined from mpMRI-target biopsy, and the percentage of clinically significant prostate cancer on concurrent systematic biopsy. According to this new nomogram, a risk of up to 7% is deemed acceptable to spare patients from ePLND, resulting in only a 1.5% oversight of patients with nodal invasion. Indeed, the 7% cutoff from this MRI-based nomogram aligns with the 5% cutoff used in previous models developed in cohorts of patients diagnosed through systematic biopsy alone (203). More recently, the latest update of the 2019 Briganti nomogram aimed to recalibrate the nomograms in the light of the results of a preoperative PSMA PET. Specifically, Gandaglia et al. (204) demonstrated that the accuracy of the MSKCC and Briganti nomogram is substantially improved by the introduction of PSMA PET and, in particular, after a negative PSMA PET the recalibrated Briganti 2019 nomogram is able to spare approximately 50% of ePLND with risk of missing only 1.5% of LNI (**FIGURE 10**).

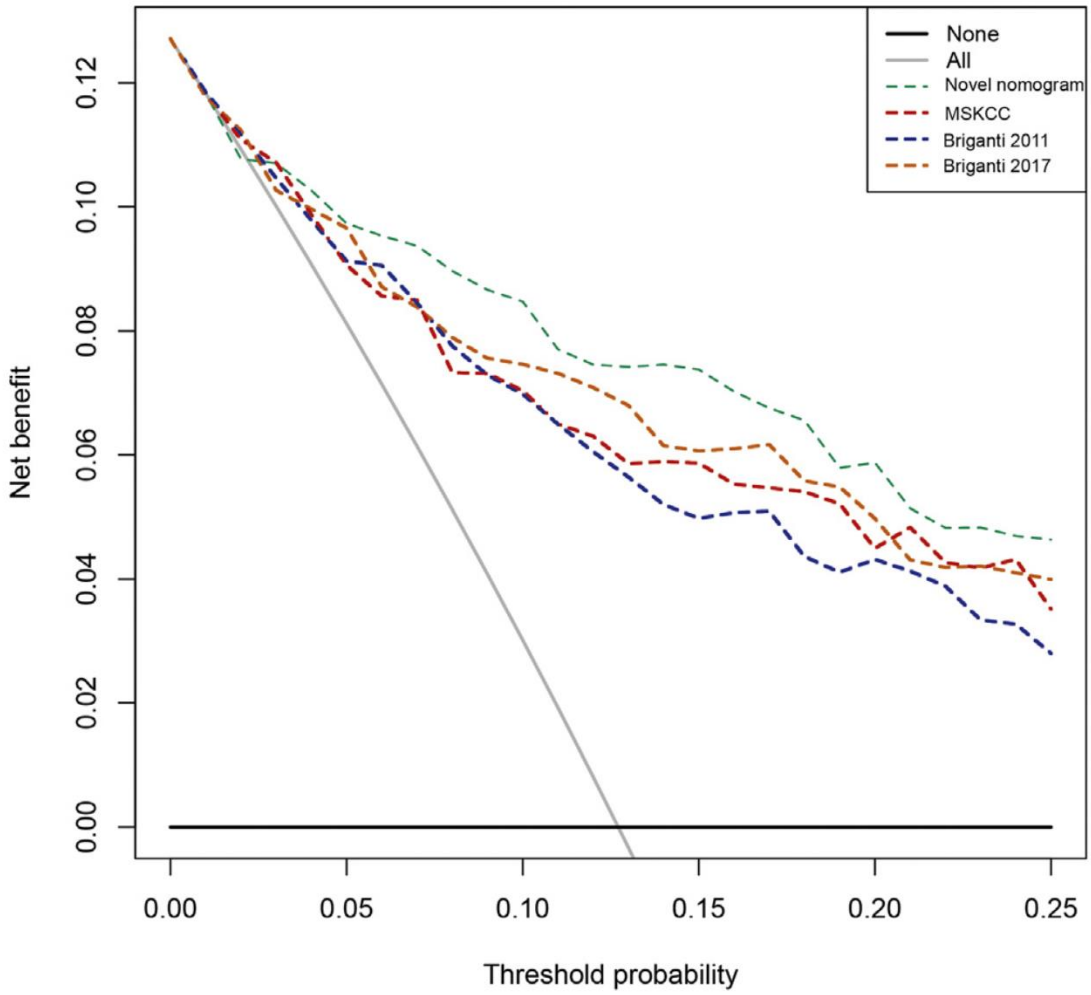

Figure 9. *Decision curve analysis demonstrating the net benefit associated with the use of the novel nomogram for detection of lymph node invasion in comparison to currently available tools (Briganti 2012, Briganti 2017 and MSKCC nomograms); (Reprinted from European Urology, Giorgio Gandaglia et al., "A Novel Nomogram to Identify Candidates for Extended Pelvic Lymph Node Dissection Among Patients with Clinically Localized Prostate Cancer Diagnosed with Magnetic Resonance Imaging-targeted and Systematic Biopsies", ©2019, with permission from Elsevier).*

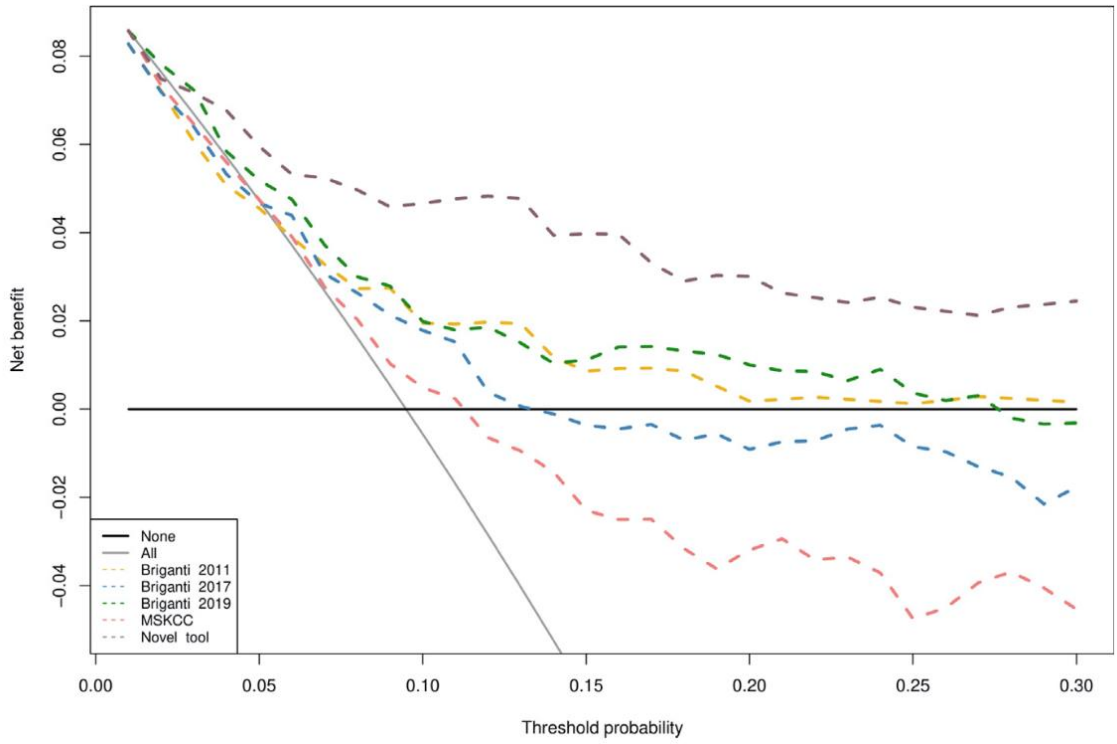

Figure 10. *Decision curve analysis demonstrating the net benefit associated with the use of the novel nomogram for prediction of lymph nodal invasion in comparison to currently available tools. (Reprinted from European Urology, Giorgio Gandaglia et al., "Identification of the Optimal Candidates for Nodal Staging with Extended Pelvic Lymph Node Dissection Among Prostate Cancer Patients Who Underwent Preoperative Prostate-specific Membrane Antigen Positron Emission Tomography. External Validation of the Memorial Sloan Kettering Cancer Center and Briganti Nomograms and Development of a Novel Tool", ©2023, with permission from Elsevier).*

4.14 – The role of PSMA in primary prostate cancer

In 1987, PSMA, a type II transmembrane glycoprotein demonstrating folate hydrolase and N-acetyl-alpha–linked acidic dipeptidase activities, was identified on the cell membrane of the LNCaP PCa cell line by Horoszewicz and team. PSMA is comprised of 750 amino acids, situated in three domains: the intracellular domain, which includes 19 amino acids; the transmembrane domain, comprising 24 amino acids; and the extracellular domain, encompassing 707 amino acids. Multiple antigenic epitopes capable

of binding to ligands within the intracellular and extracellular domains are distributed among them (205). PSMA is located on chromosome 11p11-12, coinciding with the area of the folate hydrolase gene (FOLH1), and lacks a natural ligand. This protein exhibits the enzymatic function of glutamate carboxypeptidase II (GCP-II) and is believed to play a part in the absorption of folate, as indicated by the FOLH1 gene (206,207). In non-prostatic tissues like the lacrimal gland, nervous system, duodenum, and typical prostatic tissues, PSMA expression is remarkably low. Conversely, its expression in PCa tissues escalates by 100–1000 times relative to normal tissues. Notably, expression levels are significantly elevated in poorly differentiated, metastatic, and castration-resistant tumor tissues, revealing PSMA's promising PCa tissue specificity and establishing it as a pivotal target for PCa diagnosis, staging, and treatment (208). Presently, PSMA can be targeted utilizing three primary types of ligands: monoclonal antibodies, aptamers, and small molecule inhibitors. Given that PSMA exhibits enzyme activities, small molecular inhibitors can selectively bind to the enzyme’s active sites, thereby competitively obstructing PSMA activity. Small molecule inhibitors, based on their structural traits, can be categorized into three groups: sulfur series compounds, phosphorus series compounds, and urea series compounds. Despite sulfur-containing compounds exhibiting favorable membrane permeability and oral bioavailability, their lack of specificity to PSMA and suboptimal stability have constrained their clinical use. Presently, phosphorus-containing compounds are undergoing preclinical testing due to their limited tumor uptake rate and relatively slow kinetics. Urea-containing compounds, created by connecting two amino acids via the urea group, display strong affinity and specificity to PSMA, rapidly internalizing into cells post-binding to active sites. Consequently, they are the most commonly utilized small molecule inhibitors in PCa diagnosis and treatment (209).

In 2008, the initial set of PSMA small molecule inhibitors (123I-MIP-1072 and 123I-MIP-1095) was launched for PCa clinical imaging (210). Their efficacy in tumor diagnosis and staging has catalyzed the advancement and clinical implementation of small molecule inhibitors. Currently, several small-molecule inhibitors targeting PSMA, like PSMA-I&T, PSMA-I&S, and PSMA-617, have been developed (211). Due to attributes such as low molecular weight, efficient tissue penetration, rapid blood clearance, and straightforward large-scale synthesis, small molecule inhibitors have emerged as the preferred option for molecular imaging and have found extensive use in

targeted therapy (101,212,213).

4.14.1 – PSMA PET in the local staging of prostate cancer

The established efficacy of PSMA PET in identifying tumor T stage in prostate cancer (PCa) remains unclear within this medical facility. An systematic review, encompassing 27 studies (with 4 utilizing PET/MRI and 23 applying PSMA PET/CT, accumulating a total of 1901 participating patients), revealed notable diagnostic precision of 68Ga-PSMA PET when used in tandem with MRI, exhibiting a combined diagnostic odds ratio natural logarithm for the detection of extracapsular extension (ECE) being 2.27 (95% CI 1.21–3.32) (214). On the other hand, for seminal vesicle invasion (SVI), it was recorded at 3.50 (95% CI 2.14–4.86). In the context of PET/CT, the figures stood at 2.45 (95% CI 0.75–4.14) and 2.94 (95% CI 2.26–3.63), respectively. Solely with 68Ga-PSMA PET/CT, the diagnostic precision for ECE was 2.45 (95% CI 0.75–4.14). Indicative results propose a diagnostic equivalency between PET/CT and PET/MRI, with extensive and intersecting ranges (214). To encapsulate, the discernible supplementary merit of PET for T staging (detecting extracapsular or SVI) remains ambiguous, as outcomes are predominantly swayed by the patient group chosen for these preliminary studies. Consequently, the contribution of a specialized PET tomograph remains indeterminate, warranting additional exploration.

4.14.2 – PSMA PET in the nodal staging of prostate cancer

Traditional imaging techniques, such as abdominal CT or MRI, tend to have a reduced capacity for identifying nodal metastases, a frequent site of metastasis, in patients recently diagnosed with PCa. The potential of PSMA imaging has gained attention, with new evidence suggesting its superior efficacy in comparison to CT or MRI, particularly in the context of recurrence (215). The ground-breaking proPSMA study offers a fresh perspective on staging for high-risk PCa patients (101). It stands as the inaugural multicenter, randomized study with two arms, evaluating whether PSMA PET has superior accuracy over traditional imaging or could potentially supplant it for initial staging in high-risk PCa patients. This investigation involved 302 high-risk participants,

with 152 undergoing the standard imaging protocol and 150 exclusively undergoing PSMA PET. The findings were cross-referenced with a combined benchmark that included histopathological, imaging, and lab data. About 30% of participants had metastatic conditions. PSMA PET outperformed traditional imaging with an accuracy of 92% compared to 65%, had an enhanced sensitivity of 85% versus 38%, influenced clinical choices more, at 28% versus 15%, and recorded fewer inconclusive results, 7% against 23%. The conclusion was that PSMA PET could potentially replace traditional imaging methods for staging high-risk individuals. Another research by Wondergem and colleagues evaluated 160 high-risk patients using an 18F-DCFPyL PSMA compound at the time of diagnosis. PSMA PET successfully identified 90% of the patients with local or distant metastasis. Almost all the patients (41 out of 42) who had positive CT results for at least one lymph node showed additional lymph node metastases on PSMA PET. PSMA PET changed clinical decisions for 17% of the subjects. Echoing the proPSMA study's conclusions, the researchers believed PSMA PET could be the primary imaging technique for high-risk PCa during initial diagnosis, eliminating the need for further staging procedures. Even though PSMA imaging is superior in nodal metastases detection compared to traditional methods, it isn't flawless. A prospective multicenter trial evaluated the precision of PSMA PET in identifying N1 status in 277 patients with intermediate or high risk (107). 27% of these patients were N1 according to histopathological data. In terms of detecting N1, PSMA PET had a sensitivity and specificity of just 40% and 95%. The somewhat limited sensitivity of PSMA imaging for LNI can be attributed to the PET's spatial resolution limitations, overlooking nodal metastases smaller than 3-5 mm. Larger nodes were indeed more sensitively detected by PSMA PET. Encouraging findings on PSMA imaging's superior sensitivity, in comparison to CT or bone scans, coupled with its clinical decision-making influence, have led to its extensive adoption for staging in newly diagnosed cases. Furthermore, a cost-benefit analysis based on the proPSMA study highlighted the enhanced precision, reduced costs, and lesser radiation exposure of PSMA PET over traditional imaging methods like CT and bone scans (108). Nonetheless, global clinical guidelines still refrain from endorsing this imaging technique as standard due to the absence of extended oncologic outcome data.

4.15 – PSMA radio-guided surgery

PSMA-ligand imaging, through advancements in radiochemistry and engineering, is now being explored in the context of PCa patients. One such innovation involves PSMA-guided radio-guided surgery (PSMA-RGS), which involves the preoperative injection of a PSMA-focused tracer followed by the use of specific gamma or beta probes during surgery to pinpoint sites of tracer uptake, facilitating comprehensive surgical excision (216,217). Modern research suggests that PSMA ligands, when labeled with gamma-emitting radionuclides such as 99mTechnetium (e.g., 99mTc-PSMA-I&S), can be leveraged for PSMA-RGS (218–220). This technique has the potential to enhance the surgical removal of metastatic tumors and detect micro-metastatic diseases that might go unnoticed by pre-surgical imaging (218–220). In typical procedures, a radionuclide-labeled PSMA-targeting ligand is introduced intravenously before surgery, and a probe detects gamma photons to locate lesions. Afterward, remaining cancerous tissue and associated lymph nodes are excised with the probe's guidance. Photons have high tissue penetration, leading to high sensitivity. Historically, the photon-emitting radionuclide 111In was the original choice for RGS research. In 2014, the Technical University of Munich first utilized 111In-PSMA-I&T RGS (111In-PSMA-RGS) for a patient, revealing its efficacy in locating metastatic sites during surgery (221). A study analyzing 31 patients showcased the potential of 111In-PSMA-RGS in recurrent cases, comparing intraoperative probe results with pathological analyses. Of these, 30 had PET-positive metastases identified via 111In-PSMA-RGS, and three had additional positive specimens. The method's sensitivity, specificity, and accuracy were 92.3%, 93.5%, and 93.1% respectively. However, drawbacks like unsuitable nuclear properties, high costs, and limited availability of 111In restricted 111In-PSMA-I&T's everyday clinical application. To counter these limitations, researchers developed 99mTc-labeled molecular probes for RGS (216). 99mTc, in comparison to 111In, is more affordable, widely available, and presents a lower radiation risk due to its lower energy and shorter half-life. The first PCa patient treated with 99mTc-PSMA-I&S RGS saw all SPECT/CT-detected suspected lesions exhibiting high 99mTc-PSMA-I&S uptake, facilitating successful intraoperative detection and removal (216). As recurrent PCa treatment advances, especially with the emergence of PSMA-ligand PET, targeted therapeutic approaches like salvage lymph node dissection are gaining traction for those with minimal recurrent disease (222).

However, intraoperative metastatic site detection remains a challenge. PSMA-RGS introduction has augmented surgical precision and enhanced metastatic lymph node removal capabilities. Initial clinical data attests to PSMA-RGS's safety, feasibility, and efficacy in patients with recurrent PCa post-primary treatments (218,223–225). A retrospective study involving 31 recurrent PCa patients treated with 99mTc-PSMA-RGS found that all PSMA-PET indicated lesions were excised, and metastases as small as 3 mm were discovered in two individuals (218,225). Additionally, 13 had no biochemical recurrence after an average of 13.8 months post-operation, and 20 required no further treatment after about 12.2 months. Comparing intraoperative measurements with pathological findings, 99mTc-PSMA-RGS showed a sensitivity, specificity, and accuracy of 84%, 100%, and 93% respectively. Another prospective research assessed 99mTc-PSMA-RGS's effectiveness against traditional salvage LND (225). Of the 42 participants, 29 underwent the standard procedure, while 13 experienced 99mTc-PSMA-RGS. Pathological results indicated that 99mTc-PSMA-RGS achieved superior results. The potential of PSMA-RGS is evident, but its long-term outcomes remain to be seen. Additionally, data supporting its role in primary settings or its feasibility with robot-assisted techniques remains scarce, with the most substantial study covering just 12 patients (219,220,226).

4.16 – Implication of PSMA expression and imaging accuracy

Most of the available evidences in the literature have shown that PSMA PET, despite having very high specificity, is characterized by sub-optimal sensitivity (227). One of the factors associated with reduced ability to detect nodal metastases is the metastatic size, since it has been shown that metastases smaller than 5 and 3mm are rarely detected by PSMA PET (228). However, this factor was not the only one associated with reduce uptake. In fact, among the potential additional confounders, PSMA expression level can indeed affect imaging accuracy. Several factors influence the probability of positive results in PSMA-PET/CT scans, leading to the development of various predictive models to identify patients who might benefit most from this imaging technique (229–231). However, immunohistochemistry studies have revealed that PSMA expression varies widely in both primary and metastatic tumors (232). It's also noteworthy that

approximately 10% of cases exhibit low or no PSMA expression (233–235). Notably, in these cases, a significant number of patients with diminished or absent PSMA expression tend to display infiltrative growth patterns. Furthermore, increased PSMA expression and heterogeneity has been showed to be associated with higher tumor Gleason Score (GS) and progression of PCa (236). This situation is often linked to a rise in DNA repair mutations and the emergence of hormone-resistant forms of PCa (237,238). In this context, it has been shown that the down-regulation of PSMA expression can be associated hyperexpression of SOX-2 which may also favour emerging endocrine resistance and luminal to basal transition with consequent reduction of the androgen-receptor expression (236,239).

5. Aim of the study

The presence of metastasis in lymph nodes represents an unfavorable prognostic factor, linked to an elevated risk of prostate cancer recurrence and reduced long-term survival (240). Managing individuals with lymph node involvement (LNI) necessitates the implementation of post-operative treatments, such as androgen deprivation therapy (ADT) and/or radiotherapy, which have demonstrated efficacy in enhancing the survival of these patients (241). Consequently, the pathological assessment of LNI assumes a critical role in treatment planning and post-surgical monitoring. However, an accurate determination of the extent of LNI can only be accomplished after conducting an extended pelvic lymph node dissection (PLND). Nevertheless, it is essential to acknowledge that extended PLND is not without its share of complications (170), and therefore, it should be reserved for patients with a higher likelihood of harboring LNI. In order to strike a balance between the advantages of more precise disease staging and the potential adverse effects associated with this surgical approach, concerted efforts should be undertaken to optimize detection of positive nodal metastases, while reducing the LND extent if possible. To achieve this goal, PSMA-based intraoperative guidance may represent an innovative option which can optimize the balance between benefits and harms of LND. Based on this premise, we aimed to describe the clinical implementation of an intraoperative diagnostic tool that may enhance the capability to detect LNI in PCa patients undergoing RARP with an ePLND, and to evaluate the effectiveness of 99mTc-PSMA-I&S in this context, with a particular focus on determining the pathological, clinical and PSMA-related molecular factors that may influence its accuracy. To summarize, our goals were the following:

Specific aim 1: To provide an insight on the PSMA expression levels within prostate and nodal specimens of patients with pN1 disease, with a specific focus on those patients who had false negative findings at PSMA-RGS, in order to identify whether heterogeneity in expression patterns or reduced overall PSMA expression can influence reduced PSMA RGS accuracy. At the same time, expression patterns of androgen receptor and SOX-2 were also quantified and were correlated with PSMA expression.

Specific aim 2: To identify the optimal definition of positivity for intraoperative PSMA-RGS and to assess the diagnostic accuracy of 99mTc-PSMA-RGS in the identification of

LNI in men with intermediate or high-risk prostate cancer and to compare its predictive accuracy to preoperative 68Ga-PSMA PET/MRI and 99mTC SPECT/CT.

Specific aim 3: To assess whether 99mTc-PSMA-RGS would help in the identification of positive nodes outside the ePLND template which includes the internal and external iliac as well as the obturator lymphatic landing sites.

Specific aim 3: To confirm the safety and tolerability of intraoperative 99mTC-PSMA administration, as well as to proof the feasibility of this novel procedure in terms on peri- and postoperative outcomes.

6. Materials and Methods

6.1 – Cohort definition

6.1.1 – Patient selection and ethical approval

The study cohort included patients with a diagnosis of localized prostate cancer (cTanyN0M0 at conventional imaging) who are candidate to radical prostatectomy and extended PLND. All patients received treatment at the Unit of Urology, IRCCS Ospedale San Raffaele (Milan, Italy). This is part of a pre-planned analysis of a phase 2 single-institution, national, non-comparative, non-randomized, prospective study (NCT04832958) started in November 2020 which is currently enrolling PCa patients with no evidence of nodal or distant metastases (cN0cM0) at conventional imaging who are candidates for RARP with ePLND and have a risk of LNI >5% according to the Briganti nomogram. The inclusion and exclusion criteria are the following:

Inclusion criteria:

• Male patients
• Age between 18 and 80 years
• Biopsy proven PCa with a LNI risk >5% according to the Briganti nomogram
• Planned to receive a RARP with an ePLND
• Able to understand and willing to sign a written informed consent document

Exclusion criteria:

The participant may not enter the trial if any of the following apply:
• Receipt of neoadjuvant therapies
• Inability to complete the imaging examinations according to the prospective protocol
• Evidence of metastatic disease at conventional imaging before surgery
• Evidence of clinical lymphadenopathies at conventional imaging before surgery
• Life expectancy of less than 12 months
• Previous chemotherapy
• Previous brachytherapy or external beam radiotherapy
• Unstable cardiovascular disease

• Congestive Heart Failure
• Clinically significant hepatobiliary or renal disease
• History of significant central nervous system injuries within 6 months
• Any other significant disease or disorder which, in the opinion of the Investigator, may either put the participants at risk because of participation in the trial, or may influence the result of the trial, or the participant's ability to participate in the trial
• Medical history of allergic disease or reactions likely to be exacerbated by any of the components of the radiotracers (99mTc- PSMA-I&S and 68Ga-PSMA)
• Patients who received an experimental drug in the context of clinical trials within 30 days from the administration of the radiotracers in the current investigation or within 5 half-lives of the experimental drug itself.

The prospective trial was funded through a competitive grant by the Italian Ministry of Health (Giovani Ricercatori GR2018-12368369). The current pre-planned analysis aims at reporting the diagnostic accuracy, pathological analyses, safety and feasibility of 99mTc-PSMA-RGS after the first 40 cases (36-month milestone) and to explore the molecular PSMA expression patterns associated with the results. A total of 40 patients have been enrolled between June 2021 and July 2023. Among those, 30 patients underwent 99mTc-PSMA RGS with available pathologic and 30-day and 84-days follow-up information and represented the study cohort.

6.2 – Preoperative 68Ga-PSMA PET/MRI

According to study protocol, the week before surgery patients underwent a 68Ga-PSMA PET/MRI or PET/CT scan for preoperative staging. Simultaneous PET/MRI started 60 minutes after the administration of approximately 160MBq of PSMA with the following protocol: localizer MRI scans to define the number of table positions (PET-FOV) to acquire (4-min/table position); specific attenuation correction and anatomical localization MR sequences at each PET-FOV; pelvic multi-parametric MRI protocol according to European Society of Urogenital Radiology guidelines (77) (**FIGURE 11**). A positive 68Ga-PSMA PET/MRI was defined as the presence of any uptake at the level of the pelvic and/or retroperitoneal nodes. The results of this procedure did not change the initially planned treatment.

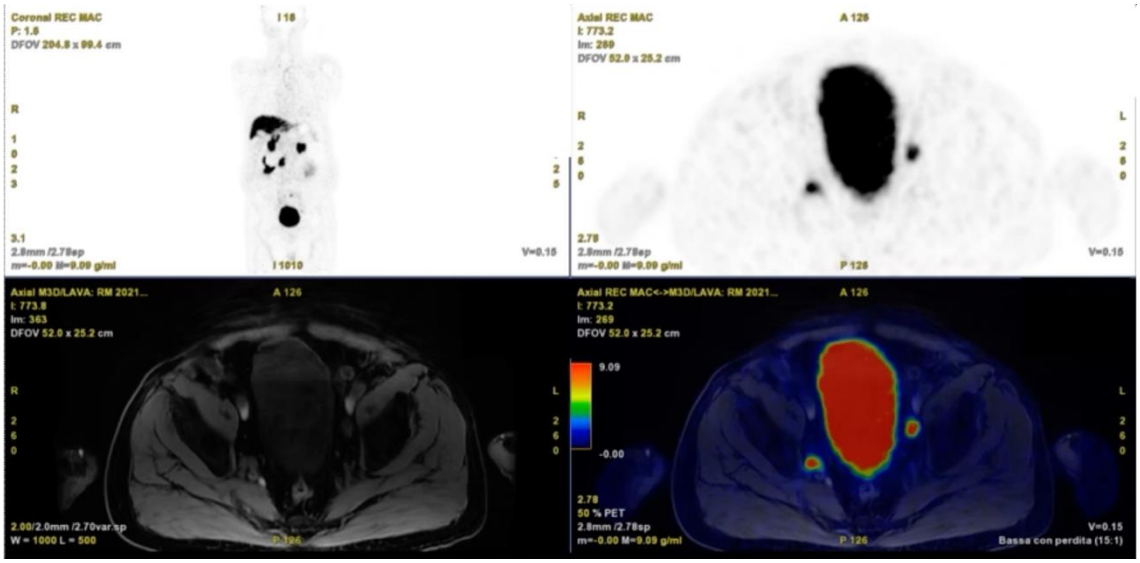

Figure 11. *Imaging report of 68Ga-PSMA PET/MRI with evidence of the level of obturator right and internal iliac left nodes.*

6.3 – Preparation of 99mTC-PSMA

The production process of the active ingredient consists of two phases that follow each other without isolation of the intermediate products and are:

1) synthesis phase which includes the reaction of the formation of the 99mTc-PSMA I&S complex (**FIGURE 12**)

2) purification phase which includes the separation of the active ingredient and its formulation.

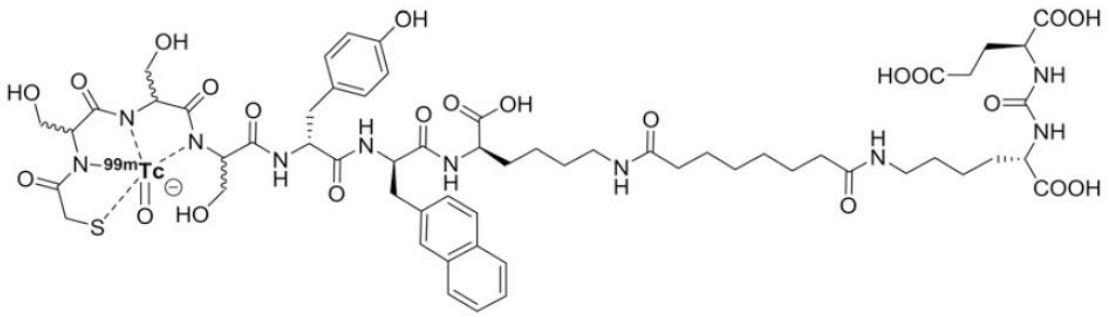

Figure 12. *Chemical structure of the 99mTc-PSMA I&S*

During the synthesis phase, the reaction vial is assembled with 40 µg of PSMA I&S /mannitol and 100 mg of sodium tartrate dissolved in 1 mL of 0.2M phosphate buffer pH7. To the mixture, 20 µL of a solution of tin chloride (2 mg/mL) and ascorbic acid (1.5 mg/mL) in 0.01 N HCl is added, and then, approximately 1 mL of [99mTc]NaTcO4 (about 2.5-3.6 GBq) is introduced. The reaction vial is transferred to a dry bath and heated to about 110°C for about 20 minutes, after which it is removed from the bath and left to cool to room temperature for about 10 minutes. The purification phase is carried out using solid-phase extraction on a Sep-Pak C-18 light cartridge (conditioned with 5 ml of 96% v/v EtOH and 5 ml 0.9% w/v NaCl) or equivalent. After loading the reaction mixture onto the cartridge, it is washed with 0.9% w/v NaCl to remove any impurities and then eluted with 2 mL of an EtOH solution (96% v/v)/0.9% w/v NaCl=1:1. The active ingredient is diluted with 8 ml of 0.9% w/v NaCl for the final formulation. The phosphate buffer and HCl solutions used in the synthesis process are filtered before use through a 0.22 µm filter. The following figure **(FIGURE 13)** describes the production process.

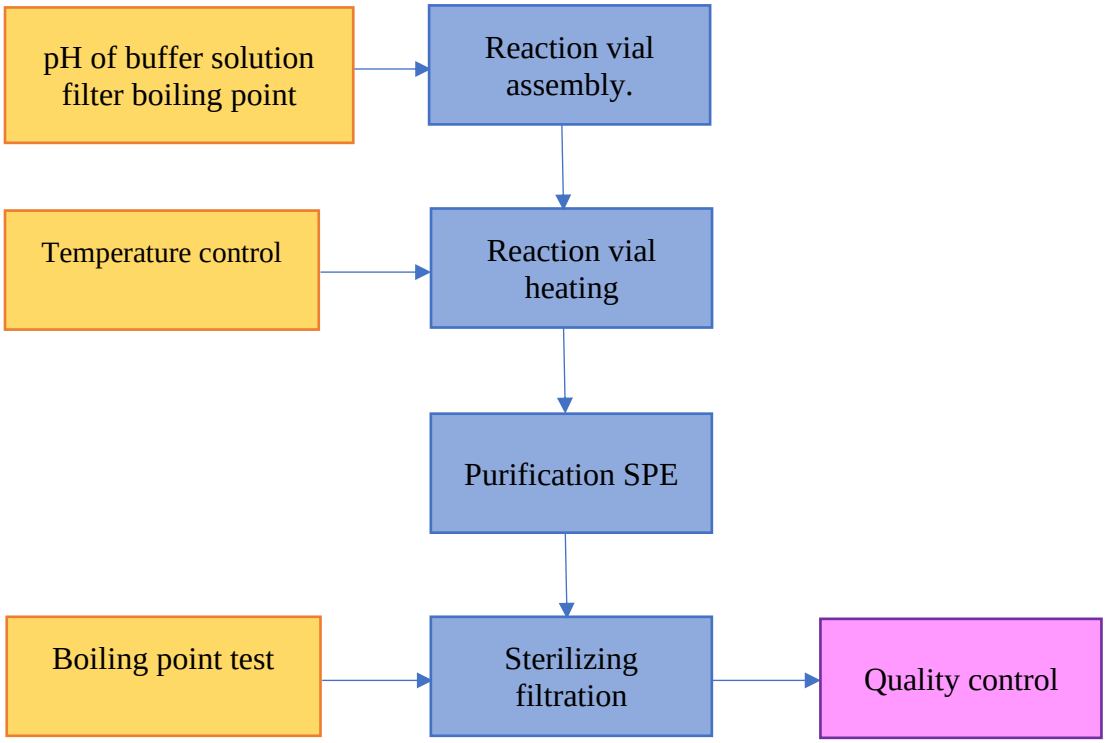

Figure 13. *Flow chart of the synthesis*

6.3.1 – Validation of the production process

Regarding the production of 99mTc-PSMA I&S, a validation was performed to demonstrate and document that the synthesis process consistently provides a product that meets predetermined specifications. The validation of the production process for the radiopharmaceutical 99mTc-PSMA I&S involves the synthesis of three production batches that must conform to the required specifications, described in the table below. The quality control tests are carried out on the finished product after sterilizing filtration since it is a continuous process that does not involve the isolation of the active ingredient. The validation tests are carried out under the same operational conditions established for the preparation process, with the same quantities of reagents and materials.

All the analyzed product batches were found to be in compliance with the required specifications, as summarized in **Table 1**.

Table 1. *Results of the validation test.*

Batch		TP15GIU20T	**Conform**	TP24GIU20T	**Conform**	TP30GIU20T	**Conform**
Aspect		Clear and colorless solution	Yes	Clear and colorless solution	Yes	Clear and colorless solution	Yes
Yield %		63.02	n.a	59.23	n.a	73.04	n.a
pH		6.6	Yes	6.2	Yes	6.7	Yes
Radiochemical purity	[^{99m}Tc]PSMA I&S	100	Yes	100	Yes	100	Yes
	[^{99m}Tc]$NaTcO_4$*	0.00%	Yes	0.00%	Yes	0.00%	Yes
	[^{99m}Tc] colloids^{+}	0.00%	Yes	0.00%	Yes	0.00%	Yes
Radioconcentration (MBq/mL)		210.5	Yes	202.2	Yes	197.2	Yes
Specific Radioactivity (MBq/nmol)		73.5	Yes	70.6	Yes	68.9	Yes

All documentation related to process validation, including complete batch records and raw data, is kept in the Nuclear Medicine department. The yield of the synthesis process is calculated as the activity obtained at the end of the process (Af) compared to the initial activity (Ai) measured using an activity calibrator:

Yield (%) = Af/Ai × 100

The activity calibrator (Actimeter) is subjected to quality checks following a protocol prepared according to the provisions in Annex A to the DM of the Ministry of Health of 29/12/97 (G.U. no. 108 of 12/5/98), which amended the DM 14/2/97 (G.U. no. 58 of 11/3/97), relating to article 113 of D.Lgs.230/95 and in annexes 1 and 2 to the DM of the Ministry of Health of 29/12/97 (G.U. no. 78 of 3/4/98), which amended the DM 14/02/97 (G.U. no. 58 of 11/3/97), relating to article 112 of D.Lgs. 230/95 (242–244). **Table 2** lists the parameters, acceptance limits, and frequency of checks.

Table 2. *Indication for routine quality control*

Controlled parameter	**Acceptability limits**	**Periodicity**
Accuracy	± 5% of the teoretical value	Every six-months
Linearity	± 5%	Yearly
Reproducibility	± 5%	At the utlization

6.4 – Surgical Technique

All surgeries were conducted via a transperitoneal approach utilizing the Da Vinci Xi robotic surgical system by three expert surgeons who followed a standardized procedure (A.B., G.G. and E.M.). Following the peritoneal incision, lateral release of the bladder to expose the endopelvic fascia, and the identification of the ureters, an autoclavable, commercially available Drop-In gamma probe with C.E. marking (Crystal Drop-In Probe; Crystal Photonics, Berlin, Germany) (**FIGURE 14**) was inserted through a 15-mm auxiliary port positioned above the right iliac crest. This gamma probe was employed for real-time intraoperative measurements to detect potential metastatic sites in the internal iliac, external iliac and obturatory regions. In case of suspicious preoperative imaging or in patients with very-high preoperative LNI risk (Briganti nomogram > 30%), intraoperative measurements using the Drop-In gamma probe was extended up to the common iliac (above the ureteric crossing), presacral, and retroperitoneal regions. Specifically designed for application in robot-assisted surgery, the Crystal Drop-In Probe features a 10-mm head, can be introduced through a 12 or 15 mm auxiliary trocar, and

can be autonomously manipulated and directed by the console surgeon using robotic ProGrasp forceps (223). A control unit provides both auditory and numerical feedback in response to 99mTc activity, aiding in intraoperative surgical guidance (**FIGURE 15**). As per-protocol indications, we initially defined a positive discovery as any lesion with a count rate at least twice that of the background reference, specifically, the fatty tissue covering the psoas muscle. Therefore, any positive lesions with a count rate exceeding double that of the background reference were surgically removed. However, as integral part of the current study, we explored additional definition of intraoperative positivity in order to optimize the diagnostic ability of RGS. After excision, ex-vivo gamma measurements were conducted to confirm the elimination of radioactive lesions or to prompt further investigation if a signal was absent. All excised tissues were categorized according to the anatomical site of removal. Subsequently, an anatomically defined extended pelvic lymph node dissection (ePLND) was carried out (245). This procedure included the excision of the lymph nodes and fibrofatty tissue along the external iliac vein, bounded laterally by the genitofemoral nerve and distally by the deep circumflex vein. Proximally, the cranial boundary was delineated by the point where the ureter intersects with the common iliac vessels. All fibrofatty tissue within the obturator fossa was meticulously extracted. The dissection was executed from the lateral aspect towards the medial region, extending up to the umbilical artery, with the bladder wall serving as the medial boundary. Lymph nodes situated along the internal iliac vessels and their medial and lateral aspects were excised. Following this ePLND, the RARP was concluded in accordance with a previously detailed technique (163).

Figure 14. *Standard set-up of the Crystal Probe within the operatory room. The flexible cable is sterilized after each utilization (on the left), while the connecting cable to the main case is reused and stored (on the right).*

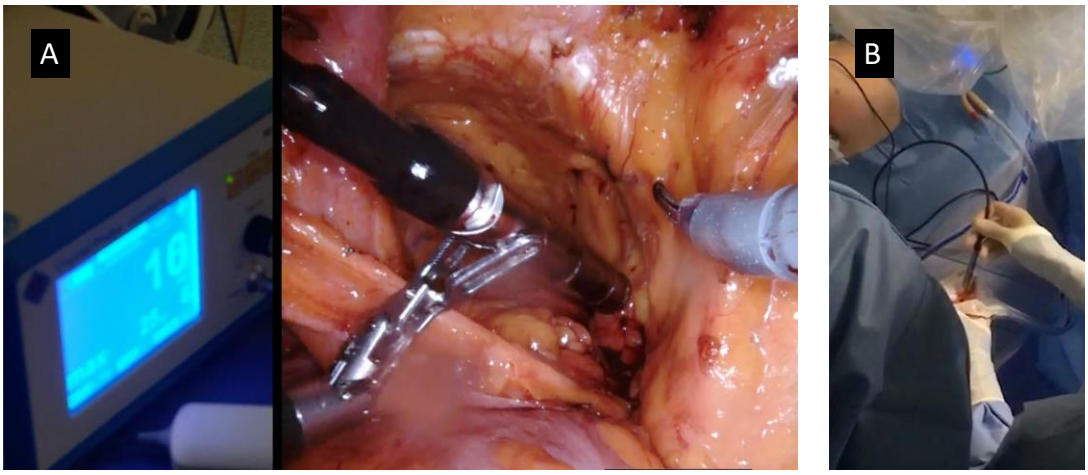

Figure 15. *Intraoperative use of gamma-probe with in-vivo evaluation during surgery*

and before starting pelvic lymph node dissection (Figure A) and ex-vivo evaluation at the table after lymph nodal removal (Figure B)

6.5 – Follow-up visits

The expected individual duration of the study is 16 weeks (follow-up at 4 and 12 weeks). The following data were collected during the follow-up visits (day 28 and day 84): vital signs; laboratory testing (absolute neutrophil count; platelets; haemoglobin; serum creatinine, serum PSA); adverse events. Additional perioperative data included: intraoperative complications; postoperative complications (according to the Clavien-Dindo system); operative time; blood loss; transfusions; length of stay; readmission (**Table 3; FIGURE 16**).

Table 3. *Protocol flow-chart*

Evaluation	Visit 1 (day -28)	Preoperative PSMA PET/MRI (day -7)	Hospitalization and Treatment Administration (day -1)	Surgery (day 0)	Visit 2 (day 28)	Visit 3 (day 84)
Patient Demography	X					
Inclusion/Exclusion Criteria	X					
Informed Consent	X					
Previous Medical/Surgical History (including the Charlson Comorbidity Index)	X					
Previous and concomitant medications	X					
Disease characteristics (namely, clinical stage, biopsy grade group, PSA at diagnosis)*	X					
Vital signs	X				X	X
Laboratory Testing	X		X		X	X
Serum PSA						X
Perioperative data including intraoperative complications, operative time, postoperative complications, length of stay					X	X
Pathologic report					X	
Procedures						
68Ga-PSMA PET/MRI		X				
Administration of 99mTc-PSMA-I&S			X			
99mTc-PSMA-I&S SPECT/CT imaging			X			
PSMA-RGS				X		
Safety						
AE /SAE recording (if any):		X	X	X	X	X

*Including the assessment of the risk of LNI calculated according to the Briganti nomogram

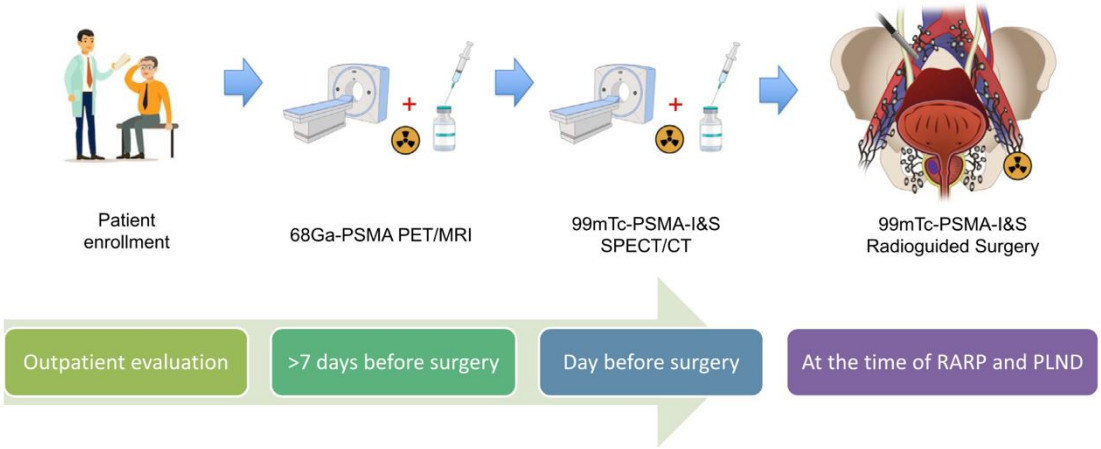

Figure 16*. Graphical representation of the protocol flow-chart. (Reprinted from European Urology, Giorgio Gandaglia et al., "Prostate-specific membrane antigen Radioguided Surgery to Detect Nodal Metastases in Primary Prostate Cancer Patients Undergoing Robot-assisted Radical Prostatectomy and Extended Pelvic Lymph Node Dissection: Results of a Planned Interim Analysis of a Prospective Phase 2 Study", ©2022, with permission from Elsevier)*

6.6 – Pathological analyses

6.6.1 Morphologic evaluation

Formalin-fixed, paraffin-embedded (FFPE) RARP specimens were retrieved for all patients included in the study and 2 μm hematoxylin and eosin (H&E)-stained sections will be evaluated. All pathological specimens of patients undergoing RARP were analysed by two board certified (R.L.; C.D.), experienced genito-urinary pathologists at IRCCS Ospedale San Raffaele, Milan. Staging and grading were done according to the WHO/ISUP/UICC guidelines. The most common histological type at final pathology was typically represented by prostate acinar adenocarcinoma (aPCa). However, in up to 40% of cases, a smaller percentage of Histological Variant (i.e Mucinous and Foamy glands), Cytoarchitectural Patterns (i.e. Glomeruloid, Cribriform, Fused and Poorly formed glands) or other histotypes (i.e. Ductal or Intraductal component, HG-PIN) is typically identified and was described, when present.

6.6.2 *Immunohistochemistry for expression patterns*

The slide harbouring the largest representative tumour area and therefore defining the dominant tumour at RP specimens in patients with LNI disease was retrieved from the study biobank and selected by a dedicated uro-pathologist. Moreover, slides including false-negative nodes and true-positive nodes were also retrieved (in case of patients in positive nodes at final pathology). IHC staining of three different IHC markers (namely, PSMA, Androgen Receptor, and SOX-2) that would be representative of the PSMA pathway activation was performed. This pathway stream involving the three markers has been assessed in in-vitro analyses but not in human specimens.

Firstly, PSMA (GCP-05) mouse monoclonal primary antibody (Thermo Fisher Scientific) will be used for IHC staining on formalin-fixed, paraffin-embedded sections. The Roche Ventana BenchMark ULTRA IHC/ISH staining system automated platform will be used. A dedicated board certified, experienced uro-pathologist had visually quantify the predominant PSMA-expression patterns using a four-tiered system (0 = negative, 1+ = weak, 2+ = moderate, 3+ = strong) for each membranous PSMA expression (mPSMA) as previously reported (236). Tumour areas without PSMA expression were be quantified in steps of 5%, 10% and further 10% increments in relation to the total tumour area, as percentage PSMA-negative tumour area (PSMA 0). A semiquantitative evaluation of PSMA expression was performed using H-score index, calculated as follow: ([{% of weak staining} x 1] + [{% of moderate staining} x 2] + [{% of strong staining} x 3]). Thereafter, intra-tumoral heterogeneity was measured using Shannon Diversity Index (SDI) as follow: $SDI = -\Sigma\ Pi(\ln Pi)$, where Pi is the proportion of each PSMA staining level in each pathological sample.

Additional staining was then performed. In particular, anti-androgen receptor (AR) rat monoclonal antibody (clone AN1-15 Thermo Fisher Scientific) were used for IHC staining to evaluate the AR expression pathway activity. Similarly, SOX-2 has been previously associated with an increased likelihood of tumour progression and, therefore, SOX-2 expression will be assessed using IHC staining (anti-SOX-2 goat polyclonal antibody, AF6655, rndsystems). Endothelial cells, lymphocytes and benign gland were used as internal positive controls. Pathological slides were digitalized using the 3DHISTECH slide viewer software (Budapest, Hungary).

6.7 – Statistical analysis

Due to the innovative nature of our research and the absence of available data on the performance characteristics of 99mTc-PSMA-RGS in nodal staging within the primary setting at the time of study design, a formal sample size calculation could not be determined. We decided to enroll a total of 100 consecutive patients in our study based on a practical and feasible approach. The present study serves as an interim analysis, as per the study protocol, following the initial ten cases, with the aim of outlining the safety and viability of the method in the primary staging context. Continuous variables were presented as medians, and categorical variables as proportions. Sensitivity, specificity, as well as positive (PPV) and negative (NPV) predictive values of PSMA-RGS in comparison to the definitive pathology (considered the gold standard) were computed using contingency tables for both per-patient and per-region analyses. In order to optimize the definition of positivity at PSMA-RGS, different target-to-background (TtB) count rate definition were compared with preoperative imaging exams and with final pathological results. Specifically, TtB count rates ≥2, ≥3 and ≥4 were explored and the one with highest correspondence with preoperative imaging and with the highest accuracy for the identification of positive nodes at final pathology was set as reference standard for further IHC analyses. Comparisons of PSMA expression between true- and false-positive nodes and correlations with intraoperative RGS data were determined using the Wilcoxon matched-pair signed rank test and with linear regression models. Locally weighted scatter plot smooth and violin plots, which combined box-plot and Kernel's density estimation, were used to graphically represent differences between groups and correlation between continuous covariates. All statistical assessments were executed employing R (version 3.6.3) and graphics were elaborated using GraphPad Prism v10.

7. Results

7.1 – Patients characteristics

The characteristics of patients from the preliminary analysis are shown in **Table 4**. The average age at the time of surgery was 68 years (interquartile range [IQR]: 62-70), and the PSA level was 8.5 ng/ml (IQR: 4.6-16 ng/ml). The majority of patients underwent systematic plus targeted biopsies after prostate mpMRI (60 vs 40%). Breaking it down, 37% of the patients had EAU intermediate-risk, 53% were classified as high-risk, and 10% had locally advanced conditions. Regarding biopsy grade groups, 7% were in grade 2, 40% in grade 3, 43% in grade 4, and 10% in grade 5. The estimated risk for LNI based on the Briganti nomogram stood at 18% (IQR: 7 – 53%). From the entire group, 23% of patients demonstrated pathologic nodal uptake when examined with 68Ga-PSMA PET/MRI, while positivity rate was 20% at preoperative 99mTc-PSMA SPECT/CT.

Table 4: *Patient demographics and clinical characteristics at diagnosis.*

Characteristics	**(n=30)**
Age (years), median (IQR)	68 (62-70)
BMI (kg/m^2), median (IQR)	25 (23-26)
CCI (Age adjusted), n (%)	
≤ 2	17 (56)
> 2	13 (44)
PSA at biopsy (ng/mL), median (IQR)	8.5 (4.6-16)
PSA density (MRI) (ng/mL/mL), median (IQR)	0.28 (0.18-0.48)
Clinical stage, n (%)	
cT1	9 (30)
cT2	15 (50)
>cT2	6 (20)
Prostate biopsy approach, n (%)	
Systematic	12 (40)
MRI targeted + systematic	18 (60)

Prostate biopsy cores, median (IQR)	
Number of overall cores	15 (14-16)
Number of positive cores	8 (6-10)
Number of systematic cores	12 (12-14)
Number of positive systematic cores	6 (3-8)
Number of MRI targeted cores	3 (2-3)
Number of positive MRI targeted cores	2 (1-3)
Biopsy Grade Group, n (%)	
2 (3 + 4)	2 (7)
3 (4 + 3)	12 (40)
4 (4 + 4)	13 (43)
5 (4 + 5 or 5 + 4)	3 (10)
EAU risk group, n (%)	
Localized, intermediate risk	11 (37)
Localized, high risk	16 (53)
Locally advanced	3 (10)
Risk of LNI according to the Briganti nomogram (median, IQR)	18 (7.3-53)
^{68}Ga-PSMA PET/CT, n of positive patients (%)	
Median activity, Mbq (IQR)	174 (145-244)
Prostate	30 (100)
Pelvic lymph nodes	7 (23)
^{99m}Tc-PSMA SPECT, n of positive patients (%)	
Median activity, Mbq (IQR)	734 (730-738)
Prostate	29 (97)

Pelvic lymph nodes	6 (20)

Legend: IQR: Interquartile Range; BMI: Body Mass Index; CCI: Charlson Comorbidity Index; MRI: Multiparametric Resonance Imaging; EAU: European Association of Urology.

7.2 – Preoperative 68Ga-PSMA PET/MRI and 99mTc-PSMA SPECT/CT results

After giving 99mTc-PSMA-I&S, there were no negative adverse events noted. The SPECT/CT conducted a day prior to the operation correctly pinpointed the six patients with positive markers seen in the 68Ga-PSMA PET/MRI. Nonetheless, it overlooked one patient among the 7 (14%) identified by the 68Ga-PSMA PET/MRI. However, when compared to final pathology, 68Ga-PSMA PET/MRI demonstrated lower false-negative rates compared to SPECT/CT resulting in higher overall accuracy (86 vs 83%). Indeed, on a per-patient level analysis, 68Ga-PSMA PET/MRI showed sensitivity, specificity, PPV and NPV of 67, 95, 86 and 87%, respectively. Conversely, 99mTc-PSMA SPECT/CT demonstrated lower sensitivity (55%) with same specificity (83%) compared to 68Ga-PSMA PET/MRI (**Tables 5 and 6**).

Table 5. *Contingency table and diagnostic accuracy on per patients analysis over a total of 30 patients according to preoperative 68Ga-PSMA PET/MRI results.*

	Pathology positive	**Pathology negative**
68Ga PSMA positive	6	1
68Ga PSMA negative	3	20
Sensitivity	67%	
Specificity	95%	
Positive Predictive Value	86%	
Negative Predictive Value	87%	
Accuracy	86%	

Table 6. *Contingency table and diagnostic accuracy on per patients analysis over a total of 30 patients according to preoperative 99mTc-PSMA SPECT/CT results.*

	Pathology positive	**Pathology negative**
68Ga PSMA positive	5	1
68Ga PSMA negative	4	20
Sensitivity	55%	
Specificity	95%	
Positive Predictive Value	83%	
Negative Predictive Value	83%	
Accuracy	83%	

7.3 – Defining optimal target-to-background (TtB) count rate for positive uptake at PSMA RGS

Nine (30%) patients had LNI at ePLND. Overall, 174 lymph nodal regions including 707 nodes were resected. Of these, 22 regions (13%) were positive including an overall number of 80 positive nodes. At PSMA RGS, when using a TtB count rate ≥2, the drop-in probe detected suspicious nodes in 33 locations at in-vivo evaluation in 12 patients. Of these, 16 contained PCa whilst 17 contained no cancer. Overall, using count rate ≥2 PSMA-RGS identified 19 additional suspicious areas in the pelvic nodal region which were not previously identified by 68Ga-PSMA PET/MRI with 80% concordance rate. However, of these additional suspicious areas, 13 (68%) resulted negative at final pathology. When compared to preoperative SPECT/CT, PSMA RGS with count rate ≥ 2 identified 18 additional nodes that were missed by SPECT/CT, with an overall concordance of 86%. The sensitivity, specificity, PPV and NPV of count rate ≥2 at a per-region analysis were 72%, 89%, 48%, and 95%. When using a count rate ≥3, the drop-in probe detected suspicious nodes in 15 locations at in-vivo evaluation in 7 patients. Of these, 12 contained PCa whilst 3 contained no cancer. Using TtB count rate ≥3, PSMA-RGS identified 4 additional suspicious areas in the pelvic nodal region which were not previously identified by 68Ga-PSMA PET/MRI with a 90% concordance rate. Of these additional suspicious areas, only 2 (50%) resulted negative at final pathology. When

compared to preoperative SPECT/CT, PSMA RGS with count rate ≥ 3 identified 4 additional nodes that were missed by SPECT/CT, with an overall concordance of 95%. The sensitivity, specificity, PPV and NPV of PSMA-RGS at a per-region analysis were 54%, 98%, 80%, and 94% (accuracy 92%). When using a TtB count rate ≥4, the drop-in probe detected suspicious nodes in 9 locations at in-vivo evaluation in 6 patients. Of these, 8 contained PCa whilst only one contained no cancer. Using count rate ≥4 PSMA-RGS identified only one additional suspicious areas in the pelvic nodal region which was not previously identified by 68Ga-PSMA PET/MRI with 89% concordance rate. When compared to preoperative SPECT/CT, PSMA RGS with count rate ≥ 4 identified 2 additional nodes that were missed by SPECT/CT, with an overall concordance of 92%. Using count rate ≥4, the sensitivity, specificity, PPV and NPV of PSMA-RGS at a per-region analysis were 36%, 99%, 88%, and 91%, with higher similar accuracy compared to count rate ≥3 (accuracy 90%). Detailed detection rates are reported in **Tables 7 and 8**. Taking together the results, a TtB count rate ≥ 3 resulted as the most accurate and with the highest concordance with preoperative 68Ga-PSMA PET/MRI and 99mTc-PSMA SPECT/CT. As such, it was used as reference for further per-patient accuracy evaluation and comparison with IHC of PSMA expression.

Table 7*. Contingency table and diagnostic accuracy on per-patient analysis over a total of 30 patients according to different definitions of RGS positivity at in-vivo or ex-vivo evaluation*

	Pathology positive	**Pathology negative**
Positivity ≥ 2 target-to-background count rate		
PSMA RGS positive	7	5
PSMA RGS negative	2	16
Sensitivity	78%	
Specificity	76%	
Positive Predictive Value	58%	
Negative Predictive Value	89%	
Accuracy	77%	
Positivity ≥ 3 target-to-background count rate		
PSMA RGS positive	6	1
PSMA RGS negative	3	20
Sensitivity	66%	
Specificity	95%	
Positive Predictive Value	86%	
Negative Predictive Value	87%	
Accuracy	87%	
Positivity ≥ 4 target-to-background count rate		
PSMA RGS positive	5	1
PSMA RGS negative	4	20
Sensitivity	55%	
Specificity	95%	
Positive Predictive Value	83%	
Negative Predictive Value	83%	
Accuracy	83%	

Table 8. *Contingency table and diagnostic accuracy on per-region analysis over a total of 174 anatomical lymph nodal regions dissected in 30 patients according to different definitions of RGS positivity at in-vivo only evaluation*.

	Pathology positive	**Pathology negative**
Positivity ≥ 2 target-to-background count rate		
PSMA RGS positive	16	17
PSMA RGS negative	6	135
Sensitivity	72%	
Specificity	88%	
Positive Predictive Value	48%	
Negative Predictive Value	96%	
Accuracy	87%	
Positivity ≥ 3 target-to-background count rate		
PSMA RGS positive	12	3
PSMA RGS negative	10	149
Sensitivity	54%	
Specificity	98%	
Positive Predictive Value	80%	
Negative Predictive Value	93%	
Accuracy	92%	
Positivity ≥ 4 target-to-background count rate		
PSMA RGS positive	8	1
PSMA RGS negative	14	151
Sensitivity	36%	
Specificity	99%	
Positive Predictive Value	89%	
Negative Predictive Value	91%	
Accuracy	91%	

7.4 – Diagnostic accuracy and concordance with preoperative Ga68-PSMA PET/CT and 99mTc-PSMA SPECT/CT

Combining in vivo and ex vivo assessments, which applied a distinct positivity threshold and reduced background interference, revealed heightened precision. On a per-patient basis using the identified TtB count rate ≥ 3, the Drop-In gamma tool for PSMA-RGS correctly pinpointed six of the nine individuals with pN1 disease in pelvic lymph nodes, yielding respective sensitivity, specificity, PPV, and NPV results of 66%, 95%, 86%, and 87% (**Table 7**). These rates perfectly replicated those of 68Ga-PSMA PET, demonstrating the highest concordance between the chosen definition of RGS positivity (count rate ≥3) and preoperative imaging. The correspondence between TtB count rate ≥3 and 99mTc-PSMA SPECT/CT resulted lower. Among patients with positive findings at RGS, three subjects with detectable LNI had significant massive nodal invasion. Meanwhile, two individuals with false negative outcome on both pre-surgery imaging and PSMA-RGS had LNI size smaller than 2 mm. Another patient had false negative findings at RGS due to high signal background in the context of extensive extracapsular tumor extension and nodal invasion. Additionally, two patients displayed LNI outside the standard ePLND region; one of those patients had LNI in the pre-vescical area which was not identified in any of the listed imaging techniques. This occurrence, however, was not considered a misstep for the PSMA-RGS since the imaging performance in this zone is not optimal due to significant background disturbances.

7.5 – Pathological report

At final pathological evaluation, 9 patients (30%) had LNI with a median number of removed nodes of 22 (IQR 18-32 nodes). Regarding local tumor stage, 3 (10%), 17 (57%) and 10 (33%) patients had respectively pT2, pT3a and pT3b disease. Tumor grading resulted in 8 patients (27%) with ISUP 3, 12 (40%) and 10 (33%) patients with ISUP 4 and 5, respectively. ISUP score upgrading from biopsy to radical prostatectomy specimens was reported in 8 (27%) patients. Conversely, ISUP score downgrading was reported in 5 (15%) patients. Regarding overall tumoral patterns, histological variants were identified in 23 patients with 77% of cribriform pattern and 27% of intraductal patterns. Overall, 6 (20%) patients had positive surgical margins (**Table 9**).

Table 9. *Patients' pathological characteristics after surgery.*

Pathological Characteristics	(n=30)
Tumor stage, n (%)	
pT2c	9 (30)
pT3a	15 (50)
pT3b	6 (20)
Pathological Grade Group, n (%)	
3 (4 + 3)	8 (27)
4 (4 + 4)	12 (40)
5 (4 + 5 or 5 + 4)	10 (33)
Surgical margins, n (%)	
Negative	24 (80)
Positive	6 (20)
Number of removed nodes (median, IQR)	22 (18-31)
Pathological N stage (%)	
pN0	21 (70)
pN1	9 (30)

Legend: IQR: Interquartile Range

7.6 – Safety profile

The median duration of the surgery and the amount of blood loss were 222 minutes (IQR 211-250 minutes) and 50 milliliters (IQR 0-100 mL), respectively. There were no intraoperative complications observed during the RARP procedure with ePLND and PSMA-RGS. Moreover, no technical issue correlated with the use of the Drop-in gamma-probe was recorded. Four patients encountered postoperative complications (13%): one patient had a respiratory issue within 28 days (pneumonia) that was managed with antibiotics (Clavien-Dindo grade 2); the second patient experiencing complications

underwent a second surgery due to pelvic hematoma (Clavien-Dindo grade 3b); the other two patients had postoperative fever linked with pelvic lymphoceles that were treated with antibiotics only (Clavien-Dindo 2). However, all cases were unlikely to be associated with PSMA-RGS and/or administration of 99mTc-PSMA. The median hospital stay length was 4 days.

7.7 – Follow-up

No adverse reactions related to the application of 99mTc-PSMA-I&S and the utilization of the commercially approved Drop-In Crystal gamma probe were documented during the initial follow-up at 28 days and at 84 days after RARP. In total, six patients (20%) displayed persistent PSA levels following RARP, defined as a first PSA measurement ≥ 0.1 ng/ml. Notably, of these patients with PSA persistence, three had extensive nodal involvement as per the final pathology report. The individuals with persistent PSA levels were recommended for salvage radiation therapy after a thorough multidisciplinary assessment.

7.8 – Immunohistochemical evaluation of prostate cancer specimens of patients with LNI

The levels of PSMA protein expression were assessed in 9 prostate specimens from the individuals with PCa and pN1 disease obtained at the time of surgery (median H-score 210; IQR: 175–240). Among the evaluated biopsies expressing PSMA, not only did considerable variation existed between patients, but there was also noticeable variation within the same patient's tissue samples, with several evaluated specimens containing regions lacking detectable PSMA (**FIGURE 17**). To quantify this intratumor variability, each prostate specimen was assigned an SDI score, revealing that all tumors with detectable PSMA displayed heterogeneous expression and that the level of intra-patient variation was inversely correlated with the PSMA H-score (coefficient -121, p=0.03) (**FIGURE 18**). To further corroborate these findings, intra-patient heterogeneity was stratified into low, moderate and high grade based on SDI tertiles. Median SDI among categories was 0.6, 0.8 and 1.2 respectively. When comparing H-score between heterogeneity groups, patients with high heterogeneity in PSMA expression had lower median H-scores (170, IQR 137-195) compared to low heterogeneity group (median 275,

IQR 225-282) (p=0.1). Conversely, prostate cancer specimens with higher SDI were characterized by higher expression proportion of area with no PSMA staining (PSMA 0) compared to patients with low heterogeneity level (30 vs 1%, p=0.03) (**FIGURE 19**). Moreover, after stratification according to tertiles, patients with high SDI were all associated with ISUP grade 5 disease while in patients with low tumor heterogeneity the maximum ISUP grade recorded was 4. These findings indicate that, in addition to a portion of patients having no detectable PSMA expression in their tumor specimens, when PSMA is present, its expression is inherently diverse, and it seems associated with more aggressive tumor patterns (**FIGURES 20**). Moreover, while the patient cohort in this study is relatively small, making it more challenging to draw conclusions about the impact of PSMA expression on outcomes, our results suggest that PSMA expression and heterogeneity is linked to a more aggressive histological phenotype, warranting further investigation in larger prospective datasets. Intriguingly, the highest SDI (1.29) were recorded in the only two patients expressing SOX-2 and with reduced AR expression, suggesting their correlation with intra-tumour heterogeneity (**FIGURE 21**). Indeed, patients expressing SOX-2 were both characterized by high proportion of area not expressing any PSMA (PSMA 0 = 40%), high grade disease (ISUP 5) and had immediate PSA persistence after surgery.

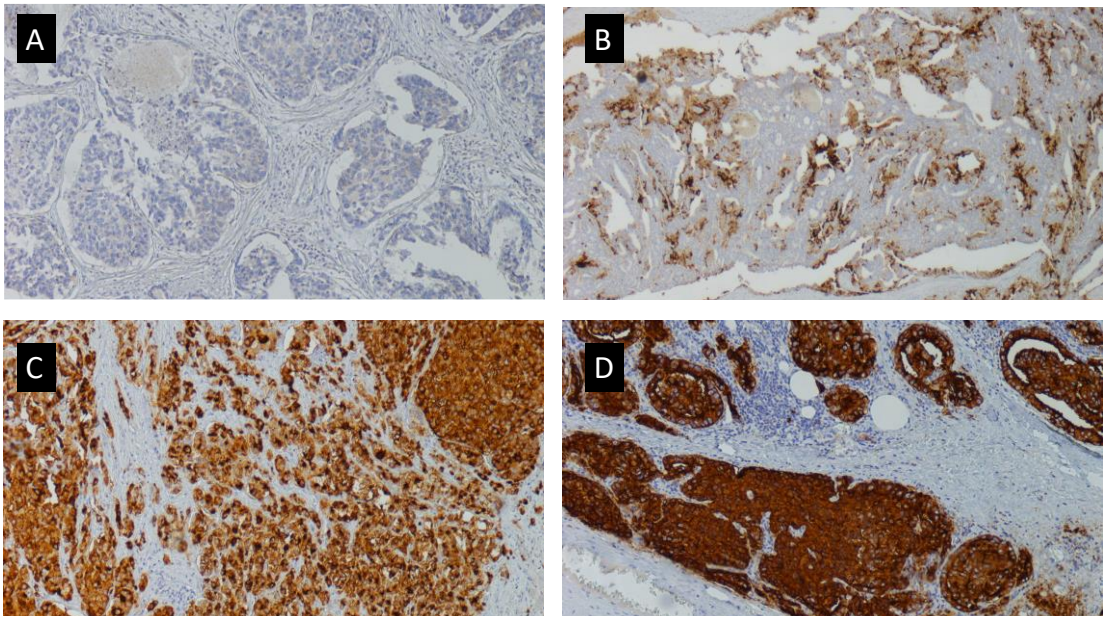

Figure 17. *Difference of PSMA expression patterns among the evaluated patient cohort. Figure A shows a PCa with absence of any PSMA antibody uptake (PSMA 0). Figure B shows low PSMA expression pattern (PSMA 1+). Figure C shows moderate signal of PSMA Uptake (PSMA 2+). Lastly, Figure D shows intense PSMA uptake (PSMA 3+)*

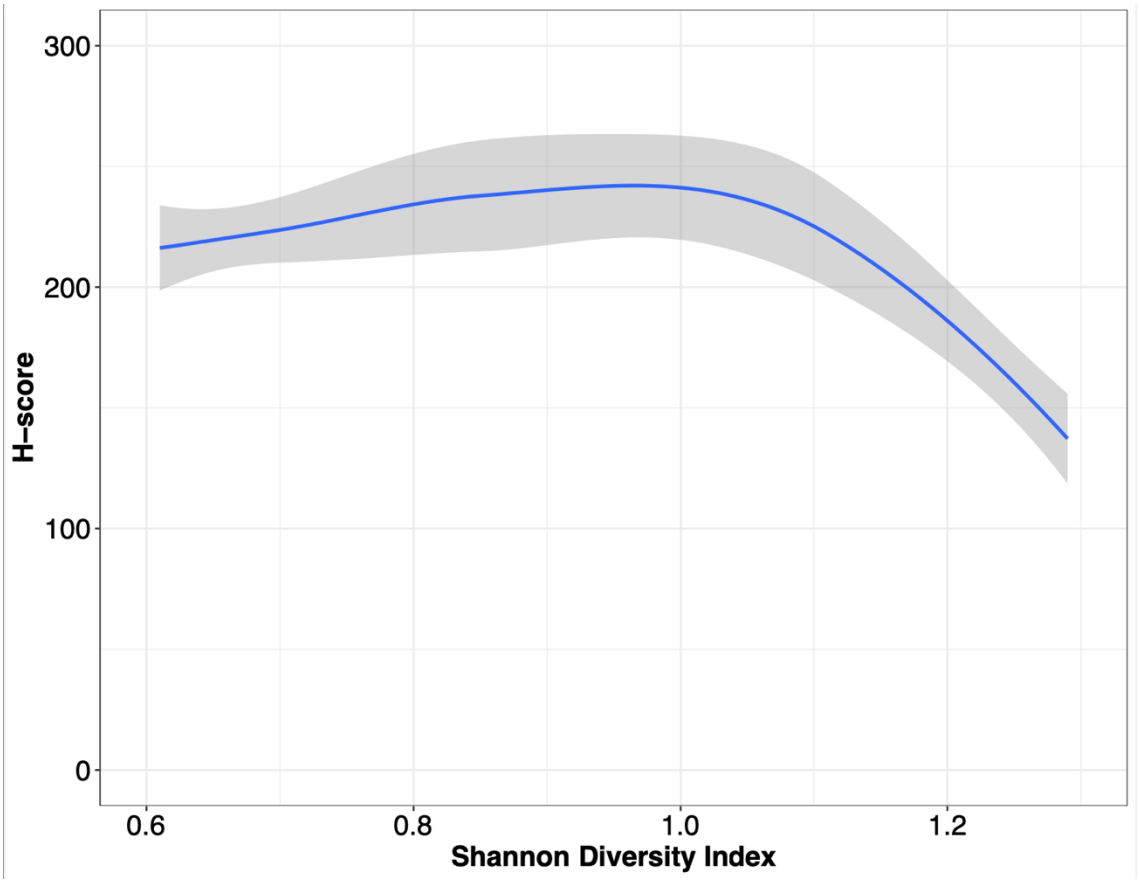

Figure 18. *Locally weighted scatter smoothed plot showing the inverse correlation between of H-score and Shannon Diversity Index of prostate cancer specimens.*

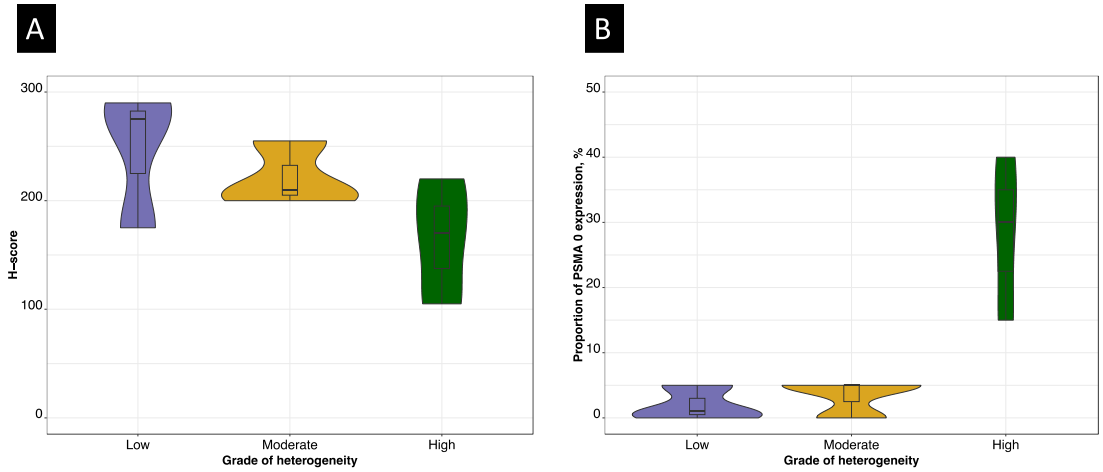

Figure 19. *Summary of H-score (A) and proportion of PSMA 0 areas (B) in prostate cancer specimens after stratification according to Shannon Diversity Index tertiles of prostate specimens*

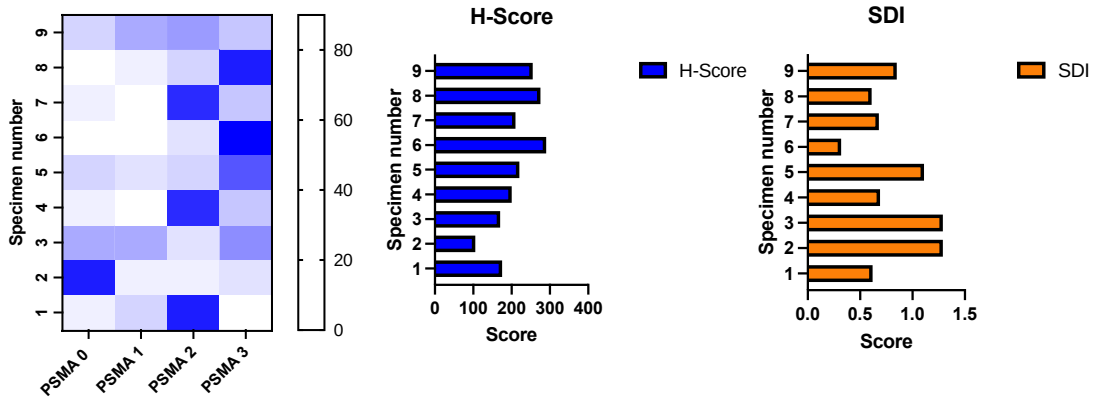

Figure 20. *Summary of the distribution of PSMA expression patterns and correlated H-score and Shannon Diversity Index distribution of prostate cancer specimens.*

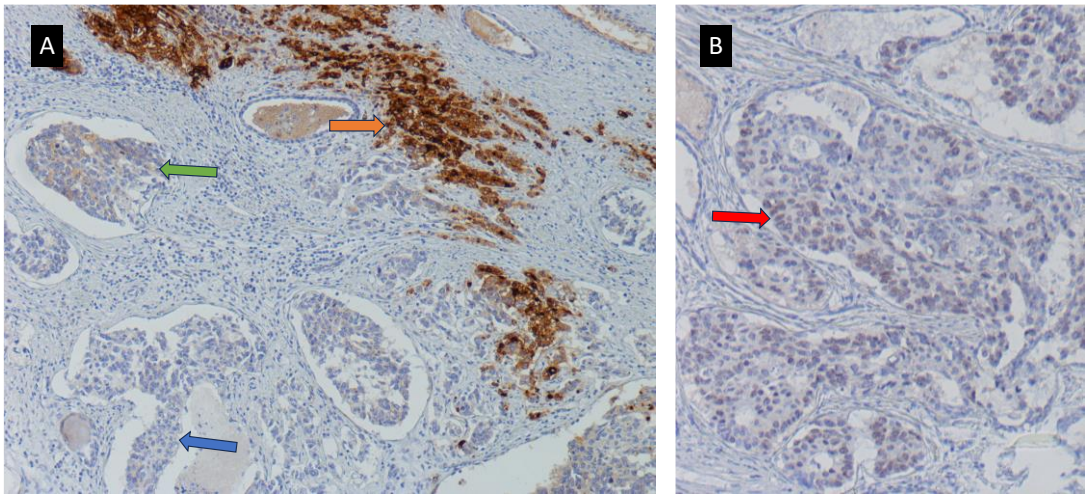

Figure 21. *IHC analysis a patient with high tumor heterogeneity and SOX-2 expression. Figure A shows the different coexistent patterns of PSMA expression: PSMA 3+ is indicated by orange arrow, patterns with low PSMA expression (PSMA 1+) are indicated by the green arrow, and the blue arrow indicates area with no PSMA uptake (PSMA 0). On the right, Figure B shows the expression of SOX-2 in prostate cancer cells of the same patient with high PSMA heterogeneity.*

7.9 – Correlation between intraoperative count and PSMA expression at nodal level

At lymph-nodes IHC of pN1 patients, median maximum diameter of the nodal metastases was 4 mm (IQR 1-10 mm). Median H-score of positive nodes at intraoperative RGS TtB count was 277 (IQR: 226-283). In negative nodes according to intraoperative TtB count rate, median H-score was 212 (IQR 160-234). Non-statistically significant differences in terms of H-score between nodal metastases resulting negative or positive at RGS were recorded while a trend towards higher H-score in RGS positive nodes was detected (p=0.08) (**FIGURE 22**). Notably, H-scores among positive lymph nodes with negative uptake at RGS did differ compared to the H-score of main tumour in the prostate (212 vs 210), while the median H-score was substantially higher in positive nodes resulting positive at RGS (277 vs 210) even though the difference was not statistically significant

(p=0.1). Similarly, SDI scores resulted lower in lymph nodes metastases when compared to SDI of the respective prostate specimens (median SDI 0.5 in lymph nodes) with no significant differences between negative and positive nodes at RGS (median SDI 0.6 vs 0.4), suggesting that tumour heterogeneity in metastatic nodal areas is less in magnitude compared to the main prostate tumour specimen. Overall, median intraoperative count was substantially higher in positive nodes at RGS with a median count per-second of 61 (IQR 42-94 count/s). On the other hand, negative nodes were characterized by low median intraoperative count per-second (Median 14, IQR 12-16 count/s) ($p<0.001$) (**FIGURE 23**). When correlating H-score and maximum metastatic diameters with intraoperative count rate, both higher H-score and increasing nodal metastatic diameters showed a positive association with higher intraoperative count rate (regression coefficients 3.13 and 0.14, respectively). However, the associated between H-score and intraoperative count rate was not statistically significant (p=0.2), while there was substantial statistical significance in the correlation between increasing intraoperative count rate and maximum diameter of the nodal metastasis ($p<0.001$) (**FIGURE 24**). When comparing true-positive and false-negative nodal findings at RGS according to positivity definition, non-significant differences in H-scores were reported (277 vs 212, p=0.8). Conversely, the maximum diameter of metastatic lesion was significantly smaller in false negative findings (10 vs 1.2mm, p=0.01), with no metastases smaller than 3mm identified at PSMA RGS (**FIGURES 25, 26 and 27**). Regarding SDI, this variable did not have a significant impact on diagnostic accuracy of PSMA RGS.

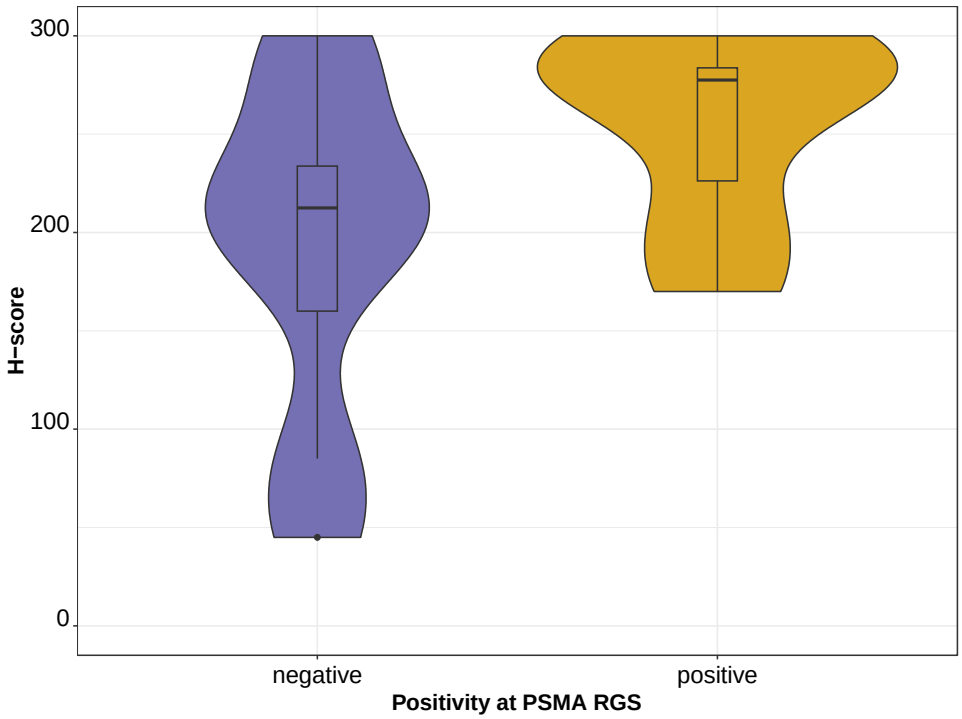

Figure 22. *Violin box-plot plot representing the difference in H-score between lymph node metastasis which resulted respectively negative or positive at PSMA RGS. Such difference was statistically non-significant (p=0.08) but relevant higher heterogeneity was reported in negative LN*

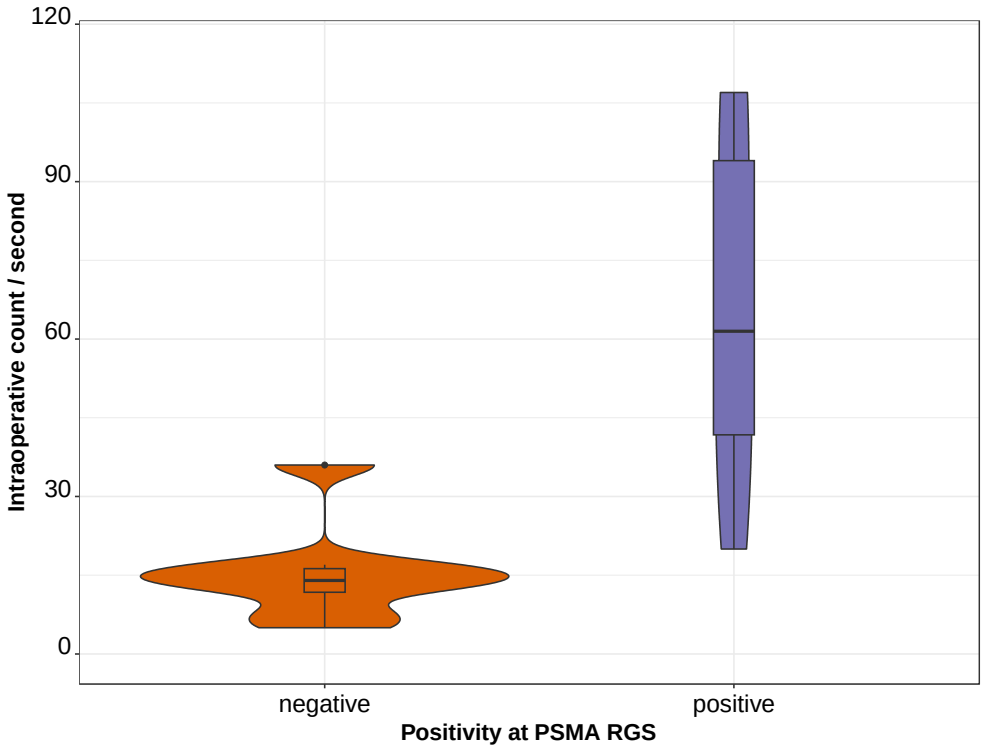

Figure 23. *Violin box-plot plot representing the difference in intraoperative count per-second between lymph node metastasis which resulted respectively negative or positive at PSMA RGS*

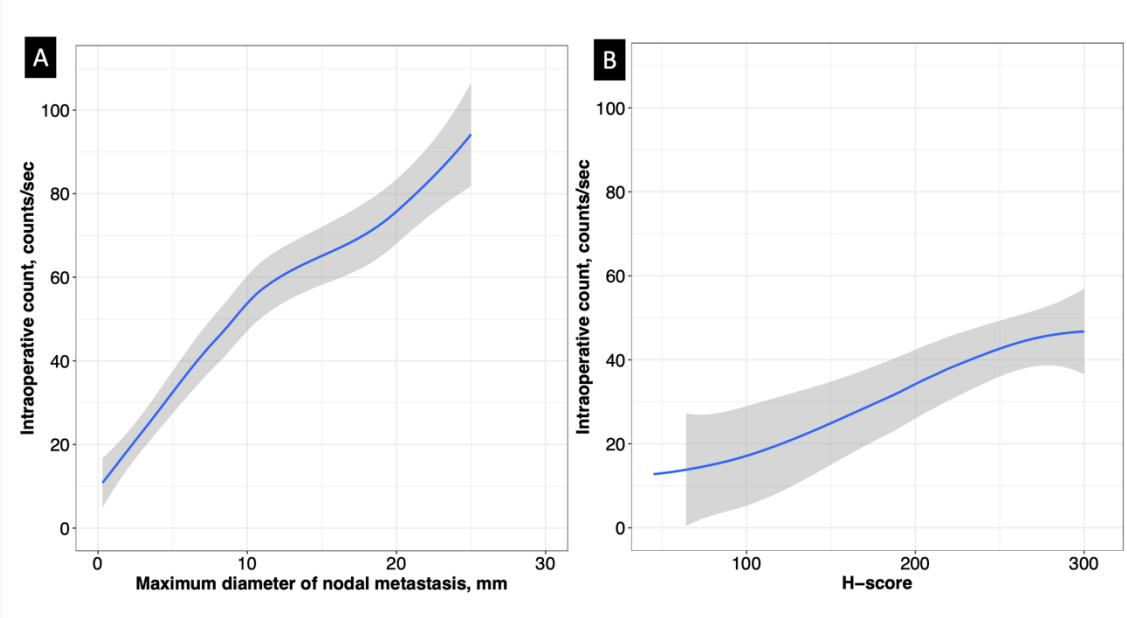

Figure 24. *Locally weighted scatter smoothed plot showing the correlation between of maximum diameter of nodal metastasis (A) and H-score (B) with the intraoperative count at RGS.*

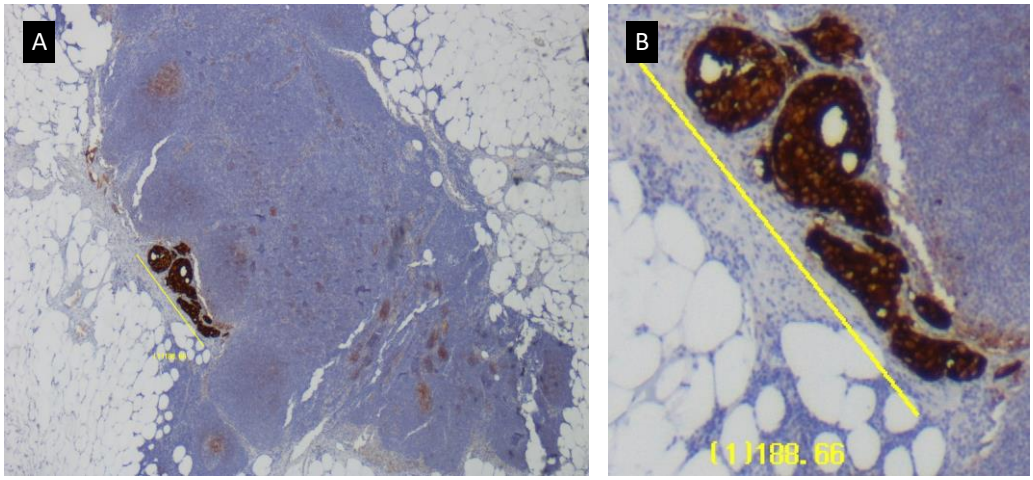

Figure 25. *Example of a patients with lymph nodal micro-metastatic disease. Sub-millimetric cancer metastasis within the entire lymph node parenchyma (Figure A) was not identified despite having a homogeneous PSMA 3+ expression (Figure 3), showing the dimensional limitation of the PSMA RGS.*

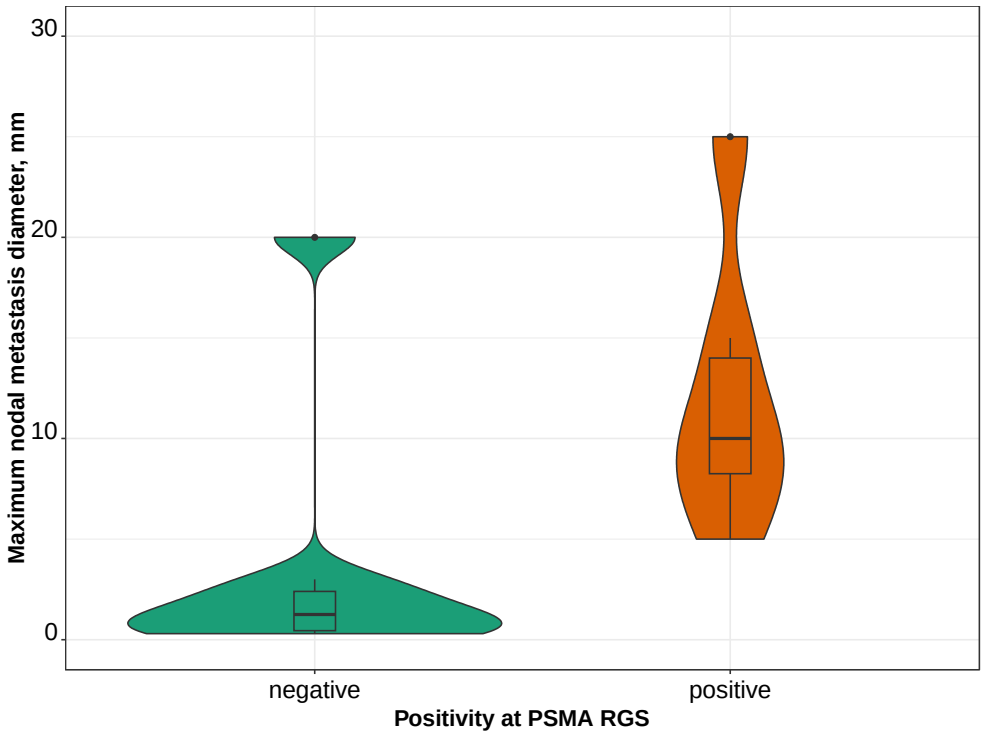

Figure 26*. Violin box-plot plot representing the difference in maximum nodal metastases diameter between lymph node metastasis which resulted respectively negative or positive at PSMA RGS*

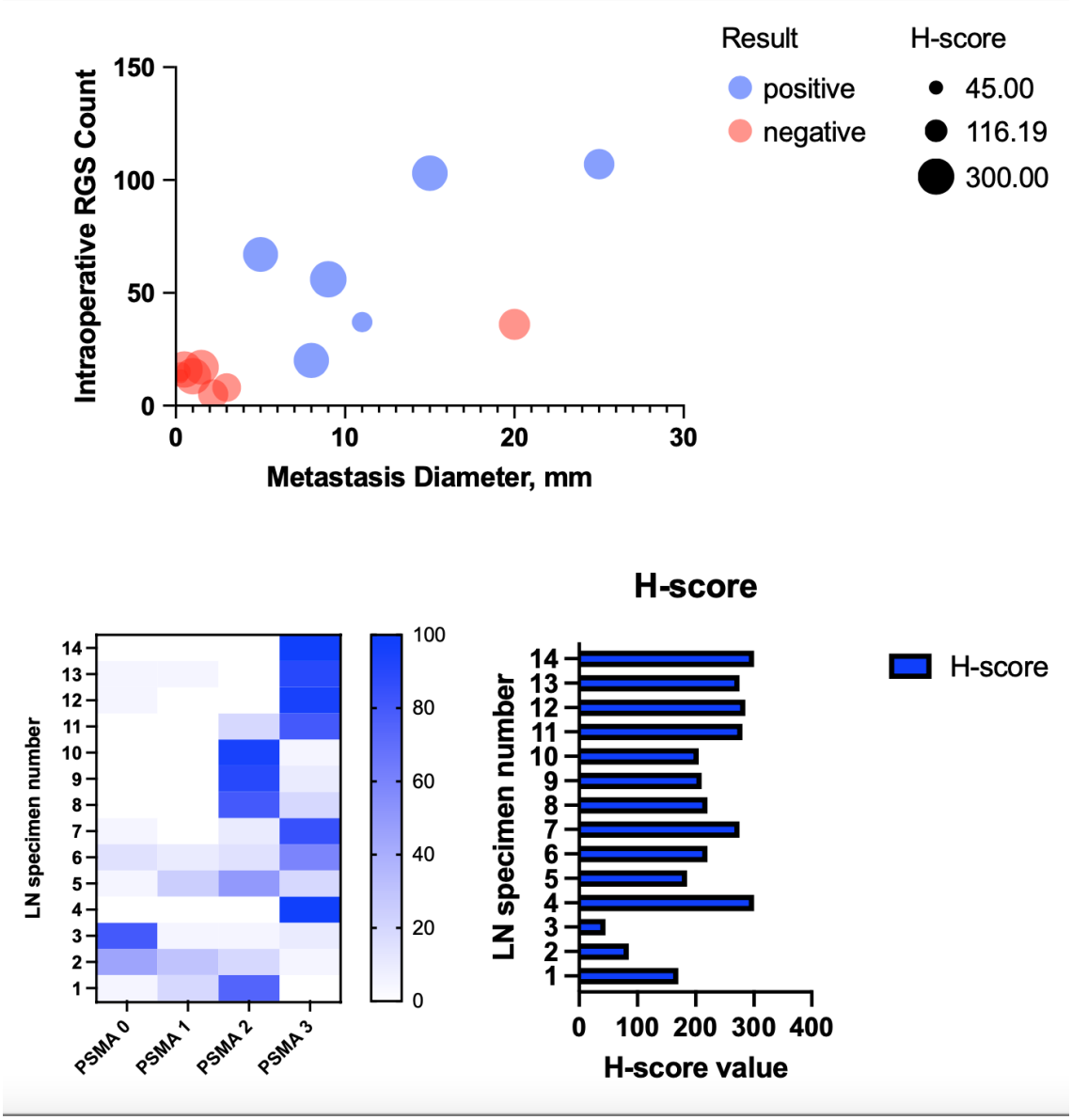

Figure 27*. Summary of PSMA expression patterns and factors associated with intraoperative positivity at PSMA RGS. Figure on top showed the distribution of positive and negative nodes over the metastatic diameter (x axis) and total intraoperative count rate (y axis), while the dimension of the dot represents in proportional to the H-score. The heat-map and histogram show respectively the distribution of PSMA expression patterns and the total H-score in the lymph nodal specimens evaluated.*

8. Discussion

Previous research has alluded to the capability of PSMA-RGS in pinpointing LNI in individuals with positive PSMA PET/CT undergoing salvage lymph node dissection (216,218,224,225). Yet, the current body of knowledge on the viability of this technique, particularly in the initial stage and with robot-assisted surgery, is sparse (220,226). Moreover, it has been reported regarding the sub-optimal accuracy of PSMA PET preoperative imaging in identifying the presence of positive nodes at final pathology (227). Indeed, such limitations are often correlated to the dimension of the metastases and/or the under-expression of PSMA (228) but it is unknown whether the intraoperative utilization of PSMA-related tracers can overcome these technical limitations of preoperative imaging modalities. In light of this information gap, our objective was to identify those clinical and pathological factors which may influence the accuracy of intraoperative use of 99mTc-PSMA for RGS and to shed further light on the safety and viability of robot-assisted PSMA-RGS, drawing from our observations in the initial 30 patients in a presently active phase 2 study. This investigation is actively recruiting individuals identified with cN0cM0 using standard imaging, showing medium to high-risk PCa, suitable for RARP with comprehensive ePLND. These evaluations were initially set in the study design. However, with the accelerated pace of participant inclusion, we can now share findings from the initial 30 participants who finalized the study protocols.

8.1 – Assessing the added value of pathological and PSMA expression patterns for detection of nodal metastases

Several findings can be derived from our IHC analyses of this patient's cohort. First, analysis of prostate specimens revealed substantial intra-tumoral heterogeneity among patients with pN1 disease, confirming what previously showed in the literature regarding the correlation between tumor heterogeneity and aggressive patterns (236). In particular, our analysis was the first to report such results in the context of non-metastatic hormone-naïve patients, thus suggesting the potential correlation between tumor instability and metastatic spread to the lymph nodes even at an early stage of the tumoral progression. Notably, we reported the concomitant presence of high intra-patient PSMA expression heterogeneity (with high proportion of PSMA 0) and the over-expression of SOX-2, as

well as under-expression of AR, in two patients with aggressive metastatic disease and with early PSA persistence after surgery. These findings, despite being only exploratory, seem to confirm the potential association between the increased expression of the reprogramming transcription factor such as SOX-2 that can promote tumor instability enabled by the loss of TP53 and RB1 function and, in consequence, a highly mutated tumor landscape which is associated with further metastatic progression even at an early disease stage and without having received and upfront androgen-deprivation therapy (239). When exploring the correlation between PSMA expression and RGS, it has been recorded a direct correlation between H-score and intraoperative count, thus confirming that the level of PSMA expression is directly correlated to the tracer uptake (i.e. 99mTc-PSMA). However, it is notable to remark that the most important factor determining the detection of positive nodes at RGS was the dimension of the tumoral metastasis, with no nodes with diameter smaller than 3mm identified at RGS. This finding seems to confirm the intrinsic limitation of preoperative PSMA PET imaging modalities, since previous studies has reported that dimensional limitation exist for the identification of micro-metastases (228). On the other hand, PSMA RGS was not able to overcome the dimensional limitation of preoperative imaging modalities.

8.2 – Optimizing intraoperative definition for positivity and exploratory analysis of the overall diagnostic accuracy

Only few evidence is available to date on PSMA RGS and data on the optimal cut-off of TtB are indeed still very limited. Previous analyses in the context of recurrent PCa [REF Maurer] have used a TtB count rate ≥ 4 as cut-off for intraoperative positivity during PMSA-guidance. However, this ratio has never been validated in the context of primary PCa. Indeed, the presence of significantly higher single background correlated with the presence of the whole prostatic tissue during primary surgery may undermine the actual value of this proposed positivity ratio cut-off. This said, we tested different ratios in order to identify the most accurate in identifying positive nodes, as well as the one with the highest correspondence with preoperative PSMA PET results. After exploring the various definition of TtB count rate (≥ 2 vs ≥ 3 vs ≥ 4), the definition of TtB count rate ≥ 3 resulted as the most accurate in detection of LNI, as well as the most concordant with preoperative

imaging modalities; indeed, perfect correspondence with preoperative 68Ga-PSMA PET was noted.

Even though our results are initial, utilizing the Drop-In gamma probe for intraoperative 99mTc-PSMA detection displayed exceptional specificity in both individual and regional assessments but exhibited less than ideal sensitivity. In fact, PSMA-RGS accurately pinpointed 6 men as pN1, all of whom showed nodal accumulation in the preceding 68Ga-PSMA PET/MRI. Yet, both PSMA-RGS and PSMA PET/MRI overlooked positive nodes in the right obturator region and in the external iliac left in two individuals with a small nodal spread (maximum size: 3 mm). Consequently, this led to a per-person sensitivity, specificity, PPV, and NPV of 66%, 95%, 86%, and 87%, respectively. Although combining both in-vivo and ex-vivo detections managed to pinpoint the majority of LNI regions at the final diagnosis, PSMA-RGS showed a sensitivity that was just slightly above 50% in a regional assessment, with specificity and NPV being ≥80%. There were 10 regions where PSMA-RGS failed to detect LNI in patients accurately categorized as pN1 (n=5). Notably, of these 5 patients with pN1 disease who exhibited uptake on PSMA-RGS but in which at least one nodal region was missed, three had extensive nodal involvement with increased background noise signal which may have caused sub-optimal identification of all the involved lymph nodal regions.

This indicates that the potential for underestimation seen with preoperative PSMA PET in individuals with substantial nodal involvement could also be a factor in PSMA-RGS. Here, PET/CT significantly undervalued the actual tumor load, irrespective of the tracer used. Notably, 68Ga-PSMA demonstrated superior performance over 11C-choline in accurately assessing the actual nodal tumor load only in patients with lower PSA levels (up to 1.5 ng/ml) and a smaller number of positive regions (two or fewer). There was no substantiated indication of 68Ga-PSMA having superior staging accuracy over 11C-choline in any other categories of patients. Collectively, these observations underline the significance of comprehensive nodal procedures, especially when considering salvage therapies for nodal recurrence (246).

It is worth noting that PSMA-RGS could not detect a micro-metastatic LNI that wasn't identified during the preoperative scan in two individuals. In essence, this method currently has limited sensitivity when it comes to identifying LNI in those with extensive nodal burden or micro-metastatic conditions. However, its high specificity, both in-vivo

and ex-vivo, should aid in verifying the extraction of nodes flagged in the preoperative PSMA PET. Negative results in PSMA-RGS could direct surgeons to a broader dissection to pinpoint positive nodes even outside the usual template (220).

Our findings should be interpreted within the framework of the limited existing research in this area. Gondoputro and colleagues recently shared findings from a study involving 12 PCa patients who underwent 99mTc-PSMA-I&S RGS in a primary setting. They found that the inpatient use of the gamma probe had a sensitivity, specificity, PPV, and NPV of 76%, 69%, 50%, and 88%, respectively. The diagnostic accuracy was higher ex-vivo, at 76%, 96%, 89%, and 91%, respectively. Among the lymph nodes missed in-vivo and ex-vivo (n=5), 90% were micro-metastases (≤3mm). No severe complications exceeding Clavien-Dindo Grade I were observed. These findings suggest the feasibility and safety of robot-assisted 99mTc-based PSMA-RGS in a primary setting, enhancing the detection of nodal metastases during RARP and ePLND. Further advancements in detector technology could refine the capabilities of robot-assisted 99mTc-based PSMA-RGS (220). The variances between our study and Gondoputro et al.'s findings should be evaluated considering the differences in trial designs. Notably, our study and theirs adopted different PSMA-RGS positivity thresholds (1.5 vs. 2 times the background reference). The performance of PSMA-RGS significantly improved in both studies with ex-vivo measurements, which reduce background noise interference, highlighting its importance in the procedure. While our research concentrated on intermediate- and high-risk patients, Gondoputro et al. included mainly high-risk PCa patients (220), leading to a higher rate of preoperative PSMA PET positivity (64 vs. 23%) and lymph node involvement (83 vs. 30%), underscoring the importance of patient selection in PSMA-directed surgeries. Furthermore, our study employed a CE-marked Drop-In gamma probe, compared to their use of a prototype. This research presents the inaugural usage of a commercially available, sterilizable Drop-In gamma probe, which maintained its performance quality in the initial 14 patients.

Yilmaz and team also highlighted that 99mTc-PSMA-RGS is a potential strategy during RARP for primary PCa, enhancing the procedure's efficiency and safety (226). Moreover, while early imaging with 99mTc-PSMA-I&S SPECT/CT does not match the diagnostic capabilities of Ga-68 PSMA-11 PET/CT for primary PCa lesions or LNM, there's ample evidence supporting PSMA-RGS's potential in guiding intraoperative resections in

recurrent PCa scenarios. As minimally invasive surgeries become more common, it's anticipated that robot-assisted techniques will increasingly be at the forefront for detecting and addressing residual or recurring PCa post-curative treatment.

8.3 – Confirming effective utilization and safety profile of intraoperative 99mTc-PSMA

Another key point of the current research study was to confirm the feasibility and safety of intraoperative utilization of 99mTc-PSMA and the related procedures. First of all, the successful creation and distribution of 99mTc- PSMA-I&S, synthesized based on prior methodologies (216), were confirmed in nearly every participant through a SPECT/CT conducted 270 minutes post-tracer injection. Radiolabeling of PSMA ligands using gamma-emitting isotopes like 111Indium (111In-PSMA imaging and therapy [111In-PSMA-I&T]) or 99mTechnetium (99mTc-PSMA assessment and surgery [99mTc-PSMA-I&S]) has been documented before. Such agents are beneficial for pre-surgery SPECT imaging and standard gamma probe surgical guidance. Yet, due to its elevated expense, significant radiation dose, and limited access, 111In-PSMA-I&T isn't ideal for regular clinical use. On the other hand, 99mTc-PSMA-I&S emerges as a practical choice due to the ease of obtaining 99mTc from 99Mo/99mTc generators, common in nuclear medicine departments, at a comparatively affordable cost (218). Robu et al. introduced a solid and trustworthy kit-labeling method, facilitating the synthesis of 99mTc-MAS3-y-nal-k(Sub-KuE) and 99mTc-PSMA-I&S with consistent radiological quality. Yet, owing to its enhanced uptake efficiency and better stability in vivo, 99mTc-PSMA-I&S was preferred for additional in vivo studies. In patients with PCa, 99mTc-PSMA-I&S displayed a relatively slow systemic clearance due to the tracer's significant plasma protein adherence (94%). However, this led to effective tracer absorption in PCa lesions over time, resulting in progressively higher lesion-to-background ratios up to 21 hours post-injection (216). Our study validates these findings, noting tracer absorption persisting even a day post-surgery.

Secondly, 99mTc-PSMA-I&S administration proved safe with no reported side effects. The only post-surgery complications were respiratory infection and/or small lymphoceles managed with antibiotics in three patients (Clavien-Dindo: 2). Only one patient experienced a major surgical complication (i.e. pelvic haematoma) treated with

reintervention (Clavien-Dindo 3b), but it was not correlated with the experimental procedure itself. Numerous reports highlight the safety of 99mTc-PSMA-I&S, primarily in a relapse scenario. As an instance, in Rauscher et al. study, 24 participants (38.1%) experienced complications from the salvage surgical procedure. Still, no specific issues linked to the PSMA-RGS technique or tracer injection emerged. Most subjects encountered mild challenges, categorized as grade 1 in the Clavien-Dindo system, such as temporary incontinence or post-surgery lymphedema. Six individuals (9.5%) necessitated follow-up surgeries due to severe complications, like ureter damage. Yet, these complication percentages align with previously published data (216). Beyond changes post-surgery and radiation treatment, the heightened complication rates in salvage surgeries compared to primary surgeries can also be attributed to the often-challenging locations of reoccurring PCa lesions (247). A crucial consideration involves the radiation exposure risks linked with the use of 99mTc-PSMA-I&S. Research by Aalbersberg et al. revealed that the radiation dose for staff involved in managing 99mTc-PSMA-I&S is on par with that from other 99mTc-based radiopharmaceuticals, confirming its safety for both imaging and RGS applications. The estimated radiation dose per procedure varied from 1.59x10^-10 μSv for imaging technicians to 9.74 μSv for scrub nurses. The actual effective dose measured ranged from 0 to 5 μSv for all involved personnel during a single 99mTc-PSMA-I&S procedure. The highest dose was recorded by the scrub nurse (3.2±1.3 μSv), while the surgical nurse received the lowest (0.2±0.5 μSv). In a scenario where a scrub nurse is involved in up to 100 99mTc-PSMA-I&S procedures annually, the cumulative effective dose would amount to 320 μSv/year. Post-administration, the radiation dose rate at 50 cm from the patient was initially 18.5±1.6 μSv/h, which decreased to 1.8±0.3 μSv/h after next-day imaging and further dropped to 0.56±0.33 μSv/h post-surgery (248). In a related study by Schmidt et al., the optimal level of radioactivity (OAR) was identified to adhere to safety limits and estimate the maximum number of 99mTc-PSMA-based RGS operations a surgeon can perform annually without necessitating comprehensive radiation monitoring. Given the mean effective half-life of 4.15 hours for 99mTc-PSMA-I&S and an average surgery duration of 2 hours at an average distance of 0.25 meters from the patient, the dose per operation was calculated to be 4.16 μSv. This allows for approximately 241 surgeries per surgeon per year without requiring full radiation protection monitoring (249).

In line with this, our research reveals that robot-assisted PSMA-RGS using a CE-approved Drop-In gamma probe controlled robotically is both feasible and safe, with only minor operative time impacts (250). Preceding studies have verified the safety and efficacy of these gamma probes in robot-assisted surgeries. Collectively, these findings suggest that during RARP with ePLND, PSMA-RGS can be executed without adding risks to the patient.

From a clinical standpoint, our study is among the first to delineate the safety and efficacy of robotic PSMA-RGS for primary staging in medium to high-risk PCa patients. We are the first to describe the employment of a sterilizable CE-certified Drop-In gamma device, which proved consistent in its first 30 uses. The tool can be swiftly controlled by the surgeon during RARP, immediately offering feedback on nodal metastasis removal. Preliminary data indicates the safety of PSMA-RGS without elevated risks during the post-operation period. The extended hospital duration compared to RARP without PSMA-RGS could be ascribed to various reasons, including mandatory prior day admissions for tracer injections and the novelty of the surgical method for initial patients. Notwithstanding these factors, our results are promising, providing insight into robot-aided PSMA-RGS's feasibility and safety. In terms of staging and diagnostic accuracy, the initial findings indicate that PSMA-RGS could enhance the detection of LNI, especially in patients showing nodal uptake in preoperative PSMA PET scans. However, this method tended to underestimate the actual nodal burden observed in final pathology, even in cases where pN1 disease was accurately detected by the Drop-In probe. Consequently, at present, PSMA-RGS should not replace ePLND when the preoperative profile suggests its necessity, and a thorough ePLND remains essential even with positive Drop-In probe findings. Nonetheless, ePLND can lead to possible complications, highlighting the need for precise surgical techniques that support lymph node dissections and can identify both micro and macro-metastases. Given that primary draining nodes may be located beyond the conventional ePLND template in some patients, sentinel node approaches have been suggested and have demonstrated value in accurate lymph node staging and reducing morbidity. While PSMA ligand PET is more sensitive than traditional imaging, it still has limitations in detecting small metastatic lesions, making it inadequate for excluding patients from ePLND based on the absence of nodal disease.

Hence, traditional lymphatic mapping remains necessary for identifying micro-metastases in lymph nodes. This raises the question of PSMA-RGS's impact on clinical care in primary PCa treatment. Theoretically, it could be utilized in high-risk, high-volume PCa cases with lymph node-positive disease identified on PSMA-ligand PET to assist in metastatic site removal. However, the presence of smaller, undetected lymph node metastases in primary PCa remains a possibility, and clinical parameters like PSA levels are less informative than in recurrent PCa. Therefore, for now, ePLND remains a recommended approach in patients with PSMA-ligand PET-positive lymph nodes undergoing surgery. The potential role of PSMA-RGS might become apparent primarily in atypical lesions not easily identified otherwise. The exact additional value of PSMA-RGS in uncovering micro-metastatic disease that both conventional and PSMA preoperative imaging miss remains to be determined. Nevertheless, it is crucial to realize that in some instances, PSMA-RGS might not capture the full scope of nodal involvement. Thus, it should not replace ePLND when prior indicators call for its application.

8.4 – Limitations

Even though this study was designed prospectively and adhered to uniform protocols for all participating patients, there are certain constraints to acknowledge. First, it should be underlined the exploratory design of the current analysis in terms of IHC analyses since only small cohort of patients has undergone comprehensive IHC evaluation. Further pathological analyses should be performed to corroborate our findings. Moreover, further methodological application to objectively quantify the PSMA expression patterns can be implemented. Similarly, it is plausible that underlying molecular mechanism such as and DNA aberration may support the progression patterns of aggressive tumors and/or the heterogeneous expression of PSMA. As such, additional next-generation-sequencing analyses may further unveil the mechanism associated with limited PSMA uptake, as well as with the metastatic spread of hormone-naïve PCa. Second, these initial results pertain to the experiences of the first 30 men who underwent PSMA-RGS, with plans to include further individuals in the context of this prospective trial. Hence, this data should be seen as early insights. It is plausible that as surgeons become more proficient with the procedure, the predictive accuracy of robot-assisted PSMA-RGS could enhance,

suggesting a potential learning curve. Moreover, we only have provided short-term findings, and extended tracking is crucial for evaluating more robust outcomes. All the tracers currently in use for PSMA-RGS exhibit urinary elimination, and any leakage from the bladder during the prostate removal can interfere with the PSMA-guided lymph node extraction process. Ideally, tracers with minimal to no urinary discharge should be crafted. Furthermore, the natural accumulation of the tracer in the rectal wall, coupled with weak signals from scattered cancer cells, complicates the precise evaluation of the prostate bed post-surgery for lingering cancer cells. Tracers without renal clearance and with diminished nonspecific rectal wall retention would be more efficient. The current PSMA tracers' tissue penetration limitations hinder their application during the assessment of the prostate specimen for any positive surgical boundaries. Generating tracers that do not seep into non-cancerous tissue and are not discharged through urine is an evident gap. An alternative approach might be optical surgical navigation. The last decade has seen commendable advancements in image-driven PCa surgery using, for example, indocyanine green-based tracers (251). Upcoming advancements are likely to shape disease handling, propelled by new technologies, innovative tracers, and optical advances. Comprehensive clinical assessments are essential to further understand the benefits, cost implications, and result consistency of these innovations. In this scenario, experiences from PSMA-focused surgeries might pave the way for introducing similar molecularly directed methods in treating diverse cancers and conditions.

9. Conclusions

Our study showed that the use of intraoperative 99mTC-PSMA cannot overcome dimensional limitation of preoperative imaging modalities based on PSMA in the identification of small tumor metastases, regardless the expression of PSMA. However, we confirmed that PSMA is indeed upregulated in many but not all PCa, and exhibits marked intra-patient heterogeneity which may be correlated with the hyperexpression of certain molecular markers such as SOX-2 which may promote tumor instability and aggressive metastatic progression. In terms of clinical application of the novel methodology, we implemented a highly accurate definition of positivity (i.e. TtB count rate ≥3) which perfectly correlates with the preoperative molecular imaging findings. Last but not least, we confirmed that with 99mTc-PSMA-RGS was both safe and practical, and can potentially facilitate the detection of nodal metastases intraoperatively in cN0cM0 PCa patients who are candidate for radical surgical treatment with ePLND.

10. References

1. Global Cancer Observatory [Internet]. [cited 2023 Aug 23]. Available from: https://gco.iarc.fr
2. Baade PD, Youlden DR, Krnjacki LJ. International epidemiology of prostate cancer: geographical distribution and secular trends. Mol Nutr Food Res. 2009 Feb;53:171–84.
3. Zhou CK, Check DP, Lortet-Tieulent J, et al. Prostate cancer incidence in 43 populations worldwide: An analysis of time trends overall and by age group. Int J cancer. 2016 Mar;138:1388–400.
4. Culp MB, Soerjomataram I, Efstathiou JA, Bray F, Jemal A. Recent Global Patterns in Prostate Cancer Incidence and Mortality Rates. Eur Urol. 2020 Jan;77:38–52.
5. Leitzmann MF, Rohrmann S. Risk factors for the onset of prostatic cancer: age, location, and behavioral correlates. Clin Epidemiol. 2012;4:1–11.
6. Timms BG. Prostate development: a historical perspective. Differentiation. 2008 Jul;76:565–77.
7. McNeal JE. Normal and pathologic anatomy of prostate. Urology. 1981 Mar;17:11–6.
8. Francis JC, Swain A. Prostate Organogenesis. Cold Spring Harb Perspect Med. 2018 Jul;8.
9. Haffner MC, Zwart W, Roudier MP, et al. Genomic and phenotypic heterogeneity in prostate cancer. Nat Rev Urol. 2021 Feb;18:79–92.
10. Porter CM, Shrestha E, Peiffer LB, Sfanos KS. The microbiome in prostate inflammation and prostate cancer. Prostate Cancer Prostatic Dis. 2018 Sep;21:345–54.
11. Rebello RJ, Oing C, Knudsen KE, et al. Prostate cancer. Nat Rev Dis Prim. 2021 Feb;7:9.
12. Epstein JI. An update of the Gleason grading system. J Urol. 2010 Feb;183:433–40.

13. Kim EH, Andriole GL. Prostate cancer: A simplified prostate cancer grading system. Vol. 12, Nature reviews. Urology. England; 2015. p. 601–2.
14. Makarov D V, Carter HB. The discovery of prostate specific antigen as a biomarker for the early detection of adenocarcinoma of the prostate. J Urol. 2006 Dec;176:2383–5.
15. Balk SP, Ko Y-J, Bubley GJ. Biology of prostate-specific antigen. J Clin Oncol Off J Am Soc Clin Oncol. 2003 Jan;21:383–91.
16. Kouriefs C, Sahoyl M, Grange P, Muir G. Prostate specific antigen through the years. Arch Ital di Urol Androl organo Uff [di] Soc Ital di Ecogr Urol e Nefrol. 2009 Dec;81:195–8.
17. Catalona WJ, Smith DS, Ratliff TL, et al. Measurement of prostate-specific antigen in serum as a screening test for prostate cancer. N Engl J Med. 1991 Apr;324:1156–61.
18. Filson CP, Marks LS, Litwin MS. Expectant management for men with early stage prostate cancer. CA Cancer J Clin. 2015;65:264–82.
19. Klotz L. Cancer overdiagnosis and overtreatment. Curr Opin Urol. 2012 May;22:203–9.
20. Ilic D, Neuberger MM, Djulbegovic M, Dahm P. Screening for prostate cancer. Cochrane database Syst Rev. 2013 Jan;2013:CD004720.
21. Moyer VA. Screening for prostate cancer: U.S. Preventive Services Task Force recommendation statement. Ann Intern Med. 2012 Jul;157:120–34.
22. Screening for prostate cancer: U.S. Preventive Services Task Force recommendation statement. Ann Intern Med. 2008 Aug;149:185–91.
23. Andriole GL, Crawford ED, Grubb RL 3rd, et al. Mortality results from a randomized prostate-cancer screening trial. N Engl J Med. 2009 Mar;360:1310–9.
24. Schröder FH, Hugosson J, Roobol MJ, et al. Screening and prostate-cancer mortality in a randomized European study. N Engl J Med. 2009 Mar;360:1320–8.

25. Desai MM, Cacciamani GE, Gill K, et al. Trends in Incidence of Metastatic Prostate Cancer in the US. JAMA Netw open. 2022 Mar;5:e222246.
26. Grossman DC, Curry SJ, Owens DK, et al. Screening for Prostate Cancer: US Preventive Services Task Force Recommendation Statement. JAMA. 2018 May;319:1901–13.
27. Gandaglia G, Albers P, Abrahamsson P-A, et al. Structured Population-based Prostate-specific Antigen Screening for Prostate Cancer: The European Association of Urology Position in 2019. Eur Urol. 2019 Aug;76:142–50.
28. Loeb S, Giri VN. Clinical Implications of Germline Testing in Newly Diagnosed Prostate Cancer. Eur Urol Oncol [Internet]. 2021 Feb 1;4:1–9. Available from: https://doi.org/10.1016/j.euo.2020.11.011
29. Siegel RL, Miller KD, Fuchs HE, Jemal A. Cancer statistics, 2022. CA Cancer J Clin. 2022 Jan;72:7–33.
30. Jaratlerdsiri W, Chan EKF, Gong T, et al. Whole-Genome Sequencing Reveals Elevated Tumor Mutational Burden and Initiating Driver Mutations in African Men with Treatment-Naïve, High-Risk Prostate Cancer. Cancer Res. 2018 Dec;78:6736–46.
31. Karunamuni RA, Huynh-Le M-P, Fan CC, et al. Performance of African-ancestry-specific polygenic hazard score varies according to local ancestry in 8q24. Prostate Cancer Prostatic Dis. 2022 Feb;25:229–37.
32. Lachance J, Berens AJ, Hansen MEB, et al. Genetic Hitchhiking and Population Bottlenecks Contribute to Prostate Cancer Disparities in Men of African Descent. Cancer Res. 2018 May;78:2432–43.
33. Pu YS, Chiang HS, Lin CC, et al. Changing trends of prostate cancer in Asia. aging male Off J Int Soc Study Aging Male. 2004 Jun;7:120–32.
34. Brandt A, Sundquist J, Hemminki K. Risk for incident and fatal prostate cancer in men with a family history of any incident and fatal cancer. Ann Oncol Off J Eur Soc Med Oncol. 2012 Jan;23:251–6.

35. Stewart RW, Lizama S, Peairs K, Sateia HF, Choi Y. Screening for prostate cancer. Semin Oncol. 2017 Feb;44:47–56.
36. Rebbeck TR. Prostate Cancer Genetics: Variation by Race, Ethnicity, and Geography. Semin Radiat Oncol. 2017 Jan;27:3–10.
37. Nyberg T, Frost D, Barrowdale D, et al. Prostate Cancer Risk by BRCA2 Genomic Regions. Eur Urol. 2020 Oct;78:494–7.
38. Karlsson R, Aly M, Clements M, et al. A population-based assessment of germline HOXB13 G84E mutation and prostate cancer risk. Eur Urol. 2014 Jan;65:169–76.
39. Tamura K, Kaneda M, Futagawa M, et al. Genetic and genomic basis of the mismatch repair system involved in Lynch syndrome. Int J Clin Oncol. 2019 Sep;24:999–1011.
40. Meyer KB, Maia A-T, O'Reilly M, et al. A functional variant at a prostate cancer predisposition locus at 8q24 is associated with PVT1 expression. PLoS Genet. 2011 Jul;7:e1002165.
41. Li-Sheng Chen S, Ching-Yuan Fann J, Sipeky C, et al. Risk Prediction of Prostate Cancer with Single Nucleotide Polymorphisms and Prostate Specific Antigen. J Urol. 2019 Mar;201:486–95.
42. Dickerman BA, Torfadottir JE, Valdimarsdottir UA, et al. Midlife metabolic factors and prostate cancer risk in later life. Int J cancer. 2018 Mar;142:1166–73.
43. Cirne F, Kappel C, Zhou S, et al. Modifiable risk factors for prostate cancer in low- and lower-middle-income countries: a systematic review and meta-analysis. Prostate Cancer Prostatic Dis. 2022 Sep;25:453–62.
44. Darcey E, Boyle T. Tobacco smoking and survival after a prostate cancer diagnosis: A systematic review and meta-analysis. Cancer Treat Rev. 2018 Nov;70:30–40.
45. Alexander DD, Mink PJ, Cushing CA, Sceurman B. A review and meta-analysis of prospective studies of red and processed meat intake and prostate cancer. Nutr J. 2010 Nov;9:50.

46. Compérat E, Varinot J, Eymerit C, et al. [Comparison of UICC and AJCC 8th edition TNM classifications in uropathology]. Ann Pathol. 2019 Apr;39:158–66.
47. Radkiewicz C, Andersson TM-L, Lagergren J. Reranking cancer mortality using years of life lost. JNCI cancer Spectr. 2023 May;7.
48. Ross HM, Kryvenko ON, Cowan JE, et al. Do adenocarcinomas of the prostate with Gleason score (GS) ≤6 have the potential to metastasize to lymph nodes? Am J Surg Pathol. 2012 Sep;36:1346–52.
49. Bill-Axelson A, Holmberg L, Garmo H, et al. Radical Prostatectomy or Watchful Waiting in Prostate Cancer - 29-Year Follow-up. N Engl J Med. 2018 Dec;379:2319–29.
50. Wilt TJ, Jones KM, Barry MJ, et al. Follow-up of Prostatectomy versus Observation for Early Prostate Cancer. N Engl J Med. 2017 Jul;377:132–42.
51. Hamdy FC, Donovan JL, Lane JA, et al. Fifteen-Year Outcomes after Monitoring, Surgery, or Radiotherapy for Prostate Cancer. N Engl J Med. 2023 Apr;388:1547–58.
52. D'Amico A V, Whittington R, Malkowicz SB, et al. Biochemical outcome after radical prostatectomy, external beam radiation therapy, or interstitial radiation therapy for clinically localized prostate cancer. JAMA. 1998 Sep;280:969–74.
53. Mazzone E, Gandaglia G, Ploussard G, et al. Risk Stratification of Patients Candidate to Radical Prostatectomy Based on Clinical and Multiparametric Magnetic Resonance Imaging Parameters: Development and External Validation of Novel Risk Groups. Eur Urol. 2022 Feb;81:193–203.
54. Merriel SWD, Funston G, Hamilton W. Prostate Cancer in Primary Care. Adv Ther. 2018 Sep;35:1285–94.
55. Sekhoacha M, Riet K, Motloung P, et al. Prostate Cancer Review: Genetics, Diagnosis, Treatment Options, and Alternative Approaches.

Molecules. 2022 Sep;27.

56. Catalona WJ, Richie JP, Ahmann FR, et al. Comparison of Digital Rectal Examination and Serum Prostate Specific Antigen in the Early Detection of Prostate Cancer: Results of a Multicenter Clinical Trial of 6,630 Men. J Urol. 2017 Feb;197:S200–7.
57. Carvalhal GF, Smith DS, Mager DE, Ramos C, Catalona WJ. Digital rectal examination for detecting prostate cancer at prostate specific antigen levels of 4 ng./ml. or less. J Urol. 1999 Mar;161:835–9.
58. Herrera-Caceres JO, Wettstein MS, Goldberg H, et al. Utility of digital rectal examination in a population with prostate cancer treated with active surveillance. Can Urol Assoc J = J l'Association des Urol du Canada. 2020 Sep;14:E453–7.
59. Cornud F, Lefevre A, Flam T, et al. MRI-directed high-frequency (29MhZ) TRUS-guided biopsies: initial results of a single-center study. Eur Radiol. 2020 Sep;30:4838–46.
60. Prebay ZJ, Medairos R, Doolittle J, et al. The prognostic value of digital rectal exam for the existence of advanced pathologic features after prostatectomy. Prostate. 2021 Oct;81:1064–70.
61. Djavan B, Milani S, Remzi M. Prostate biopsy: who, how and when. An update. Can J Urol. 2005 Feb;12 Suppl 1:44–100.
62. Loeb S, Bjurlin MA, Nicholson J, et al. Overdiagnosis and overtreatment of prostate cancer. Eur Urol. 2014 Jun;65:1046–55.
63. Giganti F, Rosenkrantz AB, Villeirs G, et al. The Evolution of MRI of the Prostate: The Past, the Present, and the Future. AJR Am J Roentgenol. 2019 Aug;213:384–96.
64. Kayat Bittencourt L, Litjens G, Hulsbergen-van de Kaa CA, et al. Prostate Cancer: The European Society of Urogenital Radiology Prostate Imaging Reporting and Data System Criteria for Predicting Extraprostatic Extension by Using 3-T Multiparametric MR Imaging. Radiology. 2015 Aug;276:479–89.

65. Hricak H, Dooms GC, McNeal JE, et al. MR imaging of the prostate gland: normal anatomy. AJR Am J Roentgenol. 1987 Jan;148:51–8.
66. Verma S, Rajesh A, Morales H, et al. Assessment of aggressiveness of prostate cancer: correlation of apparent diffusion coefficient with histologic grade after radical prostatectomy. AJR Am J Roentgenol. 2011 Feb;196:374–81.
67. Weinreb JC, Barentsz JO, Choyke PL, et al. PI-RADS Prostate Imaging - Reporting and Data System: 2015, Version 2. Eur Urol. 2016 Jan;69:16–40.
68. Delongchamps NB, Rouanne M, Flam T, et al. Multiparametric magnetic resonance imaging for the detection and localization of prostate cancer: combination of T2-weighted, dynamic contrast-enhanced and diffusion-weighted imaging. BJU Int. 2011 May;107:1411–8.
69. Nagel KNA, Schouten MG, Hambrock T, et al. Differentiation of prostatitis and prostate cancer by using diffusion-weighted MR imaging and MR-guided biopsy at 3 T. Radiology. 2013 Apr;267:164–72.
70. Turkbey B, Brown AM, Sankineni S, et al. Multiparametric prostate magnetic resonance imaging in the evaluation of prostate cancer. CA Cancer J Clin. 2016 Jul;66:326–36.
71. Li W, Dong A, Hong G, Shang W, Shen X. Diagnostic performance of ESUR scoring system for extraprostatic prostate cancer extension: A meta-analysis. Eur J Radiol. 2021 Oct;143:109896.
72. Barentsz JO, Richenberg J, Clements R, et al. ESUR prostate MR guidelines 2012. Eur Radiol [Internet]. 2012;22:746–57. Available from: https://doi.org/10.1007/s00330-011-2377-y
73. Barrett T, Rajesh A, Rosenkrantz AB, Choyke PL, Turkbey B. PI-RADS version 2.1: one small step for prostate MRI. Clin Radiol. 2019 Nov;74:841–52.
74. Simmons LAM, Kanthabalan A, Arya M, et al. Accuracy of Transperineal Targeted Prostate Biopsies, Visual Estimation and Image Fusion in Men

Needing Repeat Biopsy in the PICTURE Trial. J Urol. 2018 Dec;200:1227–34.

75. Montironi R, Cheng L, Lopez-Beltran A, et al. Original Gleason system versus 2005 ISUP modified Gleason system: the importance of indicating which system is used in the patient's pathology and clinical reports. Vol. 58, European urology. Switzerland; 2010. p. 369–73.
76. Ahmed HU, El-Shater Bosaily A, Brown LC, et al. Diagnostic accuracy of multi-parametric MRI and TRUS biopsy in prostate cancer (PROMIS): a paired validating confirmatory study. Lancet (London, England). 2017 Feb;389:815–22.
77. de Rooij M, Israël B, Tummers M, et al. ESUR/ESUI consensus statements on multi-parametric MRI for the detection of clinically significant prostate cancer: quality requirements for image acquisition, interpretation and radiologists' training. Eur Radiol. 2020 Oct;30:5404–16.
78. Kam J, Yuminaga Y, Krelle M, et al. Evaluation of the accuracy of multiparametric MRI for predicting prostate cancer pathology and tumour staging in the real world: an multicentre study. BJU Int. 2019 Aug;124:297–301.
79. Radtke JP, Wiesenfarth M, Kesch C, et al. Combined Clinical Parameters and Multiparametric Magnetic Resonance Imaging for Advanced Risk Modeling of Prostate Cancer—Patient-tailored Risk Stratification Can Reduce Unnecessary Biopsies. Eur Urol [Internet]. 2017;72:888–96. Available from: https://www.sciencedirect.com/science/article/pii/S0302283817302671
80. Eastham JA, Riedel E, Scardino PT, et al. Variation of serum prostate-specific antigen levels: an evaluation of year-to-year fluctuations. JAMA. 2003 May;289:2695–700.
81. Pradere B, Veeratterapillay R, Dimitropoulos K, et al. Nonantibiotic Strategies for the Prevention of Infectious Complications following Prostate Biopsy: A Systematic Review and Meta-Analysis. J Urol. 2021

Mar;205:653–63.

82. Wegelin O, van Melick HHE, Hooft L, et al. Comparing Three Different Techniques for Magnetic Resonance Imaging-targeted Prostate Biopsies: A Systematic Review of In-bore versus Magnetic Resonance Imaging-transrectal Ultrasound fusion versus Cognitive Registration. Is There a Preferred Technique? Eur Urol. 2017 Apr;71:517–31.
83. Hamid S, Donaldson IA, Hu Y, et al. The SmartTarget Biopsy Trial: A Prospective, Within-person Randomised, Blinded Trial Comparing the Accuracy of Visual-registration and Magnetic Resonance Imaging/Ultrasound Image-fusion Targeted Biopsies for Prostate Cancer Risk Stratification. Eur Urol. 2019 May;75:733–40.
84. Algaba F, Montironi R. Impact of prostate cancer multifocality on its biology and treatment. J Endourol. 2010 May;24:799–804.
85. Stabile A, Dell'Oglio P, De Cobelli F, et al. Association Between Prostate Imaging Reporting and Data System (PI-RADS) Score for the Index Lesion and Multifocal, Clinically Significant Prostate Cancer. Eur Urol Oncol. 2018 May;1:29–36.
86. Cheng E, Davuluri M, Lewicki PJ, Hu JC, Basourakos SP. Developments in optimizing transperineal prostate biopsy. Curr Opin Urol. 2022 Jan;32:85–90.
87. Bjurlin MA, Carter HB, Schellhammer P, et al. Optimization of initial prostate biopsy in clinical practice: sampling, labeling and specimen processing. J Urol. 2013 Jun;189:2039–46.
88. Mäkinen T, Tammela TL, Hakama M, et al. Prostate cancer screening within a prostate specific antigen range of 3 to 3.9 ng./ml.: a comparison of digital rectal examination and free prostate specific antigen as supplemental screening tests. J Urol. 2001 Oct;166:1339–42.
89. Guo CC, Epstein JI. Intraductal carcinoma of the prostate on needle biopsy: Histologic features and clinical significance. Mod Pathol an Off J United States Can Acad Pathol Inc. 2006 Dec;19:1528–35.

90. Spigelman SS, McNeal JE, Freiha FS, Stamey TA. Rectal examination in volume determination of carcinoma of the prostate: clinical and anatomical correlations. J Urol. 1986 Dec;136:1228–30.
91. Partin AW, Carter HB, Chan DW, et al. Prostate specific antigen in the staging of localized prostate cancer: influence of tumor differentiation, tumor volume and benign hyperplasia. J Urol. 1990 Apr;143:747–52.
92. Freedland SJ, Csathy GS, Dorey F, Aronson WJ. Percent prostate needle biopsy tissue with cancer is more predictive of biochemical failure or adverse pathology after radical prostatectomy than prostate specific antigen or Gleason score. J Urol. 2002 Feb;167:516–20.
93. Quinn DI, Henshall SM, Brenner PC, et al. Prognostic significance of preoperative factors in localized prostate carcinoma treated with radical prostatectomy: importance of percentage of biopsies that contain tumor and the presence of biopsy perineural invasion. Cancer. 2003 Apr;97:1884–93.
94. Eifler JB, Feng Z, Lin BM. An updated prostate cancer staging nomogram (Partin tables) based on cases from 2006 to 2011. BJU Int. 2013;111:22.
95. Smith JAJ, Scardino PT, Resnick MI, et al. Transrectal ultrasound versus digital rectal examination for the staging of carcinoma of the prostate: results of a prospective, multi-institutional trial. J Urol. 1997 Mar;157:902–6.
96. de Rooij M, Hamoen EHJ, Witjes JA, Barentsz JO, Rovers MM. Accuracy of Magnetic Resonance Imaging for Local Staging of Prostate Cancer: A Diagnostic Meta-analysis. Eur Urol. 2016 Aug;70:233–45.
97. Gandaglia G, Ploussard G, Valerio M, et al. The Key Combined Value of Multiparametric Magnetic Resonance Imaging, and Magnetic Resonance Imaging–targeted and Concomitant Systematic Biopsies for the Prediction of Adverse Pathological Features in Prostate Cancer Patients Undergoing Radical Prostatect. Eur Urol. 2020;77:733–41.
98. Martini A, Gupta A, Lewis SC, et al. Development and internal validation

of a side-specific, multiparametric magnetic resonance imaging-based nomogram for the prediction of extracapsular extension of prostate cancer. BJU Int [Internet]. 2018 Dec 1;122:1025–33. Available from: https://doi.org/10.1111/bju.14353

99. Müller A-C, Aebersold DM, Albrecht C, et al. Radiotherapy for hormone-sensitive prostate cancer with synchronous low burden of distant metastases. Strahlentherapie und Onkol Organ der Dtsch Rontgengesellschaft . [et al]. 2022 Aug;198:683–9.
100. Tosoian JJ, Gorin MA, Ross AE, et al. Oligometastatic prostate cancer: definitions, clinical outcomes, and treatment considerations. Nat Rev Urol. 2017 Jan;14:15–25.
101. Hofman MS, Lawrentschuk N, Francis RJ, et al. Prostate-specific membrane antigen PET-CT in patients with high-risk prostate cancer before curative-intent surgery or radiotherapy (proPSMA): a prospective, randomised, multicentre study. Lancet [Internet]. 2020;395:1208–16. Available from: http://dx.doi.org/10.1016/S0140-6736(20)30314-7
102. Marra G, Valerio M, Heidegger I, et al. Management of Patients with Node-positive Prostate Cancer at Radical Prostatectomy and Pelvic Lymph Node Dissection: A Systematic Review. Eur Urol Oncol. 2020 Oct;3:565–81.
103. Lebastchi AH, Gupta N, DiBianco JM, et al. Comparison of cross-sectional imaging techniques for the detection of prostate cancer lymph node metastasis: a critical review. Transl Androl Urol. 2020 Jun;9:1415–27.
104. von Eyben FE, Kairemo K. Meta-analysis of (11)C-choline and (18)F-choline PET/CT for management of patients with prostate cancer. Nucl Med Commun. 2014 Mar;35:221–30.
105. Schiavina R, Bianchi L, Mineo Bianchi F, et al. Preoperative Staging With (11)C-Choline PET/CT Is Adequately Accurate in Patients With Very High-Risk Prostate Cancer. Clin Genitourin Cancer. 2018 Aug;16:305-312.e1.

106. Tsechelidis I, Vrachimis A. PSMA PET in Imaging Prostate Cancer. Front Oncol. 2022;12:831429.
107. Hope TA, Eiber M, Armstrong WR, et al. Diagnostic Accuracy of 68Ga-PSMA-11 PET for Pelvic Nodal Metastasis Detection Prior to Radical Prostatectomy and Pelvic Lymph Node Dissection: A Multicenter Prospective Phase 3 Imaging Trial. JAMA Oncol. 2021 Nov;7:1635–42.
108. de Feria Cardet RE, Hofman MS, Segard T, et al. Is Prostate-specific Membrane Antigen Positron Emission Tomography/Computed Tomography Imaging Cost-effective in Prostate Cancer: An Analysis Informed by the proPSMA Trial. Eur Urol. 2021 Mar;79:413–8.
109. Cookson MS, Aus G, Burnett AL, et al. Variation in the definition of biochemical recurrence in patients treated for localized prostate cancer: the American Urological Association Prostate Guidelines for Localized Prostate Cancer Update Panel report and recommendations for a standard in the r. J Urol. 2007 Feb;177:540–5.
110. Suh CH, Shinagare AB, Westenfield AM, et al. Yield of bone scintigraphy for the detection of metastatic disease in treatment-naive prostate cancer: a systematic review and meta-analysis. Clin Radiol. 2018 Feb;73:158–67.
111. Zhou J, Gou Z, Wu R, et al. Comparison of PSMA-PET/CT, choline-PET/CT, NaF-PET/CT, MRI, and bone scintigraphy in the diagnosis of bone metastases in patients with prostate cancer: a systematic review and meta-analysis. Skeletal Radiol. 2019 Dec;48:1915–24.
112. Van Nieuwenhove S, Van Damme J, Padhani AR, et al. Whole-body magnetic resonance imaging for prostate cancer assessment: Current status and future directions. J Magn Reson Imaging. 2022 Mar;55:653–80.
113. Corfield J, Perera M, Bolton D, Lawrentschuk N. (68)Ga-prostate specific membrane antigen (PSMA) positron emission tomography (PET) for primary staging of high-risk prostate cancer: a systematic review. World J Urol. 2018 Apr;36:519–27.
114. Perera M, Papa N, Roberts M, et al. Gallium-68 Prostate-specific

Membrane Antigen Positron Emission Tomography in Advanced Prostate Cancer-Updated Diagnostic Utility, Sensitivity, Specificity, and Distribution of Prostate-specific Membrane Antigen-avid Lesions: A Systematic Review and Meta-. Eur Urol. 2019/02/19. 2020;77:403–17.

115. Sandblom G, Dufmats M, Varenhorst E. Long-term survival in a Swedish population-based cohort of men with prostate cancer. Urology. 2000 Sep;56:442–7.
116. Johansson JE, Adami HO, Andersson SO, et al. Natural history of localised prostatic cancer. A population-based study in 223 untreated patients. Lancet (London, England). 1989 Apr;1:799–803.
117. Adolfsson J, Tribukait B, Levitt S. The 20-Yr outcome in patients with well- or moderately differentiated clinically localized prostate cancer diagnosed in the pre-PSA era: the prognostic value of tumour ploidy and comorbidity. Eur Urol. 2007 Oct;52:1028–35.
118. Jonsson E, Sigbjarnarson HP, Tomasson J, et al. Adenocarcinoma of the prostate in Iceland: a population-based study of stage, Gleason grade, treatment and long-term survival in males diagnosed between 1983 and 1987. Scand J Urol Nephrol. 2006;40:265–71.
119. Hugosson J, Roobol MJ, Månsson M, et al. A 16-yr Follow-up of the European Randomized study of Screening for Prostate Cancer. Eur Urol. 2019 Jul;76:43–51.
120. Wilt TJ, Vo TN, Langsetmo L, et al. Radical Prostatectomy or Observation for Clinically Localized Prostate Cancer: Extended Follow-up of the Prostate Cancer Intervention Versus Observation Trial (PIVOT). Eur Urol. 2020 Jun;77:713–24.
121. Graversen PH, Nielsen KT, Gasser TC, Corle DK, Madsen PO. Radical prostatectomy versus expectant primary treatment in stages I and II prostatic cancer. A fifteen-year follow-up. Urology. 1990 Dec;36:493–8.
122. Vernooij RW, Lancee M, Cleves A, et al. Radical prostatectomy versus deferred treatment for localised prostate cancer. Cochrane database Syst

Rev. 2020 Jun;6:CD006590.

123. Thomsen FB, Brasso K, Klotz LH, et al. Active surveillance for clinically localized prostate cancer--a systematic review. J Surg Oncol. 2014 Jun;109:830–5.
124. Tosoian JJ, Mamawala M, Epstein JI, et al. Intermediate and Longer-Term Outcomes From a Prospective Active-Surveillance Program for Favorable-Risk Prostate Cancer. J Clin Oncol Off J Am Soc Clin Oncol. 2015 Oct;33:3379–85.
125. Hamdy FC, Donovan JL, Lane JA, et al. 10-Year Outcomes after Monitoring, Surgery, or Radiotherapy for Localized Prostate Cancer. N Engl J Med. 2016 Oct;375:1415–24.
126. Donovan JL, Hamdy FC, Lane JA, et al. Patient-Reported Outcomes after Monitoring, Surgery, or Radiotherapy for Prostate Cancer. N Engl J Med. 2016 Oct;375:1425–37.
127. McLeod DG, Iversen P, See WA, et al. Bicalutamide 150 mg plus standard care vs standard care alone for early prostate cancer. BJU Int. 2006 Feb;97:247–54.
128. Willemse P-PM, Davis NF, Grivas N, et al. Systematic Review of Active Surveillance for Clinically Localised Prostate Cancer to Develop Recommendations Regarding Inclusion of Intermediate-risk Disease, Biopsy Characteristics at Inclusion and Monitoring, and Surveillance Repeat Biopsy Strategy. Eur Urol. 2022 Apr;81:337–46.
129. Lam TBL, MacLennan S, Willemse PPM, et al. EAU-EANM-ESTRO-ESUR-SIOG Prostate Cancer Guideline Panel Consensus Statements for Deferred Treatment with Curative Intent for Localised Prostate Cancer from an International Collaborative Study (DETECTIVE Study). Eur Urol. 2019;76:790–813.
130. Loeb S, Bruinsma SM, Nicholson J, et al. Active surveillance for prostate cancer: a systematic review of clinicopathologic variables and biomarkers for risk stratification. Eur Urol. 2015 Apr;67:619–26.

131. Klotz L, Pond G, Loblaw A, et al. Randomized Study of Systematic Biopsy Versus Magnetic Resonance Imaging and Targeted and Systematic Biopsy in Men on Active Surveillance (ASIST): 2-year Postbiopsy Follow-up. Eur Urol. 2020 Mar;77:311–7.
132. Studer UE, Collette L, Whelan P, et al. Using PSA to guide timing of androgen deprivation in patients with T0-4 N0-2 M0 prostate cancer not suitable for local curative treatment (EORTC 30891). Eur Urol. 2008 May;53:941–9.
133. Gandaglia G, Ploussard G, Valerio M, et al. A Novel Nomogram to Identify Candidates for Extended Pelvic Lymph Node Dissection Among Patients with Clinically Localized Prostate Cancer Diagnosed with Magnetic Resonance Imaging-targeted and Systematic Biopsies. Eur Urol. 2019;75.
134. D'Amico A V, Chen M-H, Renshaw AA, Loffredo M, Kantoff PW. Androgen suppression and radiation vs radiation alone for prostate cancer: a randomized trial. JAMA. 2008 Jan;299:289–95.
135. Roach M 3rd, Bae K, Speight J, et al. Short-term neoadjuvant androgen deprivation therapy and external-beam radiotherapy for locally advanced prostate cancer: long-term results of RTOG 8610. J Clin Oncol Off J Am Soc Clin Oncol. 2008 Feb;26:585–91.
136. Pilepich M V, Winter K, Lawton CA, et al. Androgen suppression adjuvant to definitive radiotherapy in prostate carcinoma--long-term results of phase III RTOG 85-31. Int J Radiat Oncol Biol Phys. 2005 Apr;61:1285–90.
137. Zapatero A, Guerrero A, Maldonado X, et al. High-dose radiotherapy with short-term or long-term androgen deprivation in localised prostate cancer (DART01/05 GICOR): a randomised, controlled, phase 3 trial. Lancet Oncol. 2015 Mar;16:320–7.
138. Bolla M, Van Tienhoven G, Warde P, et al. External irradiation with or without long-term androgen suppression for prostate cancer with high

metastatic risk: 10-year results of an EORTC randomised study. Lancet Oncol. 2010 Nov;11:1066–73.

139. Viani GA, Viana BS, Martin JEC, et al. Intensity-modulated radiotherapy reduces toxicity with similar biochemical control compared with 3-dimensional conformal radiotherapy for prostate cancer: A randomized clinical trial. Cancer. 2016 Jul;122:2004–11.
140. Wortel RC, Incrocci L, Pos FJ, et al. Late Side Effects After Image Guided Intensity Modulated Radiation Therapy Compared to 3D-Conformal Radiation Therapy for Prostate Cancer: Results From 2 Prospective Cohorts. Int J Radiat Oncol Biol Phys. 2016 Jun;95:680–9.
141. James ND, Sydes MR, Clarke NW, et al. Addition of docetaxel, zoledronic acid, or both to first-line long-term hormone therapy in prostate cancer (STAMPEDE): survival results from an adaptive, multiarm, multistage, platform randomised controlled trial. Lancet (London, England). 2016 Mar;387:1163–77.
142. Krauss D, Kestin L, Ye H, et al. Lack of benefit for the addition of androgen deprivation therapy to dose-escalated radiotherapy in the treatment of intermediate- and high-risk prostate cancer. Int J Radiat Oncol Biol Phys. 2011 Jul;80:1064–71.
143. Kupelian PA, Ciezki J, Reddy CA, Klein EA, Mahadevan A. Effect of increasing radiation doses on local and distant failures in patients with localized prostate cancer. Int J Radiat Oncol Biol Phys. 2008 May;71:16–22.
144. Spratt DE, Malone S, Roy S, et al. Prostate Radiotherapy With Adjuvant Androgen Deprivation Therapy (ADT) Improves Metastasis-Free Survival Compared to Neoadjuvant ADT: An Individual Patient Meta-Analysis. J Clin Oncol Off J Am Soc Clin Oncol. 2021 Jan;39:136–44.
145. King MT, Keyes M, Frank SJ, et al. Low dose rate brachytherapy for primary treatment of localized prostate cancer: A systemic review and executive summary of an evidence-based consensus statement.

Brachytherapy. 2021;20:1114–29.

146. Viani GA, Arruda CV, Assis Pellizzon AC, De Fendi LI. HDR brachytherapy as monotherapy for prostate cancer: A systematic review with meta-analysis. Brachytherapy. 2021;20:307–14.
147. Morris WJ, Tyldesley S, Rodda S, et al. Androgen Suppression Combined with Elective Nodal and Dose Escalated Radiation Therapy (the ASCENDE-RT Trial): An Analysis of Survival Endpoints for a Randomized Trial Comparing a Low-Dose-Rate Brachytherapy Boost to a Dose-Escalated External Beam Boost . Int J Radiat Oncol Biol Phys. 2017 Jun;98:275–85.
148. Parry MG, Nossiter J, Sujenthiran A, et al. Impact of High-Dose-Rate and Low-Dose-Rate Brachytherapy Boost on Toxicity, Functional and Cancer Outcomes in Patients Receiving External Beam Radiation Therapy for Prostate Cancer: A National Population-Based Study. Int J Radiat Oncol Biol Phys. 2021 Apr;109:1219–29.
149. Guillaumier S, Peters M, Arya M, et al. A Multicentre Study of 5-year Outcomes Following Focal Therapy in Treating Clinically Significant Nonmetastatic Prostate Cancer. Eur Urol. 2018 Oct;74:422–9.
150. van der Poel HG, van den Bergh RCN, Briers E, et al. Focal Therapy in Primary Localised Prostate Cancer: The European Association of Urology Position in 2018. Eur Urol. 2018 Jul;74:84–91.
151. Yaxley JW, Coughlin GD, Chambers SK, et al. Robot-assisted laparoscopic prostatectomy versus open radical retropubic prostatectomy: early outcomes from a randomised controlled phase 3 study. Lancet (London, England). 2016 Sep;388:1057–66.
152. Efstathiou E, Davis JW, Pisters L, et al. Clinical and Biological Characterisation of Localised High-risk Prostate Cancer: Results of a Randomised Preoperative Study of a Luteinising Hormone-releasing Hormone Agonist with or Without Abiraterone Acetate plus Prednisone. Eur Urol. 2019 Oct;76:418–24.

153. Kumar S, Shelley M, Harrison C, et al. Neo-adjuvant and adjuvant hormone therapy for localised and locally advanced prostate cancer. Cochrane database Syst Rev. 2006 Oct;2006:CD006019.
154. Lawton CA, DeSilvio M, Roach M 3rd, et al. An update of the phase III trial comparing whole pelvic to prostate only radiotherapy and neoadjuvant to adjuvant total androgen suppression: updated analysis of RTOG 94-13, with emphasis on unexpected hormone/radiation interactions. Int J Radiat Oncol Biol Phys. 2007 Nov;69:646–55.
155. Murthy V, Maitre P, Kannan S, et al. Prostate-Only Versus Whole-Pelvic Radiation Therapy in High-Risk and Very High-Risk Prostate Cancer (POP-RT): Outcomes From Phase III Randomized Controlled Trial. J Clin Oncol Off J Am Soc Clin Oncol. 2021 Apr;39:1234–42.
156. Schuessler WW, Schulam PG, Clayman R V, Kavoussi LR. Laparoscopic radical prostatectomy: initial short-term experience. Urology. 1997 Dec;50:854–7.
157. Guillonneau B, Cathelineau X, Barret E, Rozet F, Vallancien G. [Laparoscopic radical prostatectomy. Preliminary evaluation after 28 interventions]. Presse Med. 1998 Oct;27:1570–4.
158. Binder J, Jones J, Bentas W, et al. [Robot-assisted laparoscopy in urology. Radical prostatectomy and reconstructive retroperitoneal interventions]. Urologe A. 2002 Mar;41:144–9.
159. Mazzone E, Mistretta FA, Knipper S, et al. Contemporary National Assessment of Robot-Assisted Surgery Rates and Total Hospital Charges for Major Surgical Uro-Oncological Procedures in the United States. J Endourol. 2019;33:438–47.
160. Mazzone E, Puliatti S, Amato M, et al. A Systematic Review and Meta-analysis on the Impact of Proficiency-based Progression Simulation Training on Performance Outcomes. Ann Surg. 2021 Aug;274:281–9.
161. Mottrie A, Mazzone E, Wiklund P, et al. Objective assessment of intraoperative skills for robot-assisted radical prostatectomy (RARP):

results from the ERUS Scientific and Educational Working Groups Metrics Initiative. BJU Int. 2021 Jul;128:103–11.

162. Coughlin GD, Yaxley JW, Chambers SK, et al. Robot-assisted laparoscopic prostatectomy versus open radical retropubic prostatectomy: 24-month outcomes from a randomised controlled study. Lancet Oncol [Internet]. 2018;19:1051–60. Available from: http://dx.doi.org/10.1016/S1470-2045(18)30357-7
163. Martini A, Falagario UG, Villers A, et al. Contemporary Techniques of Prostate Dissection for Robot-assisted Prostatectomy. Eur Urol. 2020 Oct;78:583–91.
164. Semerjian A, Pavlovich CP. Extraperitoneal Robot-Assisted Radical Prostatectomy: Indications, Technique and Outcomes. Curr Urol Rep. 2017 Jun;18:42.
165. Guillonneau B, Vallancien G. Laparoscopic radical prostatectomy: the Montsouris technique. J Urol. 2000 Jun;163:1643–9.
166. Mazzone E, Dell'Oglio P, Rosiello G, et al. Technical Refinements in Superextended Robot-assisted Radical Prostatectomy for Locally Advanced Prostate Cancer Patients at Multiparametric Magnetic Resonance Imaging. Eur Urol. 2021 Jul;80:104–12.
167. Kumar A, Tandon S, Samavedi S, et al. Current status of various neurovascular bundle-sparing techniques in robot-assisted radical prostatectomy. J Robot Surg. 2016 Sep;10:187–200.
168. Bai Y, Pu C, Yuan H, et al. Assessing the Impact of Barbed Suture on Vesicourethral Anastomosis During Minimally Invasive Radical Prostatectomy: A Systematic Review and Meta-analysis. Urology. 2015 Jun;85:1368–75.
169. Bubendorf L, Schöpfer A, Wagner U, et al. Metastatic patterns of prostate cancer: an autopsy study of 1,589 patients. Hum Pathol. 2000 May;31:578–83.
170. Fossati N, Willemse P-PM, Van den Broeck T, et al. The Benefits and

Harms of Different Extents of Lymph Node Dissection During Radical Prostatectomy for Prostate Cancer: A Systematic Review. Eur Urol. 2017 Jul;72:84–109.

171. Gandaglia G, Zaffuto E, Fossati N, et al. Identifying candidates for super-extended staging pelvic lymph node dissection among patients with high-risk prostate cancer. BJU Int. 2018;121.
172. Heidenreich A, Varga Z, Von Knobloch R. Extended pelvic lymphadenectomy in patients undergoing radical prostatectomy: high incidence of lymph node metastasis. J Urol. 2002 Apr;167:1681–6.
173. Allaf ME, Palapattu GS, Trock BJ, Carter HB, Walsh PC. Anatomical extent of lymph node dissection: impact on men with clinically localized prostate cancer. J Urol. 2004 Nov;172:1840–4.
174. Bader P, Burkhard FC, Markwalder R, Studer UE. Is a limited lymph node dissection an adequate staging procedure for prostate cancer? J Urol. 2002 Aug;168:514–8; discussion 518.
175. Touijer K, Rabbani F, Otero JR, et al. Standard versus limited pelvic lymph node dissection for prostate cancer in patients with a predicted probability of nodal metastasis greater than 1%. J Urol. 2007 Jul;178:120–4.
176. Briganti A, Chun FK, Salonia A. Critical assessment of ideal nodal yield at pelvic lymphadenectomy to accurately diagnose prostate cancer nodal metastasis in patients undergoing radical retropubic prostatectomy. Urology. 2007;69:147.
177. Briganti A, Suardi N, Capogrosso P, et al. Lymphatic spread of nodal metastases in high-risk prostate cancer: The ascending pathway from the pelvis to the retroperitoneum. Prostate. 2012 Feb;72:186–92.
178. Filimonova I, Schmidt D, Mansoorian S, et al. The Distribution of Pelvic Nodal Metastases in Prostate Cancer Reveals Potential to Advance and Personalize Pelvic Radiotherapy. Front Oncol. 2020;10:590722.
179. Touijer KA, Sjoberg DD, Benfante N, et al. Limited versus Extended

Pelvic Lymph Node Dissection for Prostate Cancer: A Randomized Clinical Trial. Eur Urol Oncol. 2021 Aug;4:532–9.

180. Lestingi JFP, Guglielmetti GB, Trinh Q-D, et al. Extended Versus Limited Pelvic Lymph Node Dissection During Radical Prostatectomy for Intermediate- and High-risk Prostate Cancer: Early Oncological Outcomes from a Randomized Phase 3 Trial. Eur Urol [Internet]. 2021 May 1;79:595–604. Available from: https://doi.org/10.1016/j.eururo.2020.11.040
181. Mattei A, Fuechsel FG, Bhatta Dhar N, et al. The template of the primary lymphatic landing sites of the prostate should be revisited: results of a multimodality mapping study. Eur Urol. 2008 Jan;53:118–25.
182. Mattei A, Würnschimmel C, Baumeister P, et al. Standardized and Simplified Robot-assisted Superextended Pelvic Lymph Node Dissection for Prostate Cancer: The Monoblock Technique. Eur Urol. 2020 Sep;78:424–31.
183. Preisser F, Bandini M, Marchioni M, et al. Extent of lymph node dissection improves survival in prostate cancer patients treated with radical prostatectomy without lymph node invasion. Prostate [Internet]. 2018 Feb 19;78:469–75. Available from: https://doi.org/10.1002/pros.23491
184. Cacciamani GE, Maas M, Nassiri N, et al. Impact of Pelvic Lymph Node Dissection and Its Extent on Perioperative Morbidity in Patients Undergoing Radical Prostatectomy for Prostate Cancer: A Comprehensive Systematic Review and Meta-analysis. Eur Urol Oncol [Internet]. 2021 Apr 1;4:134–49. Available from: https://doi.org/10.1016/j.euo.2021.02.001
185. Briganti A, Karnes RJ, Gandaglia G, et al. Natural history of surgically treated high-risk prostate cancer. Urol Oncol. 2015 Apr;33:163.e7-13.
186. Tosco L, Laenen A, Briganti A, et al. The EMPaCT Classifier: A Validated Tool to Predict Postoperative Prostate Cancer-related Death Using Competing-risk Analysis. Eur Urol Focus. 2018 Apr;4:369–75.
187. Hövels AM, Heesakkers RAM, Adang EM, et al. The diagnostic accuracy

of CT and MRI in the staging of pelvic lymph nodes in patients with prostate cancer: a meta-analysis. Clin Radiol. 2008 Apr;63:387–95.

188. Harisinghani MG, Barentsz J, Hahn PF, et al. Noninvasive detection of clinically occult lymph-node metastases in prostate cancer. N Engl J Med. 2003 Jun;348:2491–9.
189. Tiguert R, Gheiler EL, Tefilli M V, et al. Lymph node size does not correlate with the presence of prostate cancer metastasis. Urology. 1999 Feb;53:367–71.
190. Burkhard FC, Bader P, Schneider E, Markwalder R, Studer UE. Reliability of preoperative values to determine the need for lymphadenectomy in patients with prostate cancer and meticulous lymph node dissection. Eur Urol. 2002 Aug;42:82–4.
191. Von Eyben FE, Kairemo K. Meta-analysis of 11C-choline and 18F-choline PET/CT for management of patients with prostate cancer. Nucl Med Commun. 2014;35:221–30.
192. Van den Bergh L, Lerut E, Haustermans K, et al. Final analysis of a prospective trial on functional imaging for nodal staging in patients with prostate cancer at high risk for lymph node involvement. Urol Oncol. 2015 Mar;33:109.e23-31.
193. van Kalmthout LWM, van Melick HHE, Lavalaye J, et al. Prospective Validation of Gallium-68 Prostate Specific Membrane Antigen-Positron Emission Tomography/Computerized Tomography for Primary Staging of Prostate Cancer. J Urol. 2020 Mar;203:537–45.
194. Jansen BHE, Bodar YJL, Zwezerijnen GJC, et al. Pelvic lymph-node staging with (18)F-DCFPyL PET/CT prior to extended pelvic lymph-node dissection in primary prostate cancer - the SALT trial. Eur J Nucl Med Mol Imaging. 2021 Feb;48:509–20.
195. Bandini M, Marchioni M, Pompe RS, et al. First North American validation and head-to-head comparison of four preoperative nomograms for prediction of lymph node invasion before radical prostatectomy. BJU

Int. 2018 Apr;121:592–9.

196. Cimino S, Reale G, Castelli T, et al. Comparison between Briganti, Partin and MSKCC tools in predicting positive lymph nodes in prostate cancer: a systematic review and meta-analysis. Scand J Urol. 2017 Oct;51:345–50.
197. Yu JB, Makarov D V, Sharma R, et al. Validation of the partin nomogram for prostate cancer in a national sample. J Urol. 2010 Jan;183:105–11.
198. Abdollah F, Cozzarini C, Suardi N, et al. Indications for pelvic nodal treatment in prostate cancer should change. Validation of the Roach formula in a large extended nodal dissection series. Int J Radiat Oncol Biol Phys. 2012 Jun;83:624–9.
199. Godoy G, Chong KT, Cronin A, et al. Extent of Pelvic Lymph Node Dissection and the Impact of Standard Template Dissection on Nomogram Prediction of Lymph Node Involvement. Eur Urol [Internet]. 2011;60:195–201. Available from: https://www.sciencedirect.com/science/article/pii/S0302283811000273
200. Briganti A, Chun FK-H, Salonia A, et al. A nomogram for staging of exclusive nonobturator lymph node metastases in men with localized prostate cancer. Eur Urol. 2007 Jan;51:112–20.
201. MSKKC nomogram [Internet]. 2023. Available from: https://www.mskcc.org/nomograms/prostate/pre_op
202. Briganti A, Larcher A, Abdollah F, et al. Updated Nomogram Predicting Lymph Node Invasion in Patients with Prostate Cancer Undergoing Extended Pelvic Lymph Node Dissection: The Essential Importance of Percentage of Positive Cores. Eur Urol [Internet]. 2012;61:480–7. Available from: http://www.sciencedirect.com/science/article/pii/S0302283811012309
203. Gandaglia G, Ploussard G, Valerio M, et al. A Novel Nomogram to Identify Candidates for Extended Pelvic Lymph Node Dissection Among Patients with Clinically Localized Prostate Cancer Diagnosed with Magnetic Resonance Imaging-targeted and Systematic Biopsies. Eur Urol.

2019;75:506–14.

204. Gandaglia G, Barletta F, Robesti D, et al. Identification of the Optimal Candidates for Nodal Staging with Extended Pelvic Lymph Node Dissection Among Prostate Cancer Patients Who Underwent Preoperative Prostate-specific Membrane Antigen Positron Emission Tomography. External Validation of the Memorial Sloan Kettering Cancer Center and Briganti Nomograms and Development of a Novel Tool. Eur Urol Oncol. 2023 Jun;
205. Czerwińska M, Bilewicz A, Kruszewski M, Wegierek-Ciuk A, Lankoff A. Targeted Radionuclide Therapy of Prostate Cancer-From Basic Research to Clinical Perspectives. Molecules. 2020 Apr;25.
206. Carter RE, Feldman AR, Coyle JT. Prostate-specific membrane antigen is a hydrolase with substrate and pharmacologic characteristics of a neuropeptidase. Proc Natl Acad Sci [Internet]. 1996 Jan 23;93:749–53. Available from: https://doi.org/10.1073/pnas.93.2.749
207. Halsted CH, Ling E, Luthi-Carter R, et al. Folylpoly-γ-glutamate Carboxypeptidase from Pig Jejunum: MOLECULAR CHARACTERIZATION AND RELATION TO GLUTAMATE CARBOXYPEPTIDASE II *. J Biol Chem [Internet]. 1998 Aug 7;273:20417–24. Available from: https://doi.org/10.1074/jbc.273.32.20417
208. Ceci F, Castellucci P, Fanti S. Current application and future perspectives of prostate specific membrane antigen PET imaging in prostate cancer. Q J Nucl Med Mol imaging Off Publ Ital Assoc Nucl Med [and] Int Assoc Radiopharmacol (IAR), [and] Sect Soc of. 2019 Mar;63:7–18.
209. Pastorino S, Riondato M, Uccelli L, et al. Toward the Discovery and Development of PSMA Targeted Inhibitors for Nuclear Medicine Applications. Curr Radiopharm. 2019;13:63–79.
210. Hillier SM, Maresca KP, Femia FJ, et al. Preclinical evaluation of novel glutamate-urea-lysine analogues that target prostate-specific membrane antigen as molecular imaging pharmaceuticals for prostate cancer. Cancer

Res. 2009 Sep;69:6932–40.
211. Wester H-J, Schottelius M. PSMA-Targeted Radiopharmaceuticals for Imaging and Therapy. Semin Nucl Med. 2019 Jul;49:302–12.
212. Bouchelouche K, Choyke PL. Advances in prostate-specific membrane antigen PET of prostate cancer. Curr Opin Oncol. 2018 May;30:189–96.
213. Sartor O, de Bono J, Chi KN, et al. Lutetium-177-PSMA-617 for Metastatic Castration-Resistant Prostate Cancer. N Engl J Med. 2021 Sep;385:1091–103.
214. Ling SW, de Jong AC, Schoots IG, et al. Comparison of (68)Ga-labeled Prostate-specific Membrane Antigen Ligand Positron Emission Tomography/Magnetic Resonance Imaging and Positron Emission Tomography/Computed Tomography for Primary Staging of Prostate Cancer: A Systematic Review and Meta-analy. Eur Urol open Sci. 2021 Nov;33:61–71.
215. Roberts MJ, Maurer T, Perera M, et al. Using PSMA imaging for prognostication in localized and advanced prostate cancer. Nat Rev Urol. 2023 Jan;20:23–47.
216. Robu S, Schottelius M, Eiber M, et al. Preclinical Evaluation and First Patient Application of 99mTc-PSMA-I&S for SPECT Imaging and Radioguided Surgery in Prostate Cancer. J Nucl Med. 2017 Feb;58:235–42.
217. Maurer T, Graefen M, van der Poel H, et al. Prostate-Specific Membrane Antigen-Guided Surgery. J Nucl Med. 2020 Jan;61:6–12.
218. Maurer T, Robu S, Schottelius M, et al. 99m Technetium-based Prostate-specific Membrane Antigen–radioguided Surgery in Recurrent Prostate Cancer. Eur Urol. 2019 Apr;75:659–66.
219. Gandaglia G, Mazzone E, Stabile A, et al. Prostate-specific membrane antigen Radioguided Surgery to Detect Nodal Metastases in Primary Prostate Cancer Patients Undergoing Robot-assisted Radical Prostatectomy and Extended Pelvic Lymph Node Dissection: Results of a Planned Interim

Analysis of a Pr. Eur Urol. 2022 Oct;82:411–8.
220. Gondoputro W, Scheltema MJ, Blazevski A, et al. Robot-assisted prostate-specific membrane antigen-radioguided surgery in primary diagnosed prostate cancer. J Nucl Med. 2022 Mar;jnumed.121.263743.
221. Maurer T, Weirich G, Schottelius M, et al. Prostate-specific membrane antigen-radioguided surgery for metastatic lymph nodes in prostate cancer. Eur Urol. 2015 Sep;68:530–4.
222. Aluwini SS, Mehra N, Lolkema MP, et al. Oligometastatic Prostate Cancer: Results of a Dutch Multidisciplinary Consensus Meeting. Eur Urol Oncol. 2020 Apr;3:231–8.
223. de Barros HA, van Oosterom MN, Donswijk ML, et al. Robot-assisted Prostate-specific Membrane Antigen-radioguided Salvage Surgery in Recurrent Prostate Cancer Using a DROP-IN Gamma Probe: The First Prospective Feasibility Study. Eur Urol. 2022 Jul;82:97–105.
224. Horn T, Krönke M, Rauscher I, et al. Single Lesion on Prostate-specific Membrane Antigen-ligand Positron Emission Tomography and Low Prostate-specific Antigen Are Prognostic Factors for a Favorable Biochemical Response to Prostate-specific Membrane Antigen-targeted Radioguided Surgery in Rec. Eur Urol. 2019 Oct;76:517–23.
225. Knipper S, Tilki D, Mansholt J, et al. Metastases-yield and Prostate-specific Antigen Kinetics Following Salvage Lymph Node Dissection for Prostate Cancer: A Comparison Between Conventional Surgical Approach and Prostate-specific Membrane Antigen-radioguided Surgery. Eur Urol Focus. 2019 Jan;5:50–3.
226. Yılmaz B, Şahin S, Ergül N, et al. (99m)Tc-PSMA targeted robot-assisted radioguided surgery during radical prostatectomy and extended lymph node dissection of prostate cancer patients. Ann Nucl Med. 2022 Jul;36:597–609.
227. Stabile A, Pellegrino A, Mazzone E, et al. Can Negative Prostate-specific Membrane Antigen Positron Emission Tomography/Computed

Tomography Avoid the Need for Pelvic Lymph Node Dissection in Newly Diagnosed Prostate Cancer Patients? A Systematic Review and Meta-analysis with Backup Histology as Reference Standard. Eur Urol Oncol. 2022 Feb;5:1–17.

228. van Leeuwen FWB, Winter A, van Der Poel HG, et al. Technologies for image-guided surgery for managing lymphatic metastases in prostate cancer. Nat Rev Urol. 2019;16:159–71.
229. Rauscher I, Düwel C, Haller B, et al. Efficacy, Predictive Factors, and Prediction Nomograms for (68)Ga-labeled Prostate-specific Membrane Antigen-ligand Positron-emission Tomography/Computed Tomography in Early Biochemical Recurrent Prostate Cancer After Radical Prostatectomy. Eur Urol. 2018 May;73:656–61.
230. Ceci F, Bianchi L, Borghesi M, et al. Prediction nomogram for (68)Ga-PSMA-11 PET/CT in different clinical settings of PSA failure after radical treatment for prostate cancer. Eur J Nucl Med Mol Imaging. 2020 Jan;47:136–46.
231. Bianchi L, Castellucci P, Farolfi A, et al. Multicenter External Validation of a Nomogram for Predicting Positive Prostate-specific Membrane Antigen/Positron Emission Tomography Scan in Patients with Prostate Cancer Recurrence. Eur Urol Oncol. 2023 Feb;6:41–8.
232. Mannweiler S, Amersdorfer P, Trajanoski S, et al. Heterogeneity of prostate-specific membrane antigen (PSMA) expression in prostate carcinoma with distant metastasis. Pathol Oncol Res. 2009 Jun;15:167–72.
233. Ferraro DA, Rüschoff JH, Muehlematter UJ, et al. Immunohistochemical PSMA expression patterns of primary prostate cancer tissue are associated with the detection rate of biochemical recurrence with (68)Ga-PSMA-11-PET. Theranostics. 2020;10:6082–94.
234. Laudicella R, La Torre F, Davì V, et al. Prostate Cancer Biochemical Recurrence Resulted Negative on [(68)Ga]Ga-PSMA-11 but Positive on [(18)F]Fluoromethylcholine PET/CT. Vol. 8, Tomography (Ann Arbor,

Mich.). Switzerland; 2022. p. 2471–4.

235. Rüschoff JH, Ferraro DA, Muehlematter UJ, et al. What's behind (68)Ga-PSMA-11 uptake in primary prostate cancer PET? Investigation of histopathological parameters and immunohistochemical PSMA expression patterns. Eur J Nucl Med Mol Imaging. 2021 Nov;48:4042–53.
236. Paschalis A, Sheehan B, Riisnaes R, et al. Prostate-specific Membrane Antigen Heterogeneity and DNA Repair Defects in Prostate Cancer. Eur Urol [Internet]. 2019;76:469–78. Available from: https://doi.org/10.1016/j.eururo.2019.06.030
237. Perner S, Hofer MD, Kim R, et al. Prostate-specific membrane antigen expression as a predictor of prostate cancer progression. Hum Pathol. 2007 May;38:696–701.
238. Ross JS, Sheehan CE, Fisher HAG, et al. Correlation of primary tumor prostate-specific membrane antigen expression with disease recurrence in prostate cancer. Clin cancer Res an Off J Am Assoc Cancer Res. 2003 Dec;9:6357–62.
239. Mu P, Zhang Z, Benelli M, et al. SOX2 promotes lineage plasticity and antiandrogen resistance in TP53- and RB1-deficient prostate cancer. Science. 2017 Jan;355:84–8.
240. Preisser F, Marchioni M, Nazzani S, et al. The Impact of Lymph Node Metastases Burden at Radical Prostatectomy. Eur Urol Focus. 2019 May;5:399–406.
241. Bandini M, Fossati N, Gandaglia G, et al. Neoadjuvant and adjuvant treatment in high-risk prostate cancer. Expert Rev Clin Pharmacol. 2018 Apr;11:425–38.
242. Measurement AN, Guide GP. Protocol for Establishing and Maintaining the Calibration of Medical Radionuclide Calibrators and their Quality Control. Available from: http://publications.npl.co.uk/npl_web/pdf/mgpg93.pdf
243. Busemann Sokole E, Płachcínska A, Britten A. Acceptance testing for

nuclear medicine instrumentation. Eur J Nucl Med Mol Imaging. 2010 Mar;37:672–81.

244. Commission E, Energy D-G for. Criteria for acceptability of medical radiological equipment used in diagnostic radiology, nuclear medicine and radiotherapy. Publications Office; 2012.
245. Gandaglia G, De Lorenzis E, Novara G, et al. Robot-assisted Radical Prostatectomy and Extended Pelvic Lymph Node Dissection in Patients with Locally-advanced Prostate Cancer. Eur Urol [Internet]. 2017;71:249–56. Available from: http://dx.doi.org/10.1016/j.eururo.2016.05.008
246. Fossati N, Scarcella S, Gandaglia G, et al. Underestimation of Positron Emission Tomography/Computerized Tomography in Assessing Tumor Burden in Prostate Cancer Nodal Recurrence: Head-to-Head Comparison of (68)Ga-PSMA and (11)C-Choline in a Large, Multi-Institutional Series of Extended Salvage Lymph Node Dissections. J Urol. 2020 Aug;204:296–302.
247. Rauscher I, Horn T, Eiber M, Gschwend JE, Maurer T. Novel technology of molecular radio-guidance for lymph node dissection in recurrent prostate cancer by PSMA-ligands. World J Urol. 2018 Apr;36:603–8.
248. Aalbersberg EA, Verwoerd D, Mylvaganan-Young C, et al. Occupational Radiation Exposure of Radiopharmacy, Nuclear Medicine, and Surgical Personnel During Use of [(99m)Tc]Tc-PSMA-I&S for Prostate Cancer Surgery. J Nucl Med Technol. 2021 Dec;49:334–8.
249. Schmidt D, Grosse J, Mayr R, Burger M, Hellwig D. Dose estimates of occupational radiation exposure during radioguided surgery of Tc-99m-PSMA-labeled lymph nodes in recurrent prostate cancer. Nuklearmedizin. 2021 Dec;60:425–33.
250. Gandaglia G, Bravi CA, Dell'Oglio P, et al. The Impact of Implementation of the European Association of Urology Guidelines Panel Recommendations on Reporting and Grading Complications on Perioperative Outcomes after Robot-assisted Radical Prostatectomy. Eur

Urol. 2018;74.

251. Mazzone E, Dell'Oglio P, Grivas N, et al. Diagnostic Value, Oncologic Outcomes, and Safety Profile of Image-Guided Surgery Technologies During Robot-Assisted Lymph Node Dissection with Sentinel Node Biopsy for Prostate Cancer. J Nucl Med. 2021 Oct;62:1363–71.